A review of Early Weichselian climate (MIS 5d-a) in Europe

Barbara Wohlfarth

Department of Geological Sciences, Stockholm University

June 2013

SKB

A review of Early Weichselian climate (MIS 5d-a) in Europe

Barbara Wohlfarth

Department of Geological Sciences, Stockholm University

June 2013

Preface

This document contains information on climate and environmental conditions during the complex transition from warm interglacial to cold glacial conditions at the beginning of the Weichselian period, as recorded in marine, terrestrial and glacial archives. The information is of relevance for the analysis of long-term repository safety in e.g. SKB's safety assessment SR-PSU. In particular, the information will be used in the report "Climate and climate-related issues for the safety assessment SR-PSU" and in the "SR-PSU Main report".

Stockholm, June 2013

Jens-Ove Näslund

Person in charge of the SKB climate programme

Summary

This report addresses the transition from the last interglacial into the last glacial period in Europe, which corresponds to the time interval between approximately 122,000 and 70,000 years before present. Based on state-of-the-art paleoclimatic and paleoenvironmental information from selected terrestrial, marine and ice core records, questions regarding the magnitude, duration, and cyclicity of early glacial stadial and interstadials are discussed.

One of the most important aspects in this respect is the timing of climatic/environmental changes seen in terrestrial, marine, ice core and speleothem records, and most importantly, how and on which basis and by which proxy these climatic shifts are defined. Since correlations between archives are made to understand the sequence of events and the response of different systems to a change in climate, timescales are of uttermost importance. Independent chronologies however only exist for a few archives (Greenland ice cores, U/Th dated speleothems, Lago Grande di Monticchio varve record), while the timescales for other records and archives have been obtained through tuning to an independent chronology or to the astronomical time scale.

Ice core and speleothem isotopic records basically monitor atmospheric changes, but also contain an important local component. Marine records provide information on sea surface and deep-sea temperature and salinity changes, which vary with location; and terrestrial records (primarily pollen stratigraphies) allow reconstructing changing vegetation patterns. Each of these archives thus has its own multitude of proxies, which respond in different ways to an externally triggered shift in climate, such as changes in incoming solar radiation. Disentangling the response of these proxies in terms of climate is one challenge; another challenge is to obtain a detailed enough correlation between the archives in order to understand what is the trigger, what is the response, and which part adds additional feedbacks.

The end of the last interglacial, i.e. the Eemian or MIS5e, and the transition into the last glacial period was initially triggered by a decrease in incoming summer insolation at high northern latitudes. The change in orbital configuration subsequently led to a series of time-transgressive changes (e.g. gradual vegetation replacement; changes in sea surface temperature, salinity, strength of the North Atlantic Current). As Northern Hemisphere ice sheets started to grow and expand these changes became more and more pronounced.

The sequence of events leading from the last interglacial into the last glacial has been described using climate models with different complexity and boundary conditions, paleodata series, and comparisons between model out put and paleo data. One possible scenario involves the development of summer sea ice in the northern North Atlantic already during the later part of the Eemian interglacial, as a response to decreasing summer insolation. This would have accelerated a vegetation shift, which in turn would have led to a decrease in albedo. More extensive sea ice could, through brine formation, have increased the Atlantic meridional overturning circulation, which would have supplied more moisture to the cold high northern latitudes. This in turn would have favoured the growth of ice sheets.

A response of the vegetation in northern Europe to the decrease in summer insolation and to increased summer sea ice may be seen as early as 122–120 thousand years (ka) ago, but became most distinct around 115 ka, when North Atlantic sea surface temperatures show signs of a first minor cooling. This cold event (labelled sea surface cooling event C26) defines the Marine Isotope Stage (MIS) 5e/5d transition in marine cores and seems to correlate with Greenland stadial GS26. This first distinct cooling event on Greenland is paralleled by cold temperatures in Antarctica, which implies synchronous cooling in both hemispheres. However, while Antarctica remained cold, Greenland started to warm just before 110 ka, suggesting the start of the so-called bipolar see-saw mechanism. The first marked cooling over Greenland at 110–108 ka (GS25) was accompanied by a distinct drop in North Atlantic sea surface temperatures (C24 event), by an increase in ice-rafted debris and by marked vegetation changes in southern Europe. This shift in vegetation defines the end of the terrestrial Eemian in southern Europe, which in comparison to marine records, occurred during MIS 5d. Paleo records thus suggest that the response of the vegetation to North Atlantic cooling events was delayed in southern Europe by at least 5 ka as compared to northern Europe.

The decrease in summer insolation at high northern latitudes thus led to a series of feedback mechanisms, which gradually became stronger as ice sheets grew larger. The initiation of the bipolar see-saw mechanism at around 110–112 ka seems to have triggered the series of abrupt and recurrent shifts between warmer interstadials and colder stadials that characterised the last glacial. While tundra and steppe-tundra seem to have developed in response to severe stadial conditions, the vegetation response to warmer interstadial temperatures was regionally different.

The magnitude of temperature shifts at the last interglacial/glacial transition and between stadials and interstadials varied greatly, depending on the location of the paleo-archive and the methods and proxies used for estimating climate conditions. Summer and winter sea surface temperatures reconstructed for marine core ODP 980 at 55°N for example suggest a temperature drop of 3 and 2°C, respectively at the MIS 5e/5d transition. Stadial/interstadial shifts in summer and winter temperatures are estimated at between 2–3°C and 2–4°C, respectively. Alkenone-based temperature reconstructions in Iberian Margin core MD-2042 further to the south, show even larger temperature differences of up to 10°C between stadials and interstadials. Biological proxies derived from terrestrial sites indicate similar summer temperatures during stadials and interstadials, or only slightly higher temperatures during interstadials. In contrast winter temperatures seem to have been several degrees C colder during stadials as compared to interstadials. Probably the most detailed record of stadial/interstadial temperature shifts is derived from Greenland ice cores, where temperatures rose by between 8 and 16°C across stadial/interstadial transitions.

Cold, stadial conditions lasted between about 1 and 4 ka, while interstadials had a length of between 16 and 2 ka and became progressively shorter.

Although much progress has been made during the last years, many more independently dated terrestrial records are needed to faithfully assess leads and lags to marine, ice core and speleothem archives. At the moment only few archives provide independent chronologies to assess the duration of stadials and interstadials.

Contents

1 Introduction

Planet Earth has experienced numerous shifts between glacial and interglacial episodes (Figure 1-1), which were paced by changes in orbital parameters. The changes in orbital parameters resulted in variations in incoming solar radiation, which in turn led to a series of important feedback mechanisms, which involved all parts of the climate system – the ocean, the atmosphere, the cryosphere, the lithosphere and the biosphere. Variations in greenhouse gas concentrations, changes in atmospheric aerosol content, altered vegetation distribution, ice sheet response, ice shelf disintegration, sea level changes, sea ice extent, and freshwater flux contributed to push Earth's climate into and out of glacial states (Köhler et al. 2010). Marine, terrestrial and ice core paleoclimate archives show that rapid and abrupt sub-millennial scale climatic shifts were superimposed on interglacial/glacial cycles, and that these abrupt shifts were most distinct when large ice sheets were present.

Long and continuous paleoclimate records covering the past 2–3 million years are scarce and available information on glacial/interglacial cycles mainly relates to the past c. 150 ka (thousand years), during which Earth has experienced two glacial/interglacial cycles. These are well documented in paleoclimate archives located outside the Last Glacial Maximum (LGM; c. 21 ka) ice extent. In areas that had been covered by ice sheets and glaciers paleoclimatic and paleoenvironmental archives older than the LGM often have been destroyed by glacial erosion or are obscured by thick glacial deposits. Accordingly, these areas mainly allow documenting the climatic and environmental development since the LGM and only provide fragmented paleo information for older time intervals. Paleoclimatic and paleoenvironmental information regarding pre-LGM conditions therefore mainly has to be obtained from regions that were situated outside the extents of past ice sheets and glaciers. Ice cores from Greenland (NGRIP Members 2004) and Antarctica (EPICA Community Members 2006) are in this respect however one exception, because the ice that formed during the past 120 ka and 800 ka, respectively contains information on atmospheric changes and changes in ocean circulation.
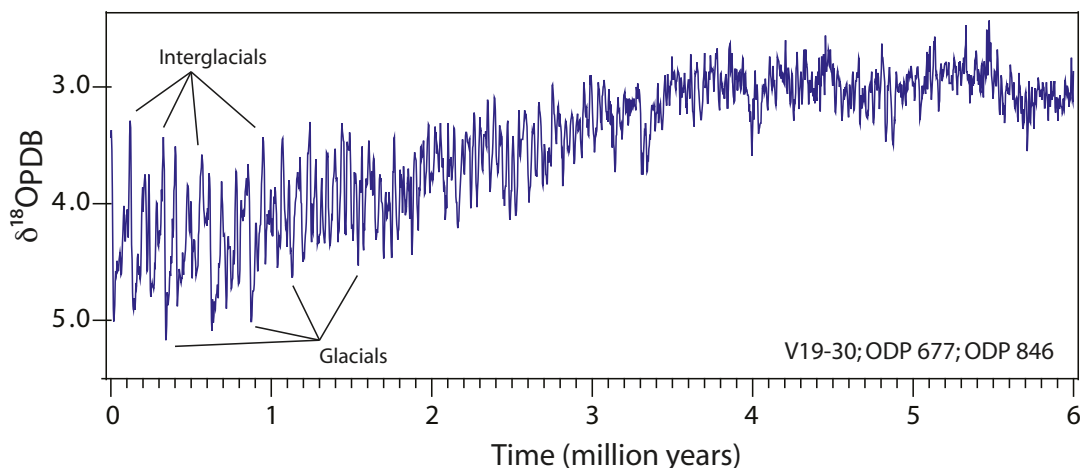
Figure 1-1. *Climate variability during the past 6 million years. This curve is based on combining oxygen isotope ($\delta^{18}O$) records measured on benthic foraminifera in marine cores V19-30 (Shackleton and Pisias 1985), ODP 677 (Shackleton et al. 1990) and ODP 846 (Shackleton et al. 1995a, b) and provides a proxy for total ice sheet volume. Original data was downloaded from http://www.esc.cam.ac.uk/research/research-groups/delphi/coredata/v677846.*
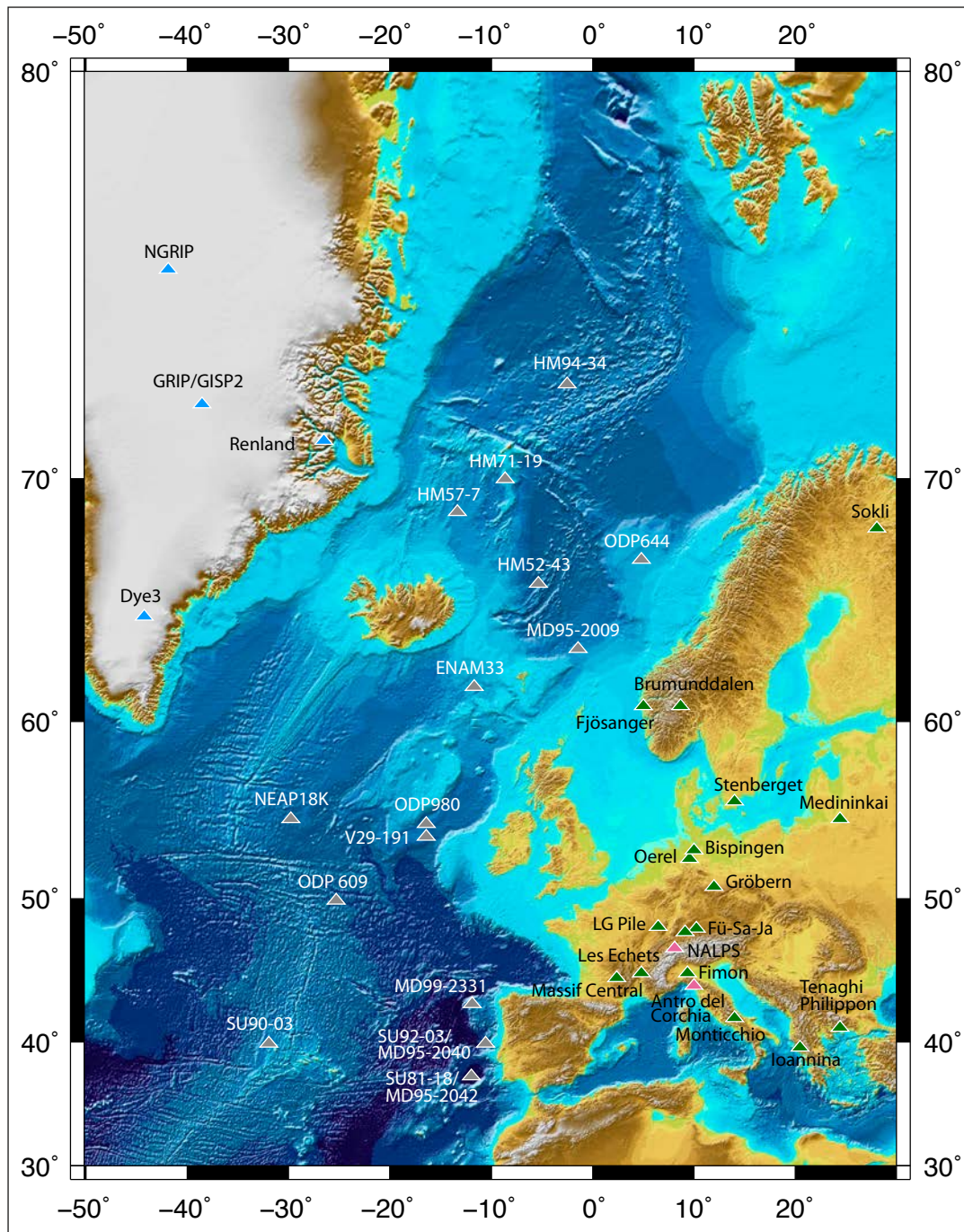
Figure 1-2. *Location of ice core, marine, and terrestrial sites discussed in the text. Blue triangles = ice core records; grey triangles = marine records; green triangles = lake/peat records; pink triangles = speleothem records. Fü = Füramoos, Sa = Samerberg, Ja = Jammertal. Massif Central = Ribain Maar lake and Lac du Bouchet. See Table 2-1 for details.*

The focus of this report is the end of the last interglacial and the early part of the last glacial period in Europe. This corresponds roughly to the time interval between 122 and 75 ka, when growth of large ice sheets took place, subsequent to a period of minimum ice volume. In terrestrial records this time frame is commonly referred to as the end of the Eemian interglacial and the subsequent early Weichselian glacial period (in northern Europe) or early Würmian glacial period (in southern Europe and in the Alps). In marine records the time interval corresponds to Marine Isotope Stages (MIS) 5e, 5d, 5c, 5b, and 5a, and in the Greenland ice core records to the last interglacial and Greenland stadials/interstadials (GS/GI) 26/25 through 19/18.

Table 1-1. Long terrestrial sequences mentioned in the text.

Site name	Coordinates (°)		Archive	References
Antro del Corchia	N 43°59'	E 10°13'	Speleothem	Drysdale et al. 2005, 2007
Baschg Cave	N46°38'	E 07°49'	Speleothem	Boch et al. 2011
Beatus Cave	N 47°26'	E 09°52'	Speleothem	Boch et al. 2011
Bispingen	N 53°06'	E 10°06'	Ancient lake	Müller 1974, Müller and Kukla 2004
Fimon	N 45°28'	E 11°32'	Lake	Pini et al. 2010
Füramoos	N 47°58'	E 09°52'	Ancient lake	Müller et al. 2003, Klotz et al. 2004
Gröbern	N 51°52'	E 12°26'	Ancient lake	Walkling and Coope 1996, Hoffmann et al. 1998, Kühl and Litt 2003
Ioannina 284	N 39°45'	E 20°51'	Ancient lake	Tzedakis et al. 2002, 2003, 2004
Jammertal	N 48°06'	E 09°43'	Ancient lake	Müller et al. 2000, 2005, Klotz et al. 2004
Klaus-Cramer Cave	N 47°26'	E 9°52'	Speleothem	Boch et al. 2011
Klinge	N 51°47'	E 14°32'	Ancient lake	Boettger et al. 2009
La Grande Pile	N 47°43'	E 06°30'	Ancient lake	Woillard 1978, de Beaulieu and Reille 1992a, Ponel 1995
Lagaccione	N 42°34'	E11°48'	Ancient lake	Magri 1999
Lac du Bouchet	N 44°29'	E 03°29'	Lake	Reille and de Beaulieu 1988
Les Echets	N 45°54'	E 04°55'	Ancient lake	de Beaulieu and Reille 1984, Klotz et al. 2004
Medininkai	N 54°33'	E 25°37'	Ancient lake	Satkunas et al. 2003
Lago Grande di Monticchio	N 40°55'	E 15°37'	Lake	Allen et al. 1999, 2000, Allen and Huntley 2009, Watts et al. 1996, Brauer et al. 2000, 2007, Wulf et al. 2012
Neumark-Nord	N 51°19'	E 11°52'	Ancient lake	Boettger et al. 2009
Oerel	N 53°28'	E 09°04'	Ancient lake	Behre and Lade 1986, Behre 1989, Behre et al. 2005
Padul	N 37°00'	W 03°40'	Ancient lake	Pons and Reille 1988
Peqiin Cave	N32°34'	E 35°11'	Speleothem	Bar-Matthews et al. 2003
Ribains	N 44°49'	E 03°49'	Ancient lake	de Beaulieu and Reille 1992b, Reille et al. 2000, Rioual et al. 2007
Samerberg	N 47°46'	E 12°13'	Ancient lake	Grüger 1979, Klotz et al. 2004
Schneckenloch Cave	N 47°26'	E 09°52'	Speleothem	Boch et al. 2011
Sofular Cave	N 41°24'	E 31°55'	Speleothem	Badertscher et al. 2011, Fleitmann et al. 2009
Sokli	N 67°48'	E 29°18'	Ancient lake	Helmens et al. 2000, 2007, 2012, Engels et al. 2010
Soreq Cave	N 31°45'	E 35°01'	Speleothem	Bar-Matthews et al. 2000
Tenaghi Philippon TP-2005	N 41°10'	E 24°19'	Ancient lake	Tzedakis et al. 2006, Müller et al. 2011
Valle di Castiglione	N 41°52'	E 12°46'	Ancient lake	Follieri et al. 1988, 1998

The main aim of this report is to address the following questions that are of relevance for the research programme at the Swedish Nuclear Fuel and Waste Management Company (SKB):

1. Can recurrent and abrupt shifts between warmer interstadials and colder stadials be observed at the last interglacial/glacial transition and during the early part of the last glacial in terrestrial, marine and ice core archives?

2. What was the magnitude of temperature and precipitation shifts at the last interglacial/glacial transition and during the early part of the last glacial based on terrestrial, marine and ice core archives?

3. How is the last interglacial/glacial transition defined in different paleo archives and how long was the duration of interstadials and stadials during the early part of the last glacial?

4. Which mechanisms can explain glacial inception at the last interglacial/glacial transition and the occurrence of rapid stadial/interstadial/stadial shifts?

These questions are addressed by summarizing available qualitative and quantitative paleoenvironmental and paleoclimatic information from continuous terrestrial sequences in Europe, selected North Atlantic marine sequences and Greenland ice core records (Figure 1-2). One crucial aspect for this overview is the discussion of the definition and chronology of the end of the last interglacial and the early part of the last glacial in different archives. This discussion is necessary because correlations between land, ocean and ice archives need to be based on independent chronologies to being able to detect leads and lags, and to discuss the sequence of events that led to glacial inception and into the last glacial period.

2 Orbital forcing, ice volume and sea level changes during MIS 5

Changes in incoming solar radiation at high northern latitudes are widely regarded as trigger for the timing of major glacial-interglacial cycles (Hays et al. 1976, Shackleton 2006, Berger 2012), and as such for the expansion/retreat of large polar ice sheets. Ice sheet expansion and disintegration lead to changes in global sea level, which can be reconstructed using radiometrically dated corals preserved below or above present-day sea level, stratigraphic information and geophysical modelling (see for example Lambeck and Chapell 2001, Dutton and Lambeck 2012). Another approach is to assess salinity changes in evaporative marine basins, which show up as shifts in the $\delta^{18}O$ composition of planktonic foraminifera shells (see for example Grant et al. 2012). These methods allow reconstructing sea level changes for the past ca 300 ka (Dutton et al. 2009), while shifts in deep-sea (benthic) oxygen isotope ($\delta^{18}O$) values are generally used for sea level reconstructions on much longer time scales (Lisiecki and Raymo 2005, Hays et al. 1976).

The influence of insolation on pacing the major climatic shifts during the past 125 ka is shown in Figure 2-1, which compares July insolation at 45, 50 and 60°N (Berger 1987) and relative sea level reconstructions (Lambeck et al. 2002, Lisiecki and Raymo 2005, Grant et al. 2012). These reconstructions can in turn be used to infer changes in past ice volumes.

July insolation decreased around 125 ka and attained a minimum at 114 ka (Berger 1987). This decrease is mirrored by a relative sea level lowering (increase in ice volume) from above present day sea levels to about –60 to –70 m and by a change in the oxygen isotope composition of deep ocean waters (Figure 2-1), marking the transition between the Eemian interglacial (MIS 5e) and the subsequent early periods of the Weichselian glacial (MIS 5d-5a). The relative sea level curve for Huon Peninsula (Figure 2-1B), which is based on raised coral reef data sets and stratigraphic information (Lambeck et al. 2002), suggests a fairly rapid drop in sea level starting around 119–118 ka. The composite curve (grey shaded in Figure 2-1C), which has been constructed using planktonic foraminifera $\delta^{18}O$ measurements in sediment core LC21 from the eastern Mediterranean Sea and chronological tie points to the U/Th dated Soreq $\delta^{18}O$ speleothem record (Grant et al. 2012), shows a much more gradual lowering, starting already at around 122–121 ka (Grant et al. 2012). If the drop in sea level started this early, it would mean that local glaciers and ice sheets had already started to grow during the later part of MIS 5e.

Insolation values show two distinct maxima at 104 and 82 ka, corresponding to MIS 5c and 5b and two distinct minima at 112, 92–94 and 70 ka, corresponding to MIS 5d, 5b and 4, respectively (Figure 2-1A). Relative sea level reconstructions mirror these trends (Figure 2-1B, C), although absolute values and the pattern for the two relative sea level curves differ. These differences could be due to a number of factors that affect far-field sites (Dutton and Lambeck 2012, Lambeck et al. 2012), and are likely also influenced by the type of proxies used in the reconstructions, i.e. [14]C and U/Th dated corals versus $\delta^{18}O$ measured in planktonic foraminifera. Lower relative sea levels during MIS 5d and MIS 5b show the growth of ice sheets, and the marked drop in sea level during MIS 4 suggests considerably larger ice volumes. Higher sea levels of between –20 and –40 m and thus lower ice volumes can be inferred for MIS 5c and 5a (Figure 2-1B, C).

Although relative sea level as reconstructed from various sources, broadly follows changes in Northern Hemisphere summer insolation (Figure 2-1A–C), minor sea level shifts of <20 m during MIS 5c and 5a suggest that global ice volume changes were also driven by sub-orbital scale climatic fluctuations.
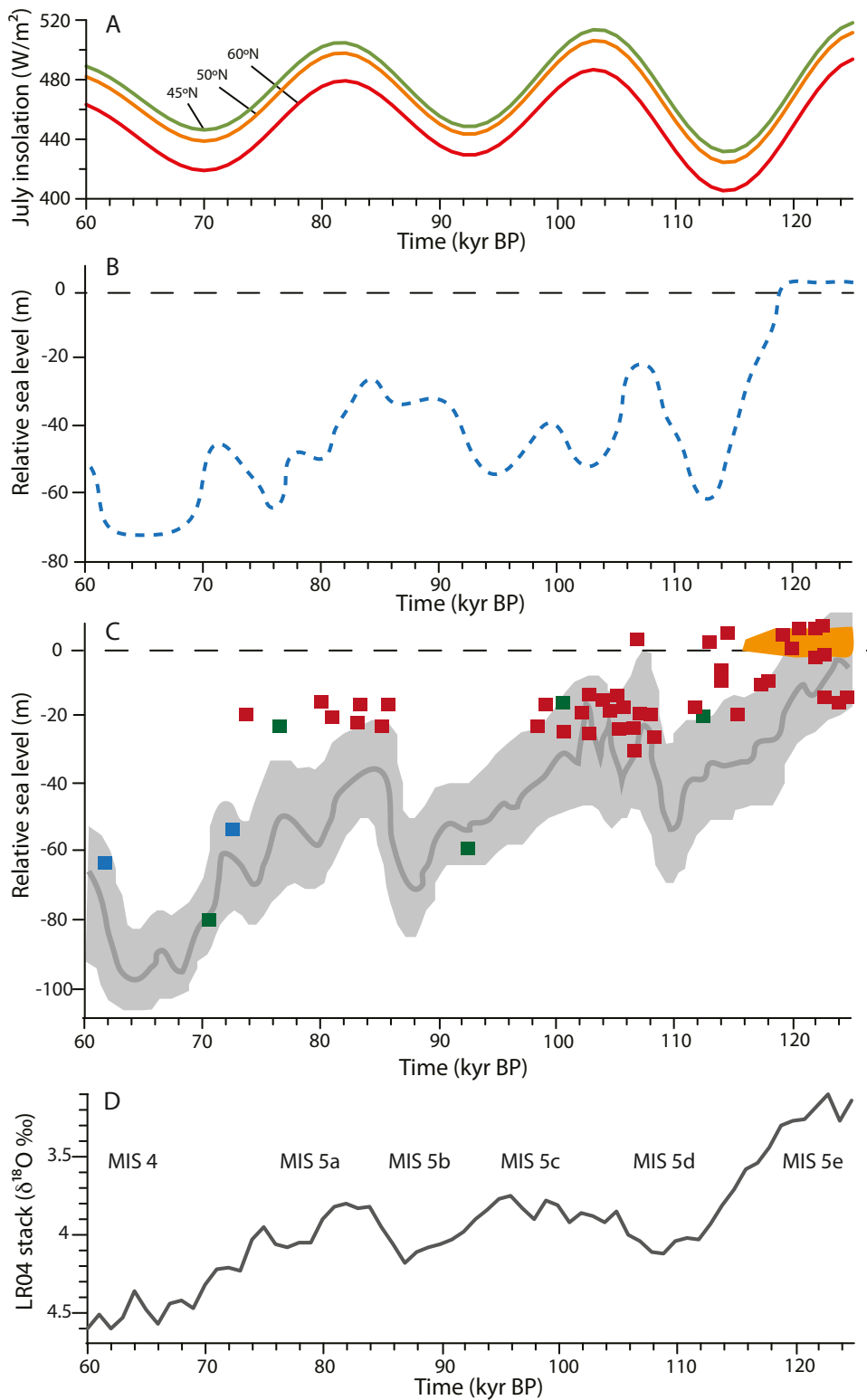
Figure 2-1. *(A) July insolation computed for 45, 50 and 60°N (Berger 1978). (B) Relative sea-level curve for parts of the last glacial cycle for Huon Peninsula based on U/Th and 14C dated corals and other stratigraphic evidence (Lambeck et al. 2002). (C) Red Sea relative sea-level curve compared to coral-based sea level data (Grant et al. 2012). The light grey envelope shows the 95% confidence interval for the Red Sea reconstruction and the dark grey line is the probability maximum. Coral data are derived from Chapell (2002) (blue), Cutler et al. (2003) (green), Thompson and Goldstein (2005) (red) and Dutton and Lambeck (2012) (orange). (D) Stack of 57 globally distributed δ¹⁸O records showing marine isotope stages (MIS) 5e to 4 (Lisiecki and Raymo 2005). Original data for (A) was obtained from MF Loutre; for (B) redrawn from Figure 2 in Lambeck et al. (2002); for (C) redrawn from Figure 2 in Grant et al. (2012); and for (D) downloaded from http://www.lorraine-lisiecki.com/stack.html.*

3 Marine isotope stratigraphy of MIS 5

Changes in calcium carbonate accumulation measured in deep-sea cores from the East Equatorial Pacific allowed for the first time a subdivision of the major climatic changes during the Quaternary (Arrhenius 1952). This sub-division and numbering was subsequently used by Emiliani (1955) and has, since the work of Shackleton (1967) and Hays et al. (1976) found wide spread application as marine isotope stratigraphy (MIS), a global stratigraphic framework for marine sediments (Martinson et al. 1987, Shackleton et al. 2003). Warm interglacial intervals are depicted as even numbers in this stratigraphic scheme and cold glacial intervals received odd numbers.

Shackleton (1969) further subdivided MIS 5 into the sub-stages MIS 5e, 5d, 5c, 5b and 5a (see the stacked deep-sea oxygen isotope curve in Figure 2-1D), since it had become obvious that the terrestrial Eemian interglacial only corresponded to parts of MIS 5 (Shackleton et al. 2003) (Figure 3-1). The stratigraphic scheme of Shackleton (1969) is now widely employed for marine sediment sequences and has subsequently been used for correlations to terrestrial and ice core archives.

Chronologies for marine sequences covering the last glacial are often based on a combination of ^{14}C dates on foraminifera and tuning of benthic foraminifera δ^{18}O measurements to the standard orbital chronology (SPECMAP stack) (Martinson et al. 1987). In some cases, known tephra layers have been used as additional age tie points (for example Rasmussen et al. 2003). Correlations of benthic and planktonic δ^{18}O sequences to the δ^{18}O record of Greenland ice cores (for example Shackleton et al. 2000) also provided alternative chronologies. The time scale of core MD95-2042 from the Iberian Margin is such an example (Figures 1-2, 3-1).

The detailed oxygen isotope record for MD95-2042 depicts a number of high frequency fluctuations during the interstadials and stadials of MIS 5, especially in the planktonic δ^{18}O curve (Figure 3-1), suggesting marked shifts in surface water conditions. The benthic δ^{18}O record on the other hand mirrors changes in continental ice volume (Shackleton et al. 2000) (Figure 3-1). Based on this observation Shackleton et al. (2003) later refined the chronology for MD95-2042 and related the benthic δ^{18}O curve to ice volume and consequently U/Th dated sea level changes. Radiometric ages on corals for these latter changes then formed new chronological tie points for MD95-2042.

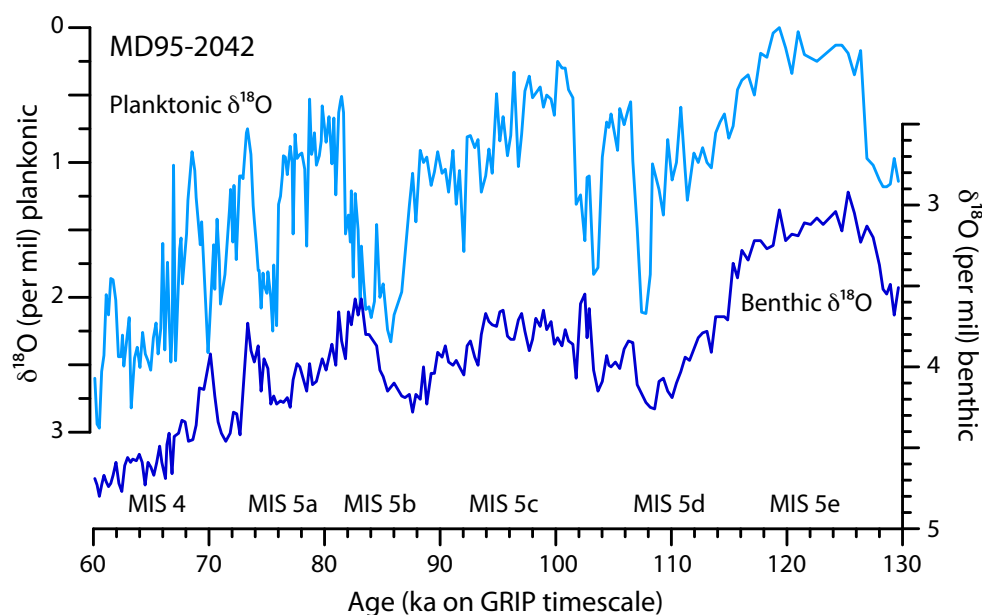**Figure 3-1.** *Planktonic and benthic δ^{18}O record for marine core MD95-2042 from the Iberian Margin. See Figure 1-2 for the location of the core. The chronology is shown on the timescale of Greenland ice core GRIP. Based on the data set of Shackleton et al. (2000). Original data was downloaded from doi:10.1594/ PANGAEA.58228.*

4 Terrestrial (pollen-) stratigraphy of MIS 5

Pollenstratigraphic records from long continuous terrestrial sequences in southern, central and northern Europe provided already more than 30 years ago evidence for two distinct cold and two warm intervals subsequent to the Eemian interglacial (Table 1-1). The sites of La Grande Pile (Woillard 1978), Les Echets (de Beaulieu and Reille 1984) and Oerel (Behre 1989) are among several for which detailed pollenstratigraphies had been established (Figure 1-2).

The pollen zones, pollen assemblages and the inferred vegetation for La Grande Pile in the Vosges Mountains (Woillard 1978) and for Oerel (Behre 1989) in northern Germany are shown here as examples (Tables 4-1, 4-2), since they provided early stratigraphic evidence for the succession of two stadials and two interstadials subsequent to the Eemian interglacial in central and northern Europe.

Initially the major zones that were recognized in the different records, were given local names. However lately most researchers use Mélisey I and II and St. Germain I and II for southern Europe to denote stadials and interstadials. For northern Europe, the corresponding zones are Herning and Rederstall for stadials and Brörup and Odderade for interstadials.

Table 4-1. Simplified description of the La Grande Pile pollen record according to Woillard (1978). The ages for the stadial and interstadial boundaries are according to Guiot et al. (1993) and based on tuning of the record to the insolation curve. PZ = pollen zone. See Figure 1-2 for the location of the site and Table 1-1 for further details.

Zone	PZ	Pollen	Vegetation
	5	*Pinus, Betula, Picea* forest with *Juniperus*	Boreal forest
	4	*Quercus, Carpinus, Corylus* forest with *Pinus,*	Temperate forest
St Germain		Betula, Picea, Alnus, Ulmus, Fraxinus, Tilia, Viscum,	
II	3	*Quercetum mixtum, Corylus* forest with *Betula,*	Temperate forest
		Pinus, Alnus, Carpinus, Picea	
	2	*Betula, Pinus, Juniperus* forest	Boreal forest
	1	Betula, Juniperus	Subarctic tundra
			84 ka
Mélisey II		Open Graminae, *Artemisia*, Chenopodiaceae,	Steppe
		Helianthemum, Thalictrum, Calluna vegetation	
			96 ka
	5	*Pinus, Betula, Picea* forest with some *Quercus*	Boreal forest
	4	*Carpinus, Picea, Quercus, Pinus, Betula* forest	Cold temperate forest
St Germain	3	*Carpinus, Quercetum mixtum, Picea* forest	Warm temperate forest
Ic	2	*Corylus, Quercetum mixtum* forests	Warm temperate forest
	1	Pinus-Betula forests with Picea and Juniperus	Boreal forest
Montaigu event		Expansion of Graminae and *Artemisia*	Slight cooling
	6	*Pinus, Betula, Picea* forest	Boreal forest
	5	*Carpinus, Picea, Quercus, Corylus, Pinus, Betula* forest	Cold temperate forest
St Germain	4	*Pinus, Betula* forest	Boreal forest
Ia	3	*Pinus, Betula, Quercetum mixtum, Corylus, Picea* forest	Boreal forest, slightly warmer
	2	*Pinus, Betula* forest with *Picea* and *Juniperus*	Boreal forest
	1	*Juniperus, Betula, Salix,* herbs	Sub-arctic tundra
			104 ka
Mélisey I		Graminae, *Artemisia, Thalictrum,*	Steppe
		Chenopodiaceae, *Calluna, Helianthemum*	
			112 ka
Late Eemian	7	*Pinus, Picea, Betula* forest with *Juniperus*	Boreal forest

The pollenstratigraphic record of La Grande Pile (Woillard 1978, Woillard and Mook 1982) was interpreted as a succession of warmer (St Germain I and II) interstadials and colder stadials (Mélisey I and II) following the declining stage of the Eemian interglacial (Table 4-1). Interstadials were characterised by a typical successional vegetation cycle with tundra, boreal forest, temperate forest, and boreal forest, and stadials by open steppe, or steppe-tundra vegetation. High frequency fluctuations in pollen assemblages during interstadials suggested a number of short-term climate shifts. Woillard (1978) moreover described a short cold phase, the Montaigu event, within the warm interstadial St. Germain I.

The paleoenvironmental record of Oerel in northern Germany is based on pollenstratigraphy and on plant macrofossil and coleopteran analyses (Behre 1989, Behre et al. 2005) and represents a standard profile for the last interglacial and the early glacial in northern Europe (Behre and Lade 1986). Similar to La Grande Pile, two distinct cold/warm intervals were recognized subsequent to the Eemian interglacial (Table 4-2). Pine and birch forests dominated during the interstadials Brörup (WE II) and Odderade (WE IV), while open tundra/steppe characterized the stadials Herning (WE I) and Rederstall (WE III). Both interstadials show a two-step development from a birch-dominated to a pine-dominated vegetation. The birch phase of the Brörup interstadial was further subdivided into three parts (WE IIa$_1$, WE IIa$_2$, WE IIa$_3$) (Behre 1989), based on distinct changes in vegetation (Table 4-2). This sub-division showed that the vegetation development was not uniform during interstadials, but that a number of short-term climate fluctuations may have occurred.

Several sites with organic deposits that can be attributed, based on their pollen assemblages and their stratigraphic position, to post-Eemian interstadials have been described from Scandinavia (see for example Berglund and Lagerlund 1981, Lagerbäck and Robertsson 1988, Houmark-Nielsen 1989, Larsen and Sejrup 1990, Robertsson 1991, Robertsson and García Ambrosiani 1992, Hättestrand 2008, Mangerud et al. 2011). All of these deposits represent however fragmented records and/or are present within discontinuous stratigraphies. Therefore correlations to continuous records in northern Europe and an attribution to either of the two last glacial interstadials has proven to be difficult (Hättestrand 2008).

A number of attempts have been made to correlate long pollen records over larger regions in Europe to assess differences in vegetation development and vegetation gradients (see for example Behre 1989, Grüger 1989. Allen and Huntley 2000). Given the lack of independent chronologies for individual sites, these correlations had to be based on the assumption that the vegetation response to stadial and interstadial climate shifts had been more or less synchronous across Europe. As such the St. Germain I interstadial of southern Europe was correlated to the Brörup interstadial of northern Europe, the Mélisey I stadial to Herning, the St. Germain II interstadial to Odderade and the Mélisey II stadial to Rederstall. In all available pollen records, the same pattern became obvious: two cold stadials with steppe/tundra vegetation in most of Europe, and two warmer post-Eemian interstadials with forest/woodland expansion (see for example Lang 1994 and Fletcher et al. 2010 for summaries and overviews).

Table 4-2. Vegetation zonation for Oerel, northern Germany after Behre (1989) and Behre and Lade (1986). See Figure 1-2 for the location of the site and Table 1-1 for further details.

Zones		Vegetation	Comments
Odderade	(WE IVb)	Pine period	Increase in herb pollen, increase in Ericales
			Slight expansion of *Picea* and *Larix*
	(WE IVa)	Birch period	Spread of tree birch
Rederstall	(WE III)	Open tundra/steppe	Increase in heliophytes
Brörup	(WE IIb)	Pine period	Decrease in *Larix, Picea*; increase in Ericales (mainly *Calluna*)
	(WE IIa$_3$)		Increase in herb pollen, *Picea, Larix*
	(WE IIa$_2$)	Birch period	
	(WE IIa$_1$)		Spread of tree birch
Herning	(WE I)	Open tundra/steppe	Grasses, heliophytes and shrubs (*Betula nana, Juniperus*)
			Expansion of Ericales heaths (*Empetrum, Calluna*)
Eem	(E VI–VII)	Pine period	Dominance of *Pinus, Betula*, increase in herb pollen

Allen and Huntley's (2000) tentative correlation between pollen records from southern Italy (Lago Grande di Monticchio, Valle di Castiglione), Spain (Padul), France (Lac du Bouchet, Les Echets, La Grande Pile), Greece (Tenaghi Philippon), and northern Germany (Oerel) (Figure 1-2), furthermore showed that the first post-Eemian interstadial (St. Germain I/Brörup), was characterized by a shift in vegetation from temperate deciduous forest to temperate deciduous forest/cool mixed forests in southern Europe, but to boreal forests in northern Europe. The following stadial (Mélisey II/Rederstall) saw an expansion of cold/warm steppe in southern Europe and of cold steppe in northern Europe (Allen and Huntley 2000). Temperate forests became re-established both in southern and northern Europe during the upper interstadial (St. Germain II/Odderade), but these were successively replaced by boreal forests in northern Europe.

Some of the earlier investigated, long terrestrial sequences have been subject to new investigations, and more sites have been added, providing a better spatial and temporal picture of the response of the European vegetation to climatic changes (see for example de Beaulieu and Reille 1992b, Hoffmann et al. 1998, Boettger et al. 2000, 2007, Allen and Huntley 2000, Tzedakis et al. 2003, 2004, Müller and Kukla 2004, Sánchez Goñi et al. 2005, Müller and Sánchez Goñi 2007, Sánchez Goñi 2007, Allen and Huntley 2009, Fletcher et al. 2010, Pini et al. 2010, Müller et al. 2011, Helmens et al. 2012, Table 1-1 and further discussions in Chapters 6 to 9).

Many of the available long pollen records however still lack an independent chronology and are consequently tuned or tied to Greenland ice cores, to the marine isotope stratigraphy and/or to the astronomical timescale using marker events. Lago Grande di Monticchio in Italy is in this respect an exception, since its chronology is based on varve counting, tephrochronology, and Ar/Ar dating of tephra layers (Allen and Huntley 2000, 2009, Brauer et al. 2000, 2007, Wulf et al. 2012).

5 Greenland ice core records and North Atlantic sea surface temperature changes

5.1 Greenland ice core records

Distinct and high frequency climatic fluctuations during the last glacial period had for the first time been recognized in Greenland ice core $\delta^{18}O$ records from e.g. Renland, Dye 3 and Camp Century (Figure 1-2) and had suggested much greater climate instability (Dansgaard et al. 1993) than previously assumed based on pollenstratigraphies. Greenland ice cores GRIP and GISP however provided the first independent chronologies against which terrestrial and marine records could be compared. Although both ice cores did not extend back to the last interglacial due to disturbances in the basal ice, they did show that the time interval corresponding to MIS 5d-a contained many more distinct and rapid shifts between cold stadials and warm interstadials (Grootes et al. 1993, Dansgaard et al. 1993), than those that had been reported from pollenstratigraphic records on land (e.g. Woillard 1978, de Beaulieu and Reille 1984, Reille et al. 1998, Behre 1989) or from marine records.

The continuous NGRIP ice core from the Greenland Summit (Figures 1-2, 5-1) finally allowed extending the Greenland record back into the last interglacial and confirmed the high frequency climatic shifts during the last glacial (NGRIP Members 2004). The chronology for the NGRIP $\delta^{18}O$ record, which is based on annual layer counting back to 60 ka and an ice flow model (ss09sea time scale) as far back as 123 ka (Svensson et al. 2008), now provides an excellent template against which last interglacial/glacial climatic and environmental changes in marine and terrestrial records can be compared and discussed (NGRIP Members 2004).

Ice core $\delta^{18}O$ values combine information on evaporation and atmospheric transport of air masses, as well as site-specific temperature changes and thus allow monitoring of colder and warmer climatic intervals. Lower $\delta^{18}O$ values signify colder conditions and higher $\delta^{18}O$ values warmer conditions. These assumptions are supported by a multitude of other ice core geochemical proxy studies (NGRIP Members 2004, EPICA Community Members 2006).
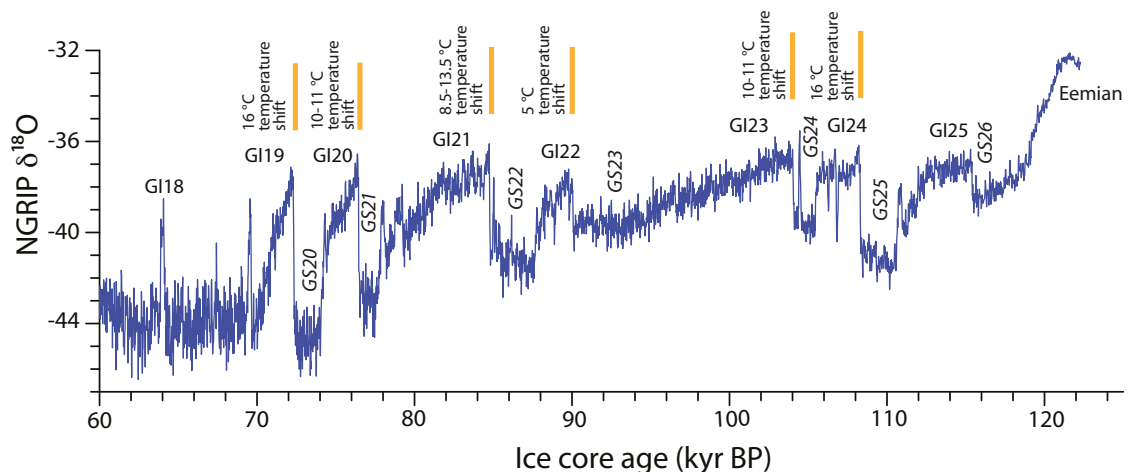
Figure 5-1. *The $\delta^{18}O$ record of the Greenland ice core NGRIP between 60 and 125 ka (NGRIP Members 2004) on the GICC05modelext time scale (Andersen et al. 2006, Svensson et al. 2008). GI = Greenland interstadial; GS = Greenland stadial. The temperature shift between stadials and interstadials is according to Landais et al. (2005) and Capron et al. (2010). See Figure 1-2 for the location of the site. Original data was downloaded from www.iceandclimate.dk/data.*

Each of the distinct climatic shifts in $\delta^{18}O$ values seen in the NGRIP ice core consists of an abrupt warming that occurred within decades and a subsequent gradual cooling. These so-called Dansgaard-Oeschger or D-O events comprise Greenland stadials (GS) and Greenland interstadial (SGI) (NGRIP Members 2004, Svensson et al. 2006). As shown in Figure 5-1, $\delta^{18}O$ values in the NGRIP ice core start to decline gradually after 121 ka and attain minimum values around 116 ka. Subsequent to this first cooling (GS26) a series of shorter and longer interstadials (GI) and stadials (GS) are observed. Each stadial and interstadial has its own specific signature in respect to length, internal oscillations and temperature shift. Interstadial GI23 for example was the longest in this series, lasting for around 10 ka while GI22 had a length of less than 2 ka. During certain stadials and interstadials shorter, abrupt warming/cooling events occurred (Capron et al. 2010), such as during GS24 and GI24, which would suggest climate instability even under stadial and interstadial conditions. Moreover, $\delta^{15}N$ and $\delta^{40}Ar$ measurements, which allow quantifying the magnitude of abrupt temperature shifts between stadials and interstadials, show that very large temperature shifts of 16°C had occurred across the GS25/GI24 and GS20/GI19 transitions (Landais et al. 2006, Capron et al. 2010). In contrast, a temperature shift of only 5°C was reconstructed for the GS23/GI22 transition (Landais et al. 2005, 2006, Capron et al. 2010) (Figure 5-1). These differences imply that temperature amplitudes across stadial/interstadial transitions had varied considerably.

Deuterium excess ($d=\delta D-8\delta^{18}O$), which is a proxy for temperature changes in the moisture source region, also varies greatly between stadials and interstadials, but shows a different pattern as compared to δD and $\delta^{18}O$ values. Deuterium excess values remain more or less stable throughout an interstadial, but shift abruptly at its end and start. Jouzel et al. (2007) argued that the Deuterium excess record monitors shifts in the polar front, which had a more parallel position close to the Greenland coast during interstadials, but had moved further south to a more zonal position during stadials.

Greenland ice cores thus demonstrate that climate variability during the glacial period, subsequent to the Eemian, was highly variable and alternated between colder stadials and warmer interstadials, each with its own specific signature. Compared to the terrestrial records described in the previous chapter, many more stadials and interstadials are recognized. These imply significant atmospheric reorganizations, which also involved the ocean and land areas.

5.2   North Atlantic sea surface temperature changes

Using the GRIP ice core $\delta^{18}O$ record as a template, McManus et al. (1994) could demonstrate that each Greenland interstadial corresponded to warmer sea surface temperatures (SST) in the North Atlantic and that SSTs cooled during each stadial. Comparisons between the ice rafted detritus (IRD) and planktonic foraminifera contents of North Atlantic marine records ODP 609 and V29-191 (Figure 1-2) had shown an early increase in IRD at around the MIS 5e/5d transition as far south as 50°N (McManus et al. 1994). Marked increases in IRD and distinct SST cooling events (termed C24, C21, C20) seemed to have occurred coincident with GS25, GS22, and GS20 on Greenland and implied that local glaciers and ice sheets had expanded to the coast and that debris-loaded icebergs had reached North Atlantic waters. SST cooling events C23 (correlated to GS24) and C22 (correlated to GS23), however did not coincide with IRD layers at ODP site 609 and at V29-191, although cooling of surface waters was observed (McManus et al. 1994). Subsequent to the work of McManus et al. (1994), North Atlantic SST cooling events were labelled 'C'.

The work by McManus et al. (1994) was further extended to the northern North Atlantic (for example Fronval and Jansen 1997, Rasmussen et al. 2003) and to the sub-polar North Atlantic (for example Chapman and Shackleton 1999, Shackleton et al. 2000, Sánchez Goñi et al. 2005, Oppo et al. 2006, Sánchez Goñi 2007, Salgueiro et al. 2010) and provided a larger regional and temporal context on the extent of IRD and coinciding North Atlantic SST cooling events.

At sites in the Norwegian, Iceland and Greenland Seas (Figures 1-2, 5-2), a first, but time-transgressive IRD increase was already noted during the later part of MIS 5e (Fronval and Jansen 1997). The amount of IRD was minor in these MIS 5e sediments, but suggested nevertheless that local glaciers and/or ice sheets had reached the coast and that surface conditions in the Nordic Seas had become colder. Earliest IRD occurrences were noted at c. 122 ka in the northern Greenland Sea, slightly later at c. 119 ka in the southern Iceland Sea and at c. 117 ka in the northern Iceland Sea and in the Norwegian Sea (Fronval and Jansen 1997) (Figure 5-2). A late MIS 5e SST cooling was also observed north
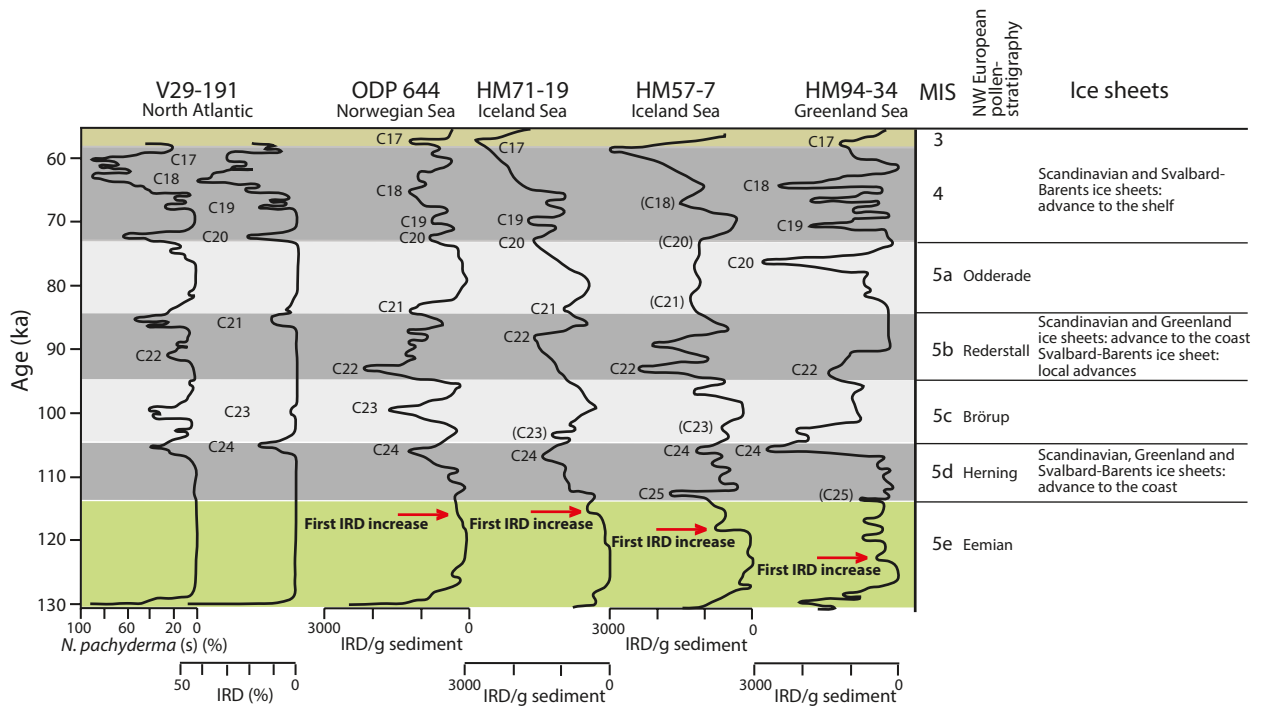
Figure 5-2. *Planktonic foraminifera (N. pachyderma s.) percentages and ice rafted debris (IRD) in marine cores from the North Atlantic, and the Norwegian, Iceland and Greenland Seas on a common time scale. Fronval and Jansen (1997) tentatively compared the IRD and sea surface cooling events (C25-C17) to the Northwest European pollenstratigraphy, and suggested possible ice advances to the coast or shelf. See Figure 1-2 for the location of the marine cores. Redrawn after Figure 11 in Fronval and Jansen (1997).*

of the Iceland-Scotland Ridge (MD95-2009) (Figure 1-2), where the dominance of *N. pachyderma* (s) (Rasmussen et al. 2003) indicated cold SSTs both during stadials and interstadials. Generally higher stadial and interstadial SSTs however seemed to have prevailed south of the Iceland–Scotland ridge (ENAM33). These temperature differences caused a distinct temperature gradient between the two regions (Rasmussen et al. 2003). At the location of ODP site 980 at around 55°N (Figure 1-2), two subsequent IRD events (C27a, b) and a decline in mean SSTs by c. 1°C were noted after the peak MIS 5e warmth (Oppo et al. 2006) (Figure 5-3). IRD events C27a and C27b have not been described from NEAP18K, a marine core located further to the west of ODP site 980 (Figure 1-2), but planktonic foraminifera δ18O values in NEAP19K nevertheless suggest a distinct cooling of surface waters during the later part of MIS 5e (Chapman and Shackleton 1999) (Figure 5-4). Also further to the south, at the location of Iberian Margin cores MD99-2331, MD95-2040 and MD95-2042 (Figure 1-2), SSTs already start to decline after the MIS 5e SST peak (Figure 5-3) (Shackleton et al. 2000, Sánchez Goñi et al. 2005, Sánchez Goñi 2007, Salgueiro et al. 2010).

Fronval and Jansen's (1997) first distinct IRD event in the northern Iceland and Greenland Seas, suggesting ice sheet expansion on Greenland, is labelled C25 and is assigned to the MIS 5e/5d transition (Figure 5-2). This transition also coincides with some IRD at the location of NEAP18K (Chapman and Shackleton 1999) and with a major cooling of summer and winter SSTs of c. 3°C at the location of ODP site 980 (Oppo et al. 2006) (Figures 5-3, 5-4). The minor SST cooling event at the MIS 5e/5d transition recognized in MD99-2331 and MD95-2042 was however assigned to C26 (Shackleton et al. 2000, Sánchez Goñi et al. 2005, Sánchez Goñi 2007, Salgueiro et al. 2010) (Figure 5-3). This discrepancy makes it unclear whether C26 in the Iberian Margin cores corresponds to Fronval and Jansen's (1997) first distinct IRD event (C25), or whether the event seen in the Iceland and Greenland Seas should be compared with the later sea surface cooling event C25. Since IRD is highly dependent on sources and transport pathways, which seem to have varied considerably between different stadials (Chapman and Shackleton 1999), the use of IRD events to align different records with each other does not seem appropriate. Independent of these labelling differences, a clear trend towards cooling of North Atlantic surface waters is observed in several records during the final part of MIS 5e. Following for example Shackleton et al. (2000), Sánchez Goñi et al. (2005), Oppo et al. (2006) and Sánchez Goñi (2007), among several others, SST cooling event C26 would define the MIS 5e/5d transition.
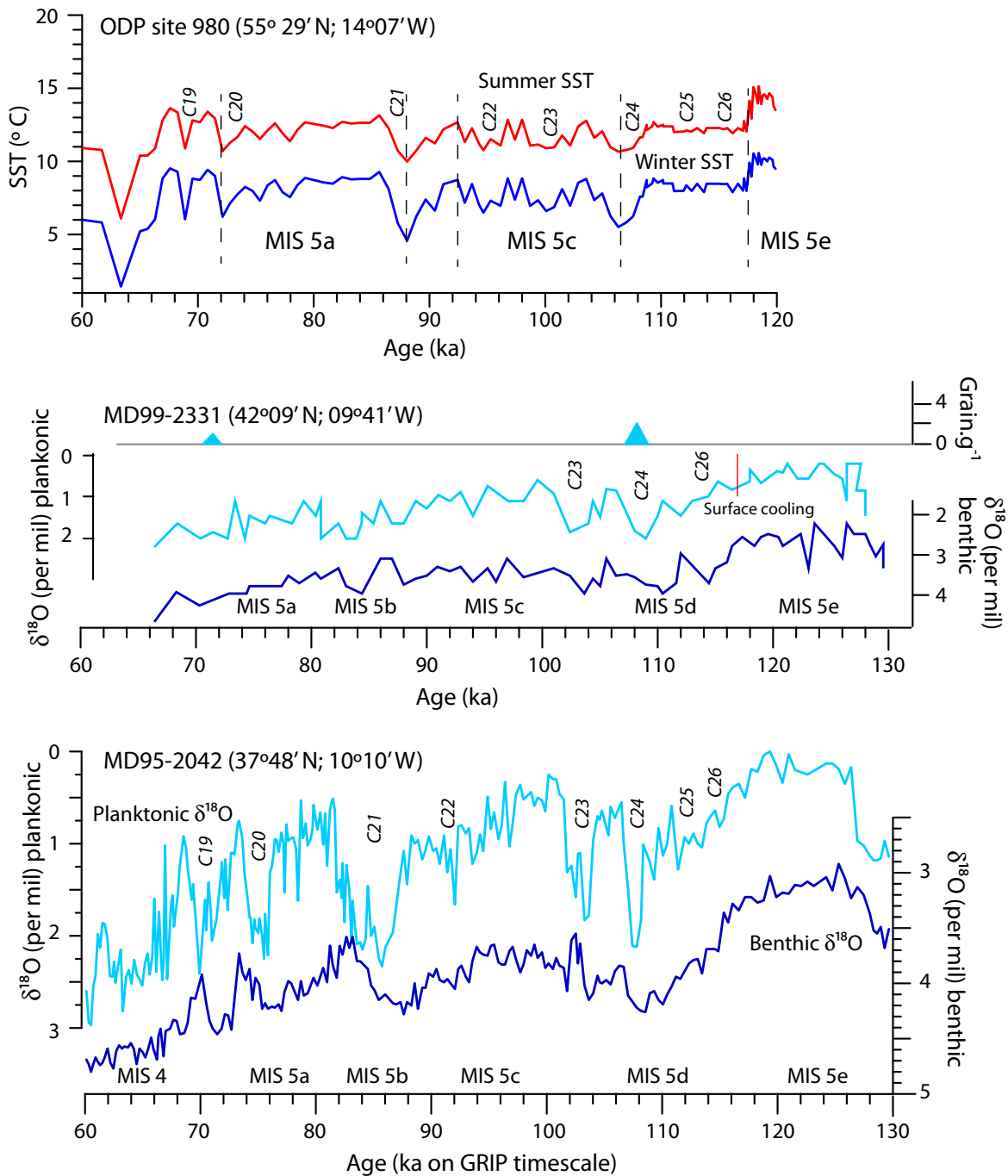
Figure 5-3. *Upper panel: North Atlantic sea surface temperature reconstructions for ODP site 980 (Oppo et al. 2006) based on planktonic foraminiferal assemblages. Original data was downloaded from ftp://ftp.ncdc.noaa.gov/pub/data/paleo/contributions_by_author/oppo2006/oppo2006.txt. Middle panel: IRD, planktonic and benthic δ¹⁸O values for Iberian Margin core MD99-2331. Modified from Figure 3 in Sánchez Goñi et al. (2005). Lower panel: Planktonic and benthic δ¹⁸O record for Iberian Margin core MD95-2042 shown on the timescale of Greenland ice core GRIP (Shackleton et al. 2000). The position of the surface-water cooling events C26 to C19 are according to Sánchez Goñi (2007). Original data for MD95-2042 was downloaded from doi:10.1594/PANGAEA.58228.*

IRD attributed to event C25 is present in core MD95-2009 north of the Iceland-Scotland Ridge, but less distinct in ENAM33 south of the Iceland–Scotland ridge (Figure 1-2) (Rasmussen et al. 2003). Minor IRD peaks are also registered at NEAP18K (Chapman and Shackleton 1999) and ODP site 980 (Oppo et al. 2006) and further cooling of surface waters is recorded in the Iberian Margin cores (Shackleton et al. 2000, Sánchez Goñi et al. 2005, Sánchez Goñi 2007) (Figures 5-3, 5-4). Rasmussen et al. (2003) had argued that the first significant cooling event south of the Iceland-Scotland ridge only occurred at the MIS 5d/5c transition. This would agree with the fairly stable SSTs recorded at the location of ODP site 980 (Oppo et al. 2006), with only a minor increase in IRD in NEAP18K (Chapman and Shackleton 1999), and with slightly cooler SSTs off the Iberian Peninsula, correspond-ing to cooling event C25 (Figures 5-3, 5-4). Subsequent to SST cooling event C25, an increase in SSTs and a decrease in IRD is seen in most North Atlantic marine records (Figure 5-3).

SST cooling event C24 is the first pronounced IRD peak in cores from the northern North Atlantic (Fronval and Jansen 1997, Rasmussen et al. 2003) (Figures 1-2, 5-2) and in cores NEAP18K, ODP 980 and MD99-2331 further to the south (Chapman and Shackleton 1999, Sánchez Goñi et al. 2005, Oppo et al. 2006) and is assigned to MIS 5d. Summer and winter SSTs decreased by 2–3°C at the location of ODP site 980 (Oppo et al. 2006) and by 6–7°C at the location of SU90-03 (Chapman and Shackleton 1999, Chapman et al. 2000) and MD95-2042 (Shackleton et al. 2000, Sánchez Goñi 2007) (Figures 1-2, 5-3, 5-4). The large amount of IRD recorded in these marine cores suggests that northern hemisphere glaciers and ice sheets had extended onto the shelf edge and that ice sheet surging had produced large amounts of icebergs. The marked decrease in SSTs indicates that this event had had a wide geographical impact.

Two sea surface cooling events (C23, C22) punctuated interstadial MIS 5c (Figure 5-3) (Sánchez Goñi et al. 2005, Oppo et al. 2006, Sánchez Goñi 2007), although Fronval and Jansen (1997), Chapman and Shackleton (1999) and Chapman et al. (2000) assign the latter event to the MIS 5c/5b transition (Figures 5-2, 5-4). IRD event C23 is pronounced in the Norwegian Sea record, but to a lesser extent in the Iceland and Greenland Sea cores (Fronval and Jansen 1997) (Figure 5-2). An increase in IRD can also be observed further to the south in NEAP18K, V29-191 and ODP 980 (McManus et al. 1994, Chapman and Shackleton 1999, Oppo et al. 2006) and coincidently SSTs decreased over a wide area (Chapman et al. 2000, Shackleton et al. 2000, Sánchez Goñi 2007) (Figures 1-2, 5-3, 5-4). Although IRD seems to have been restricted during this event, large scale cooling of surface waters did occur. SSTs increased again by a few degrees C, as shown by the records of ODP 980, MD99-2331 and MD95-2042 (Sánchez Goñi et al. 2005, Oppo et al. 2006, Sánchez Goñi 2007) subsequent to C23.

IRD and sea surface cooling event C22 is very pronounced in sediment cores from the Norwegian, Greenland and Iceland Seas, which suggested major ice advances onto the shelf in the Norwegian-Iceland Seas (Fronval and Jansen 1997). However, this event is only registered as a minor IRD increase and as a slight SST decrease of 1–2°C in marine cores further to the south (McManus et al. 1994, Chapman and Shackleton 1999, Oppo et al. 2006, Sánchez Goñi et al. 2005, Sánchez Goñi 2007). It is thus likely that Fronval and Jansen's (1997) event C22 actually corresponds to the much more severe sea-surface cooling event C21 of MIS 5b (Figures 5-2, 5-3, 5-4).

Sea surface cooling event C21 is assigned to MIS 5b (Sánchez Goñi et al. 2005, Sánchez Goñi 2007) or to the MIS 5b/5a transition (Fronval and Jansen 1997, Chapman and Shackleton 1999, Oppo et al. 2006). It is marked by less or no IRD in the Iceland, Greenland and Norwegian Sea cores (Fronval and Jansen 1997), but by a distinct increase in IRD in cores V29-191 and ODP 980 (Figure 5-3) (Chapman and Shackleton 1999, Oppo et al. 2006). Temperature reconstructions suggest a marked cooling of North Atlantic surface waters of c. 4°C at ODP site 980 (Oppo et al. 2006), of 6–7°C at site SU90-03 (Chapman and Shackleton 1999, Chapman et al. 2000) and of c. 5°C at site MD95-2042 (Sánchez Goñi 2007) (Figure 5-3). An even larger summer SST cooling of 10°C has been reported for Iberian Margin core MD95-2040 (Salgueiro et al. 2010). The regional impact of C21, as seen in several North Atlantic cores, makes it likely that this event is correlative to Fronval and Jansen's (1997) event C22, or that IRD events C22 and C21 recognized in the Norwegian, Iceland and Greenland Seas correspond to North Atlantic sea surface cooling event C22. The wide distribu-tion of IRD suggests massive surging of glaciers and ice sheets surrounding the North Atlantic.
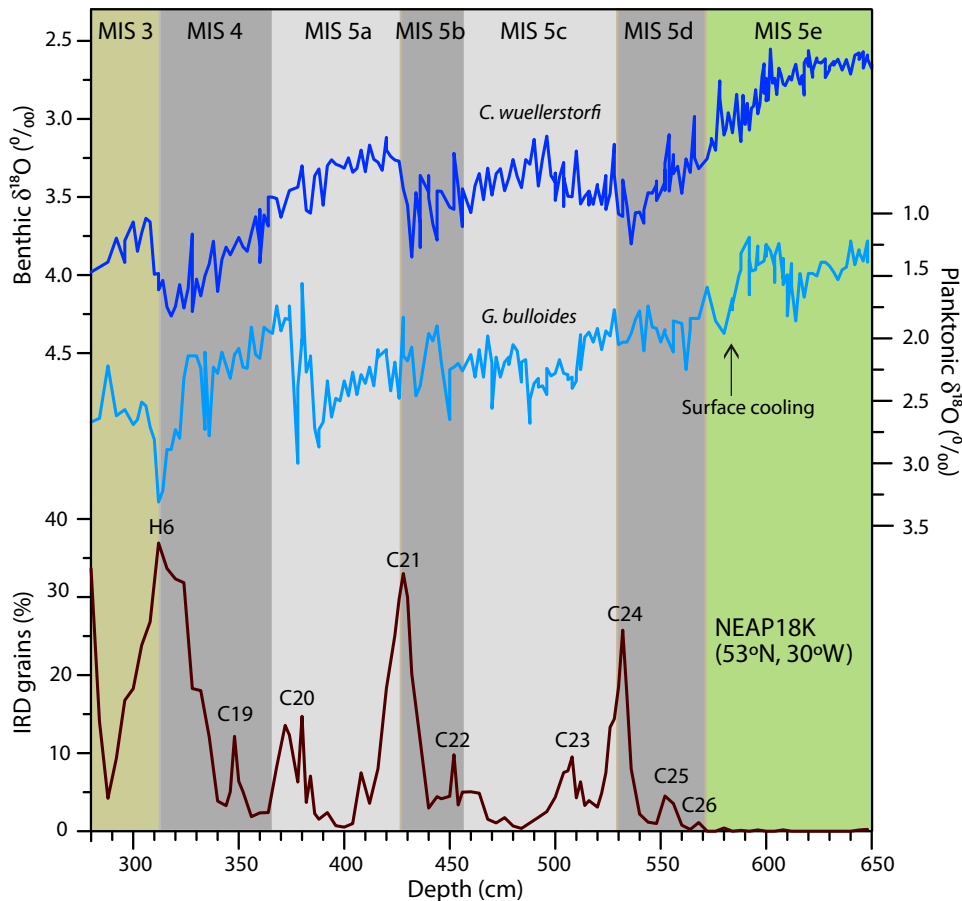
Figure 5-4. *δ¹⁸O isotope records from North Atlantic core NEAP18K measured on epibenthic Cibicidoides wullerstorfi and planktonic Globigerina bulloides and abundance of ice rafted debris (IRD) shown on a depth scale. IRD event C26, which had not been marked by Chapman and Shackleton (1999) is added here. See Figure 1-2 for the location of the site. Modified from Figure 2 in Chapman and Shackleton (1999).*

SST cooling event C20 was recognized at sites in the northern North Atlantic (Fronval and Jansen 1997) and in the sub-polar North Atlantic (McManus et al. 1994, Chapman and Shackleton 1999, Chapman et al. 2000, Oppo et al. 2006) by an increase in IRD during the end of interstadial MIS 5a (Figures 5-3, 5-4). However, no IRD increase was observed at sites SU90-03, MD99-2331 and MD95-2042 (Chapman and Shackleton 1999, Sánchez Goñi et al. 2005, Sánchez Goñi 2007), suggesting that IRD bearing icebergs did not reach as far south as 37°N. Planktonic foraminifera variations and planktonic δ¹⁸O records for SU90-03 indicate, however, that event C20 was associated with a widespread intermediate decrease in SSTs (Chapman and Shackleton 1999, Chapman et al. 2000). Similarly, distinctly lower SSTs are reconstructed for MD95-2042 (Shackleton et al. 2000, Sánchez Goñi 2007, Salgueiro et al. 2010).

Planktonic foraminifera assemblages from cores in the Norwegian, Iceland and Greenland Sea cores had suggested that large parts of the Nordic Seas were at least seasonally ice free during interstadials MIS 5c and 5a, and that interstadial SSTs in the Norwegian Sea had been relatively warm (Fronval and Jansen 1997). Relatively warm interstadial summer and winter SSTs have also been noted for ODP site 980 (Oppo et al. 2006), except during IRD/sea surface cooling events. Summer SSTs reconstructed for ODP site 980 were on average around 13°C during MIS 5c and 5a, and winter SSTs were around 8–9°C (Figure 5-3). Interstadial SSTs reconstructed for SU90-03 (Chapman et al. 2000) suggested summer temperatures of around 18–21°C during MIS 5c and 5a, and winter temperatures of around 13–15°C, while alkenone- and foraminifera-based SSTs for MD95-2042 are around 18°C (Sánchez Goñi 2007, Salgueiro et al. 2010).

All marine sequences discussed above show that SSTs had started to decrease during the later part of MIS 5e and first minor IRD increases suggest an expansion of local glaciers to the Greenland coast (Fronval and Jansen 1997). The first distinct SST cooling step is labelled C26 and is generally assigned to the MIS 5e/5d transition. Although six subsequent SST cooling events are registered in North Atlantic marine sequences, cooling events C24, C21 and C20 seem to have been the most severe, given the localized distinct increase in IRD and the marked decrease in SSTs.

5.3 Linking Greenland ice cores and North Atlantic sea surface temperature changes

Correlations between the oxygen isotope records of Greenland ice cores and marine sediments had been explored in a number of studies (for example Bond et al. 1992, 1993, McManus et al. 1994, Fronval and Jansen 1997, Rasmussen et al. 2003), but these relied on tuning/aligning records on a common time scale. Shackleton et al. (2000) attempted to circumvent this by establishing a more or less independent chronology for the marine oxygen isotope record of Iberian Margin core MD95-2042 (Figure 5-5). Although revised several times, its latest version (Shackleton et al. 2003, 2004) is based on (i) calibrated radiocarbon dates and correlations between the planktonic $\delta^{18}O$ record, which is a proxy for sea surface temperatures and sea surface salinity, to the Greenland ice core record GRIP; this provided a time scale for MIS 2 and MIS 3 back to 50 ka; (ii) comparisons of the benthic $\delta^{18}O$ record, which is a proxy for ice volume changes and as such for sea level variations, to U/Th dated corals, which in turn provides ages for sea level high and low stands; this correlation provided a time scale for MIS 5 between 83 and 140 ka; and (iii) interpolations between the two time scales to cover the gap. The time scale constructed for MD95-2042 was later transferred to Iberian Margin core MD99-2331 using the pattern of the $\delta^{18}O$ curves (Sánchez Goñi et al. 2005).
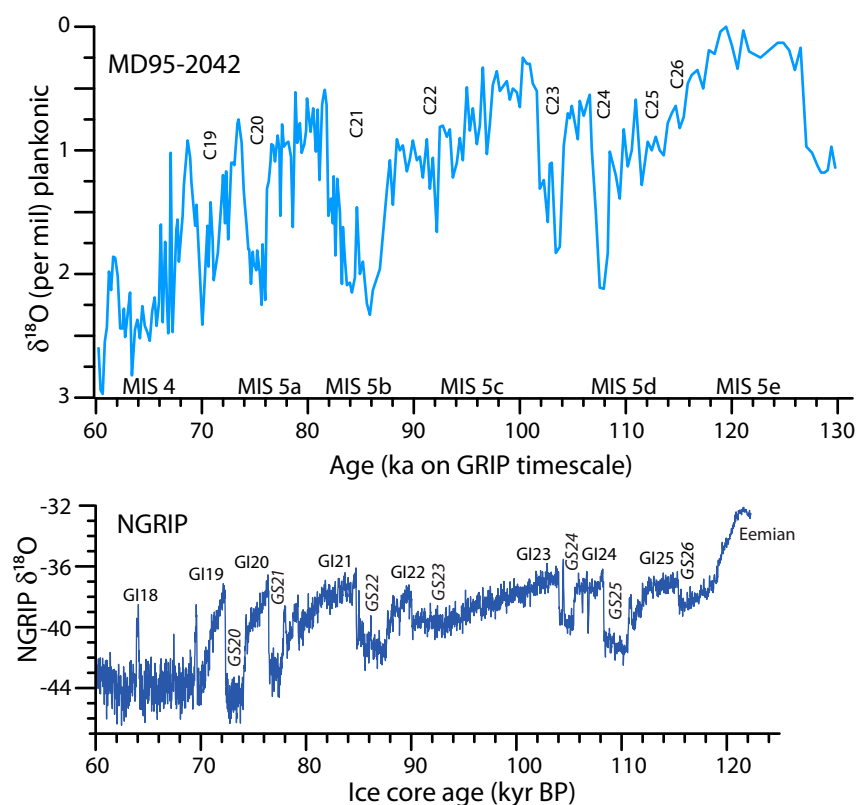
Figure 5-5. *The planktonic oxygen isotope record of core MD95-2042 from the Iberian Margin (Shackleton et al. 2000) compared to the NGRIP isotopic profile on the GICC05modelext time scale (NGRIP Members et al. 2004, Andersen et al. 2006, Svensson et al. 2008). Greenland interstadials (GI) and stadials (GS) are according to NGRIP Members (2004) and North Atlantic sea surface cooling events C26 to C19 according to Sánchez Goñi (2007). Original data for MD95-2042 was downloaded from doi:10.1594/ PANGAEA.58228 and for NGRIP from www.iceandclimate.dk/data.*

Comparisons between the planktonic $\delta^{18}O$ record of marine core MD95-2042 (Shackleton et al. 2000, Sánchez Goñi 2007) and the $\delta^{18}O$ record of the NGRIP ice core clearly show that each of the sea surface cooling events C26 to C19 corresponds to a Greenland stadial (NGRIP Members 2004) (Figure 5-5). C26, which defines the MIS 5e/5d transition in MD95-2042 (Sánchez Goñi 2007), has no clear correspondence in the ice core, but compares to an interval of gradually higher $\delta^{18}O$ values, subsequent to the Eemian, which lead into GS26. Given the good correlation between SST cooling event C24 and Greenland stadial G25, I assume here that SST cooling event C25 corresponds to GS26. SST cooling events C23, C21, C20 and C19 are paralleled by distinct cold stadials in the Greenland ice core record (GS25, GS24, GS22, GS21, GS20), while less cold SST events C25 and C22 correspond to less severe stadials in the ice (GS26, GS23) (Figure 5-5).

The Iberian Margin cores were not only analysed for marine proxies, but also proved to be an excellent recorder for vegetation changes on adjacent land areas. Pollen analyses performed on cores MD99-2331 and MD95-2042 (Shackleton et al. 2000, Sánchez Goñi et al. 2005, Sánchez Goñi 2007) show for example, that each cold event recognized in marine proxies corresponds to distinct vegetation changes on land. The excellent match between the marine response reconstructed in the Iberian Margin cores and NGRIP temperature variations, could thus be taken a step further to also include terrestrial environmental changes.

6 Terrestrial – marine correlations based on the Iberian Margin cores

The detailed pollen stratigraphic work of for example Woillard (1978), de Beaulieu and Reille (1984), Reille et al. (1998), Behre (1989) and Allen and Huntley (2000) had shown great fluctuations in pollen percentages and had thus allowed identifying several pollen sub-zones during the last inter-glacial and during the subsequent stadials and interstadials, but correlations of these to the marine record relied on the assumption of time synchroneity. Most authors thus assumed that the terrestrial Eemian corresponds to MIS 5e, and that the subsequent cold/warm stages on land are coeval with MIS 5d–MIS 5a, respectively (see for example Shackleton 1969, Mangerud et al. 1979, Woillard and Mook 1982, Behre 1989).

Accordingly, Woillard and Mook (1982) correlated the La Grande Pile (Figure 1-2) pollenstratigraphy to MIS 5e-a and also suggested a possible correlation to the North European vegetation development (Table 6-1). Similarly, de Beaulieu and Reille (1984) correlated the Les Echets pollen sequence (Figure 1-2) to the North European pollen stratigraphy on the assumption that steppe/tundra and forested intervals had occurred more or less time synchronously across Europe.

Terrestrial pollenstratigraphies and marine records (for example Larsen and Sejrup 1990, Sejrup and Larsen 1991, Fronval and Jansen 1997, Behre 1989, Allen and Huntley 2000) seemed to agree that the last glacial following the Eemian interglacial (MIS 5e) was characterized by two cold phases or stadials – MIS 5d ≈ Mélisey I/Herning and MIS 5b ≈ Mélisey II/Rederstall, and by two warmer interstadials – MIS 5c ≈ St Germain I/Brörup and MIS 5a ≈ St Germain II/Odderade (Table 6-1) and that shifts between different climate states occurred more or less synchronously on land and in the ocean (see discussion in Tzedakis 2003).

Table 6-1. Tentative correlation of cold stadials and warmer interstadials recognized in La Grande Pile with those described from Oerel in northern Germany and the marine isotope stratigraphy (MIS) according to Woillard and Mook (1982). Mélisey I and II, and Herning and Rederstall are cold stadials; St. Germain I and II, and Brörup and Odderade are interstadials. A further cold event, the Montaigu event, had been recognized in the La Grande Pile record. See Figure 1-2 and Table 1-1 for the location of the sites.

MIS	La Grande Pile, Vosges (Woillard and Mook 1982)	Oerel, northern Germany (Behre 1989)	
5a – interstadial	St Germain II	Odderade	(WE IVb)
			(WE IVa)
5b – stadial	Mélisey II	Rederstall	(WE III)
5c – interstadial	St Germain I	Brörup	(WE IIb)
			(WE IIa$_3$)
	Montaigu		(WE IIa$_2$)
	St Germain I		(WE IIa$_1$)
5d – stadial	Mélisey I	Herning	(WE I)
5e – interglacial	Eemian	Eem	(E VI–VII)

6.1   The end of the Eemian interglacial

Given the assumed synchroneity between European terrestrial and marine sequences, Tzedakis et al. (1997) had used the SPECMAP δ^{18}O chronology (Martinson et al. 1987) and glacial-interglacial transitions as tie points to obtain a time scale for long terrestrial sequences. This exercise had indicated that the forested Eemian in southern and central Europe had a length of 17 ka, extended into MIS 5d and ended around 111 ka. By tuning the La Grande Pile pollenstratigraphy to North Atlantic core V29-191 (Figure 1-2), Kukla et al. (1997) on the other hand argued for a much longer duration (23 ka) of the terrestrial Eemian and suggested that it extended until 107 ka, i.e. into MIS 5d. However, counting of annual layers in the Eemian diatomite of Bispingen in northern Germany (Figure 1-2) had estimated a length of 11 ka for the duration of the Eemian (Müller 1974), which was much shorter than that estimated by Tzedakis et al. (1997) and Kukla et al. (1997). Using the Bispingen pollen record and chronology as a template for the pollenstratigraphy of Gröbern in northern Germany (Figure 1-2), Caspers et al. (2002) and Kühl and Litt (2003) calculated an age of 115.5 ka for the end of the terrestrial Eemian in northern Europe. This meant a difference of 4.5 ka for the end of the Eemian in northern as compared to southern Europe. The astronomical time scale computed for the long pollen record from Ioannina 284 in northwest Greece (Figure 1-2) however confirmed an age of 111 ka for the decrease in temperate tree pollen percentages, which marks the end of the Eemian in southern Europe (Tzedakis et al. 2002, 2003, 2004). Obviously, the end of the terrestrial Eemian, as defined in pollen records from northern and southern Europe, did not occur at the same time.

This diachrony in respect to the end of the terrestrial Eemian in northern and southern Europe and its correlation to MIS 5e/5d became even clearer when Müller and Kukla (2004) compared a set of marine and terrestrial records. To create a common time scale for the different data sets, Müller and Kukla (2004) defined Heinrich event H11 at 128 ka and IRD event C24 at 107 ka as tie points for the marine records, and assumed that each of the two events had occurred synchronously across the North Atlantic region. The north – south correlation of IRD and cold-water planktonic foraminifera assemblages from the polar and sub-polar North Atlantic showed that SST cooling at the MIS 5e/5d transition and during MIS 5d-c did not occur synchronously. For terrestrial records, Müller and Kukla (2004) assigned an age of 126 ka to the rapid increase in tree taxa at the onset of the Eemian and correlated the post-Eemian increase in steppe pollen taxa to sea surface cooling event C24. This latter alignment assumed that reforestation at the start of the Eemian interglacial and the main abundance peak of steppe species during the first stadial had been two synchronous events across Europe (Müller and Kukla 2004). The data comparison showed that the decrease in total tree pollen percentages, which defines the end of the Eemian interglacial in terrestrial records, was diachronous and occurred several thousand years later in southern Europe as compared to northern and central Europe. The decline in tree pollen percentages was observed at 115 ka in northern Germany (Bispingen, Gröbern), coincident with SST cooling event C26, while tree pollen percentages only declined at around 108–110 ka in central (e.g. Füramoos, Samerberg, Les Echets) and southern Europe (Iberian Peninsula, Greece) coincident with SST cooling event C25 (Müller and Kukla 2004), i.e. during MIS 5d.

Further evidence for diachrony in respect to the end of the terrestrial Eemian and MIS 5e/5d came from the multi-proxy record of Iberian Margin core MD95-2042 (Figure 1-2). The sediments, which had been analysed for benthic and planktonic δ^{18}O, SSTs and terrestrial pollen (Sánchez Goñi et al. 1999, Shackleton et al. 2002, 2003), provided for the first time unequivocal evidence that the terrestrial Eemian on the Iberian Peninsula ended at 110 ka, i.e. 5 ka later than the MIS 5e/5d transition seen in marine proxies off the Iberian Margin (Figure 6-1). As seen in the MD95-2042 record, the rise in steppic pollen percentages, the drop in Eurosiberian tree pollen values and the disappearance of Mediterranean pollen, occurred shortly before high positive benthic δ^{18}O values signal the growth of large ice sheets (Shackleton et al. 2002) and prior to SST cooling event C24 (Figure 6-1).

An age of 110 ka for the end of the terrestrial Eemian in southern Europe was recently confirmed by the independent chronology for Lago Grande di Monticchio in southern Italy (Figure 1-2). Varve counting, tephra layers, and ^{40}Ar/^{39}Ar ages of tephras (Brauer et al. 2007) provided an age of 109.50 varve years for the transition from cool mixed forest biomes to wooded steppe biomes, which defines the end of the last interglacial in southern Italy (Allen and Huntley 2009).
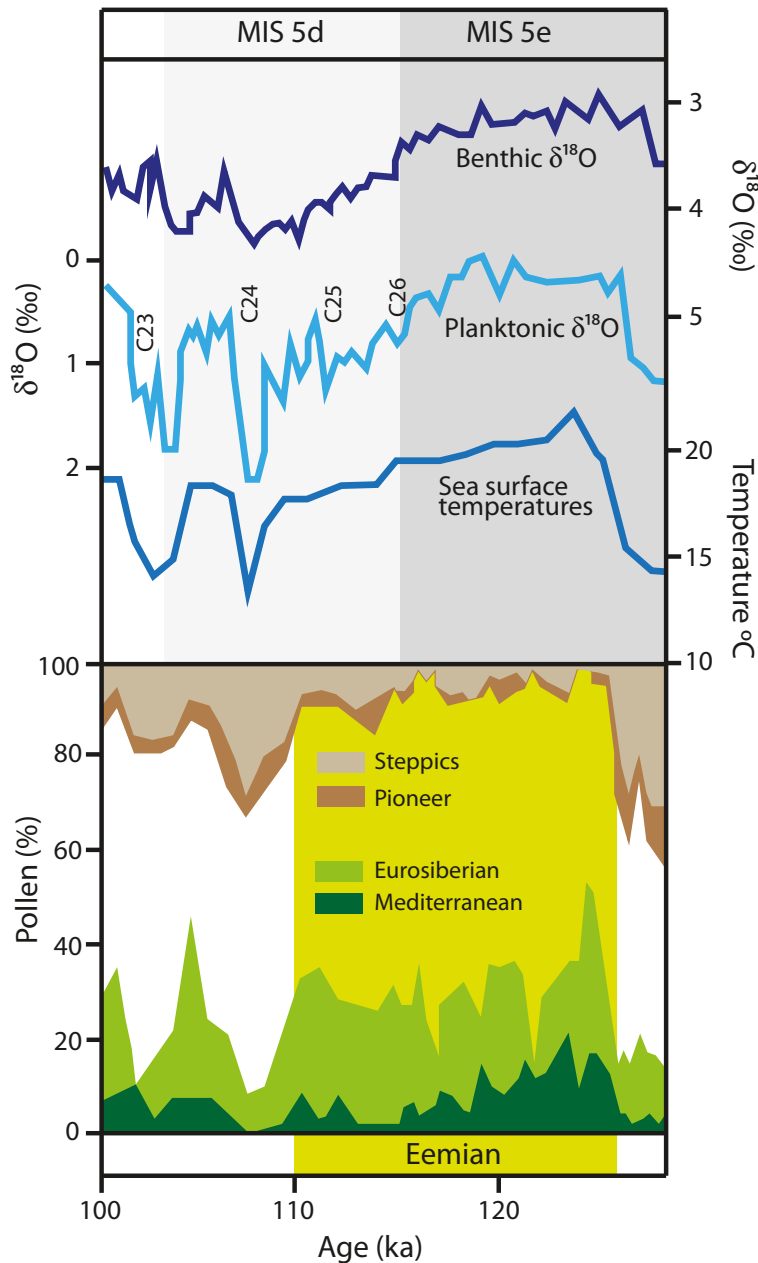
Figure 6-1. *Marine and terrestrial records in Iberian Margin core MD95-2042 for parts of MIS 5e and for MIS 5d. Sea surface temperature cooling event C26 defines the MIS 5e/5d transition. The marked increase in steppic pollen percentages, on the other hand, marks the end of the terrestrial Eemian on the Iberian Peninsula. The comparison of different proxies analysed in the same sediment core shows that the terrestrial Eemian extended into MIS 5d and ended around 110 ka. Modified after Figure 2 in Shackleton et al. (2003).*

Tuning of the pollen record of Füramoos in southern Germany to the Iberian Margin core MD95-2042, and subsequent interpolations between Füramoos and Gröbern in northern Germany (Figures 1-2, 6-2) further supported an early decline of the Eemian woodlands in the north (Müller and Kukla 2004, Müller and Sánchez Goñi 2007). The time difference between the end of the Eemian in northern (115 ka) and southern Germany (110 ka) thus amounted to approximately 5 ka.

Figure 6-2. *Correlation of last interglacial records from northern and southern Germany. Tie point (1) is placed at the beginning of the Eemian at 126 ka; tie point (2) at the peak abundance of non-arboreal taxa during the first Weichselian stadial at 107 ka. Green curve = Pinus pollen %; black curve = total tree pollen %; red curve = total thermophilous taxa Redrawn after Figure 19.4 in Müller and Sánchez Goñi (2007).*
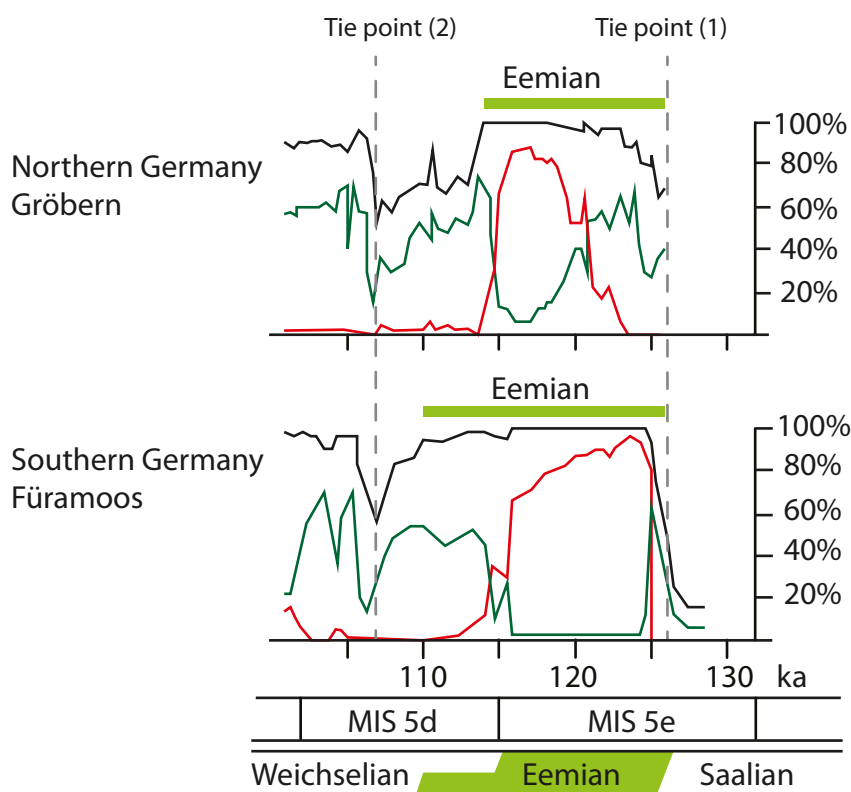
6.2   Stadials and interstadials

Subsequent work on cores MD99-2331 and MD95-2042 (Figure 1-2) showed that glacial vegetation changes on the Iberian Peninsula compare well with SST changes (Sánchez Goñi et al. 2005, Sánchez Goñi 2007). Each cold stadial on land was found to correlate to a SST cooling event in the marine records and each interstadial to warmer SSTs (Figure 6-3). The pollen records thus suggested much higher frequency changes in vegetation cover and a more or less rapid response of the vegetation to SST changes.

The pollen assemblages in the two sequences moreover showed clear differences regarding the type of vegetation, and regarding vegetation shifts and responses both during different stadials and interstadials. These differences reflect the location of the coring sites in respect to the Iberian Peninsula (MD99-2331 at 42°N and MD95-2042 at 37°N) and implied that the response of the vegetation to colder and warmer events was markedly different even within a comparably constrained region (Sánchez Goñi et al. 2005).

The pollen assemblages of MD99-2331 and MD95-2042 show a close correspondence (Sánchez Goñi et al. 2005) to those described for the last interglacial and glacial in France (Woillard 1978, de Beaulieu and Reille 1984, 1992a, b, Reille and de Beaulieu 1990). This good correspondence allows transferring the vegetation zonation, which had been established in France, to the Iberian Margin record (Figure 6-3) (Sánchez Goñi et al. 2005).

SST cooling events C26 and C25 are not very distinct in the Iberian pollen record, although MD99-2331 shows a slight increase in steppic plants and MD95-2042 an increase in semi-desert plants (Figure 6-3), suggesting slightly drier conditions and only a minor opening of the forests. The first major cooling event, Mélisey I, which occurred synchronously with SST cooling event C24, however led to marked vegetation changes on the Iberian Peninsula. Steppic and semi-arid plants increased, and temperate and humid tree taxa decreased. Similar changes are observed
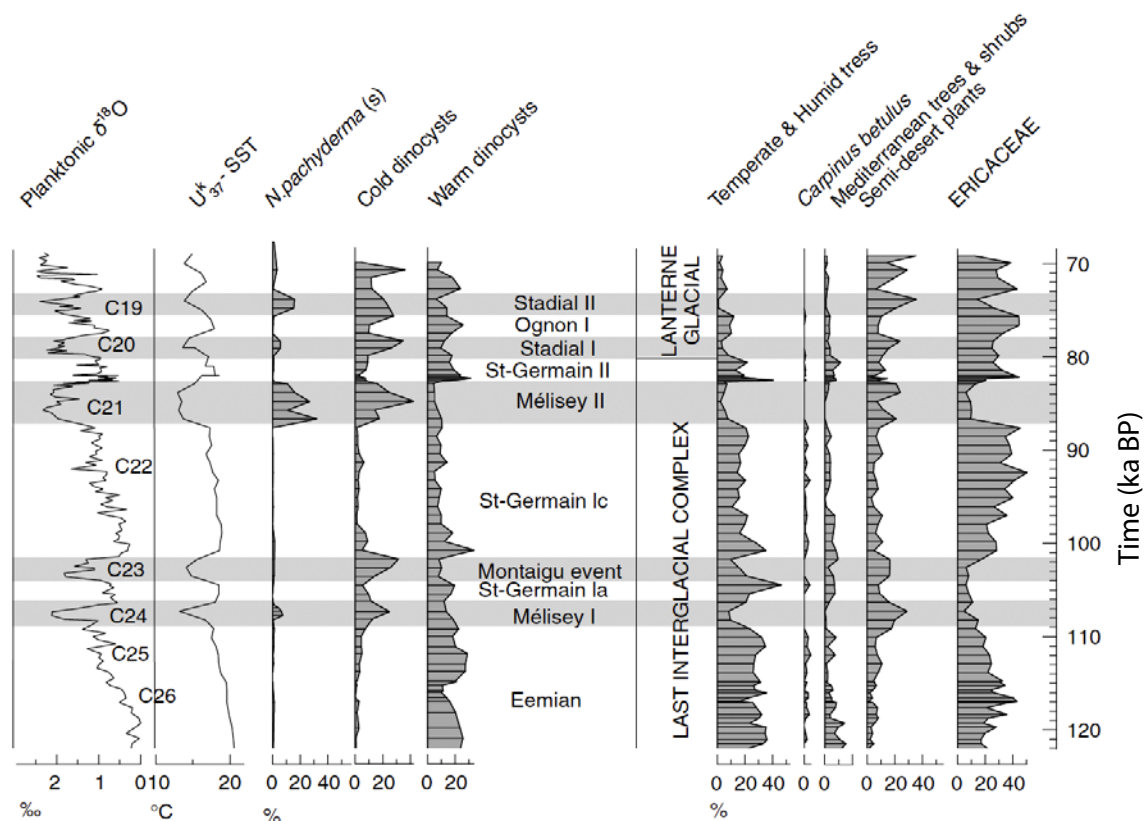
Figure 6-3. *Comparison of marine and terrestrial proxies in core MD95-2042 from the Iberian Margin between 70 and 120 kyr BP. The planktonic oxygen isotope curve reflects sea surface temperature and salinity changes. U^k_{37} is a proxy for sea surface temperature; the polar foraminifera Neogloboquadrina pachyderma (s) and cold dinocysts are proxies for incursions of cold surface waters. The marine proxies are compared to stadial and interstadial vegetation changes on the Iberian Peninsula. Modified from Sánchez Goñi (2007).*

for the Montaigu event (correlated to C23) and for Mélisey II (correlated to C21), whereas SST cooling event C22 did not seem to have had a major effect on the Iberian vegetation. Interstadials St. Germain Ia, b and St. Germain II were characterised by a re-expansion of temperate and humid trees and Mediterranean trees and shrubs (Figure 6-3).

The comparison between the planktonic oxygen isotope record of MD95-2042 and the NGRIP oxygen isotope record had shown a good correspondence between the timing of ice core stadials and marine SST cooling events (Figure 5-5) (NGRIP Members 2004, Sánchez Goñi 2007). Adding the pollen record of MD95-2042 moreover allowed for detailed correlations between vegetation changes on the Iberian Peninsula and the Greenland ice core record (Figure 6-4, Table 6-2).

Correlations between the terrestrial record of MD95-2042 and the astronomically tuned pollen record of Ioannina 284 in Greece (Figure 1-2) (Tzedakis et al. 2004, Tzedakis 2005) had suggested that the end of the Eemian and the timing of post-Eemian stadials and interstadials was more or less time synchronous across southern Europe (Figure 6-5). This assumption may however not be entirely correct, given that the independently dated multi-proxy record of Lago Grande di Monticchio in Italy (Figure 1-2) (Brauer et al. 2007, Allen and Huntley 2000, 2009), provided slightly different age estimates for some of the stadials and interstadials (Table 6-2).

Age estimates for the start/end of most of the stadials and interstadials in the Greenland NGRIP ice core and in Iberian Margin core MD95-2042 agree well with each other and show age differences of less than 1 ka (Table 6-2). Exceptions are the end of GI 24/St Germain Ia with a difference of 2 ka and the end of GS 24/Montaigu event with a difference of 2.5 ka.
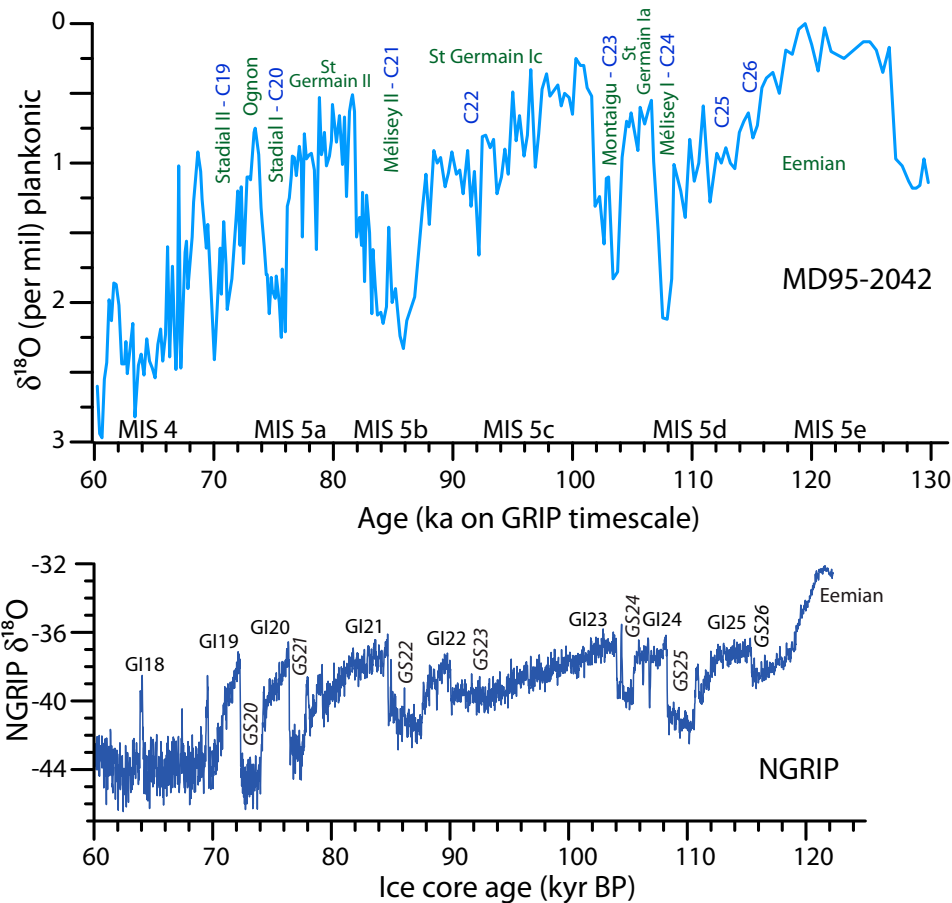
Figure 6-4. *The NGRIP δ¹⁸O record (NGRIP Members 2004) on the GICC05modelext time scale compared to marine core MD95-2042 (Sánchez Goñi 2007). The North Atlantic sea surface cooling events (C26 to C19) (marked in blue colour) and the terrestrial vegetation zones (shown in green colour) follow Sánchez Goñi (2007). The correlation between the marine and terrestrial events and the NGRIP record was inferred from Figure 13.1 in Sánchez Goñi (2007). GS = Greenland stadials; GI = Greenland interstadials. Original data for MD95-2042 was downloaded from doi:10.1594/PANGAEA.58228 and for NGRIP from www.iceandclimate.dk/data.*
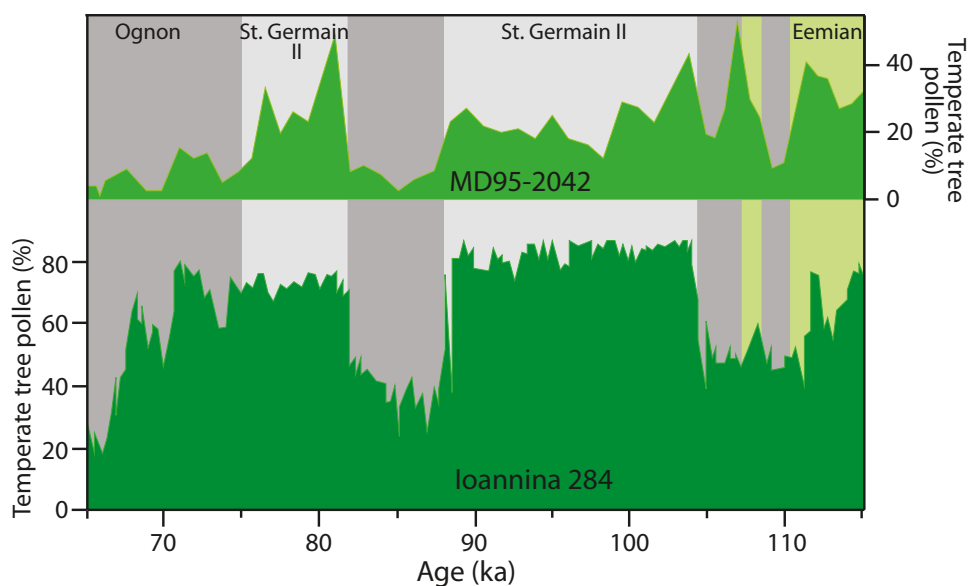
Figure 6-5. *Temperate tree pollen percentages from Ioannina 284 in Greece (lower panel) compared to those of core MD95-2042 from the Iberian Margin (upper panel). Cold stadials are shown in dark grey and warm interstadials in light grey. Redrawn after Figure 5 in Tzedakis (2005).*

Table 6-2. Comparison of stadial and interstadial ages in the NGRIP ice core (NGRIP Members 2004) and in MD95-2042 on the Iberian Margin (Sánchez Goñi et al. 2005, Sánchez Goñi 2007, Sánchez-Goñi M F, personal communication). C = North Atlantic sea-surface cooling event; GS = Greenland stadial; GI = Greenland interstadial.

NGRIP		MD95-2042	
End of GS20	72.5 ka	End of Stadial II (C19)	73 ka
End of GI20	74 ka	End of Ognon I	74 ka
End of GS21	77 ka	End of Stadial I (C20)	76 ka
End of GI 21	78 ka	End of St Germain II	78 ka
End of GS22	85 ka	End of Mélisey II (C21)	82.5 ka
End of GI 23/22	88 ka	End of St Germain Ic	87 ka
End of GS24	104 ka	End of Montaigu event (C23)	101.5 ka
End of GI24	106 ka	End of St Germain Ia	104 ka
End of GS25	108.5 ka	End of Mélisey I (C24)	107 ka
End of GI25	111 ka	End of Eemian	109.7 ka

The fairly good correspondence between stadial and interstadial ages reported for NGRIP and MD95-2042 have made the Iberian Margin core a useful tuning target. Müller and Sánchez Goñi (2007) for example tuned the pollen records of Füramoos and Samerberg in southern Germany (Figure 1-2) to the age model of MD95-2042, assuming synchronicity between major climatic events. This exercise provided a tentative chronological framework for the vegetation development during MIS 5 in central Europe.

7 Speleothem records

Speleothems are, apart from the Greenland ice core records and Lago Grande di Monticchio, the only archives with a completely independent chronology. During the last few years a number of speleothem records have been investigated in Italy (Drysdale et al. 2005, 2007), in the Swiss and Austrian Alps (Spötl and Mangini 2006, Meyer et al. 2008, Boch et al. 2011), in Turkey (Fleitmann et al. 2009, Badertscher et al. 2011), and in Israel (Bar-Matthews et al. 2000, 2003, Grant et al. 2012) (Table 1-1, Figure 1-2). Their $\delta^{18}O$ and $\delta^{13}C$ records, which show rapid shifts comparable to those reconstructed in ice cores, have been precisely dated using U/Th series and thus provide independent terrestrial timescales for the climatic changes during the last interglacial and glacial.

The NALPS data set combines speleothems from several caves in the northern Alps (Beatus cave, Baschg cave, Klaus-Cramer cave, Schneckenloch cave) (Boch et al. 2011) and displays rapid and large shifts in $\delta^{18}O$ values. Since the oxygen isotopic composition of regional meteoric precipitation in the Alps is strongly connected to temperature, high $\delta^{18}O$ values correspond to warm climatic conditions, and low $\delta^{18}O$ values to cold climates. The rapid and large shifts in $\delta^{18}O$ values seen in the NALPS data set occurred within decades to centuries and strongly resemble Greenland GS and GI (Figure 7-1). NALPS moreover shows several short-lived climate shifts within cold Greenland stadials and warm interstadials, similar to those that had been noted by Capron et al. (2010). Slight differences between the NALPS and NGRIP time scales (Figure 7-1) suggest that the new U/Th ages might help adjusting the ages for Greenland stadials and interstadials (Boch et al. 2011). The last interglacial/glacial transition is not clearly recorded in the NALPS data set, but seen in the speleothem from Entriche Kirche cave in Austria, which grew continuously between 127 and 114 ka (Meyer et al. 2008). This speleothem demonstrates an abrupt drop in $\delta^{18}O$ values at 118–119 ka, synchronous with SST cooling event C26. The rapid shift in $\delta^{18}O$ values may be explained by enhanced seasonality at the end of the last interglacial. Cold winters, relatively warm summers and a vegetated and stable catchment as indicated by the $\delta^{18}O$ and $\delta^{13}C$ data sets, seemed to have prevailed until a growth hiatus at 114 ka (Meyer et al. 2008). Another Austrian speleothem, the Inntal flowstones cover the time interval between 101 and 70 ka. They show several growth phases and hiatuses, which seem to correlate in time to warmer and colder events, respectively registered in the NGRIP ice core (Spötl and Mangini 2006).

Shorter records derived from the speleothems from Antro del Corchia in Italy (Drysdale et al. 2007) show for example two events with distinctly higher $\delta^{18}O$ values and lower speleothem growth rates at 112–109 ka and 105–103 ka (Figure 7-1). Higher $\delta^{18}O$ values and lower growth rates suggest that less moisture was evaporated from a cooler North Atlantic. These latter arguments and the timing of the two distinct speleothem events led Drysdale et al. (2007) to argue that they are time equivalent to SST cooling events C24 and C25, and to Greenland stadials GS 25 and 24 (Figure 7-1).

The $\delta^{18}O$ and $\delta^{13}C$ records of Soreq and Peqiin caves in Israel are excellent recorders for climatic shifts in the Eastern Mediterranean region. The location of Soreq cave in central Israel and of Peqiin cave in the northern part of the country is reflected in the slight difference in $\delta^{18}O$ values, which are generally lower for Peqiin cave (Figure 7-1) (Bar-Matthews et al. 1997, 1999, 2000, 2003). Both records however depict clear shifts between higher and lower $\delta^{18}O$ values, which are more or less in concert with each other. Bar-Matthews et al. (2000, 2003) interpret lower $\delta^{18}O$ values as reflecting high rainfall in the region, and higher $\delta^{18}O$ values as a proxy for lower rainfall and drier conditions. Intervals with distinctly lower $\delta^{18}O$ values in Soreq cave (event V, 124–119 ka with a main peak at 122 ka; event IV, 108–100 ka with peaks at 107 and 102 ka; event III, 85–79 ka with a peak at 80 ka) thus indicate intervals with high rainfall (Figure 7-1) and compare to the interglacial and interstadials recognized in NGRIP. Higher $\delta^{18}O$ values on the other hand correspond to stadials, during which conditions were dry in the Eastern Mediterranean region (Bar-Matthews et al. 2000, 2003). The Soreq cave $\delta^{18}O$ record moreover displays a number of high-frequency variations, which seem to broadly match the NGRIP $\delta^{18}O$ record.
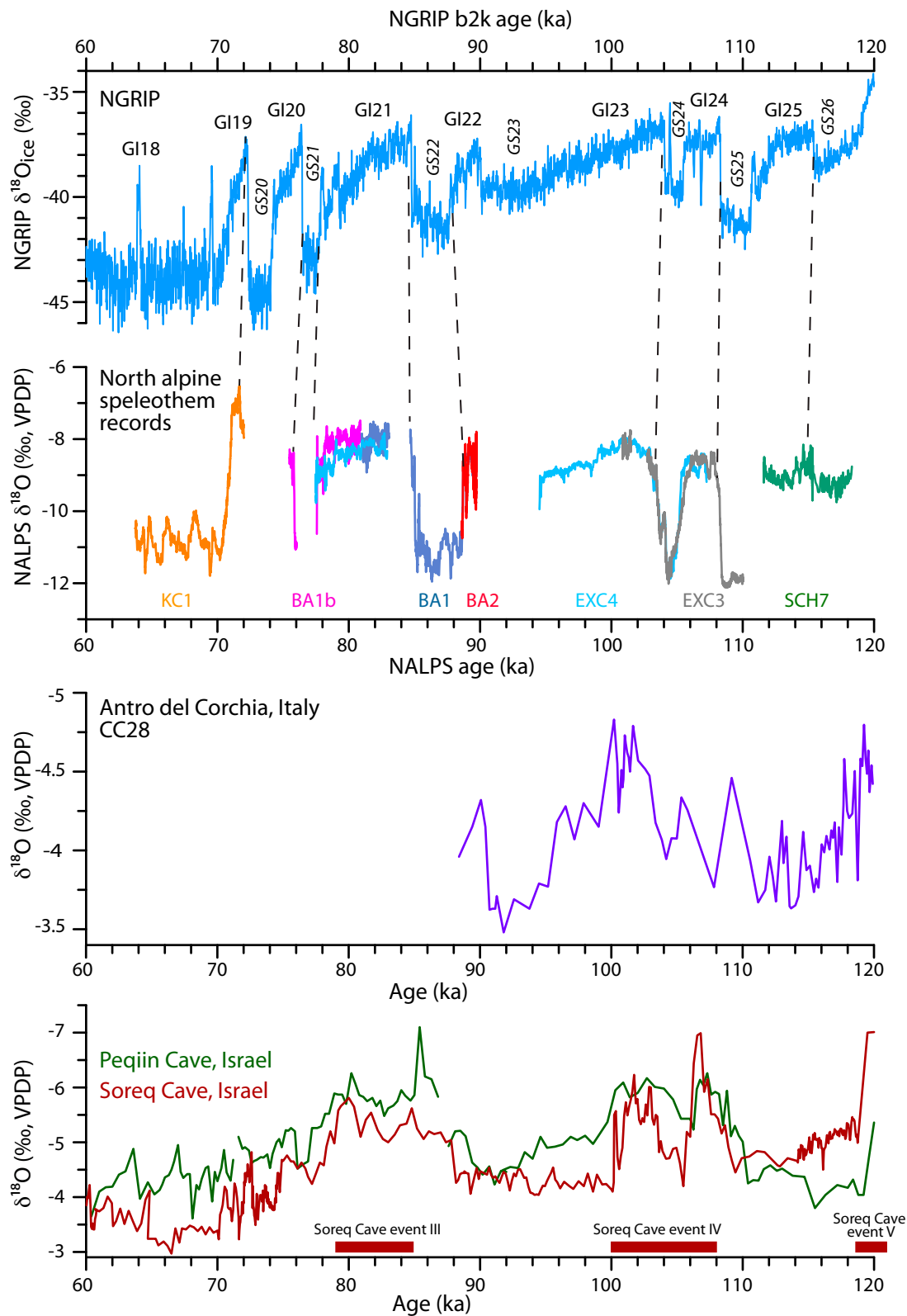
Figure 7-1. *Upper panel: δ¹⁸O values of speleothem records from the northern Alps (NALPS data set) (Boch et al. 2011) compared to the NGRIP δ¹⁸O record. The correlation between NALPS and NGRIP is based on Figure 2 in Boch et al. (2011). KC = Klaus Cramer Cave; BA = Baschg Cave, SCH = Schneckenloch Cave, EXC = Beatus Cave. Middle panel: δ¹⁸O values of the Antro del Corchia speleothems, Italy (Drysdale et al. 2005, 2007). Lower panel: δ¹⁸O values of Peqiin and Soreq caves in Israel (Bar-Matthews et al. 1997, 1999, 2003). Each speleothem record is shown on its own time scale. Original speleothem data was downloaded from ftp://ftp.ncdc.noaa.gov/pub/data/paleo/speleothem/ and ice core data from www.iceandclimate.dk/data.*

8 Chronology of MIS 5d-a and duration of MIS 5 interstadials and stadials

Only few records covering all or parts of MIS 5 can be regarded as being entirely based on their own independent chronology:

* Greenland ice core NGRIP (NGRIP Members 2004), for which the chronology was established by annual layer counting back to 60 ka and by using an ice flow model (ss09sea time scale) as far back as 123 ka (Svensson et al. 2008). NGRIP δ^{18}O values are proxies for the evaporation and atmospheric transport of air masses, as well as for site-specific temperature changes and allow monitoring shifts between warmer (interstadial) and colder (stadial) conditions.

  The start/end of stadials and interstadials are defined at the midpoint of the transition between a rapid shift from low to high or high to low δ^{18}O values. However over the course of a Greenland interstadial δ^{18}O values show different patterns: values remain stable for some time and then decline gradually (GI25); values decline gradually soon after the peak warming is attained (e.g. GI23, GI21); or values decline fairly rapidly (e.g. GI20, GI19) before the final abrupt drop to stadial values. Moreover, a number of interstadials show internal variability, such as a cold spike within GI24, or a return to warmer conditions before the final drop into stadial values (GI25, GI21) (Figure 8-1). The definition of when an interstadial ends thus depends on the pattern of the δ^{18}O curve and is a combination of an atmospheric and of a local signal.

* Speleothem data sets from the Alps, Italy and Israel (for example Drysdale et al. 2005, 2007, Bar-Matthews et al. 2000, 2003, Spötl and Mangini 2006, Meyer et al. 2008, Boch et al. 2011), were dated using high-resolution U/Th measurements. However, only the speleothem records from Peqiin and Soreq caves constitute continuous records. Those from Antro del Corchi only cover the time interval 120–88 ka, and those of the NALPS data set have a number of gaps (Figure 7-1).

  Speleothem δ^{18}O values in Italy and in the Alps monitor, similar to ice core δ^{18}O values, the atmospheric transport of colder/warmer air masses from a colder/warmer North Atlantic. More negative δ^{18}O values translate into colder temperatures and less negative values into warmer temperatures. In contrast, speleothem δ^{18}O values from caves in Israel are a proxy for precipitation changes, with higher negative values indicating higher precipitation and less negative values indicating lower precipitation. The most precisely dated speleothem data set is probably the NALPS data series, although the record is discontinuous (Figure 7-1), especially regarding the end of several interstadials. The timing of cold stadials and warm interstadials compares however excellently to the Greenland ice core δ^{18}O record, and shows that the phasing of cold/warm intervals occurred with little or possibly no time lag.

* The varved lake sediment sequence from Lago Grande di Monticchio in Italy (Allen and Huntley 2000, 2009, Brauer et al. 2007) is based on varve counting, tephra layers, and ^{40}Ar/^{39}Ar ages on tephra (Brauer et al. 2007, Wulf et al. 2012). The original chronology for this long sequence was recently revised and the new chronology (Brauer et al. 2007) is slightly different from that published by Allen and Huntley (2000). In Allen and Huntley (2000), pollen zones 19a, b were assigned to the St. Germain I interstadial, pollen zone 18 to the Mélisey II stadial, and pollen zones 17e, d, c to the St. Germain II interstadial. Brauer et al. (2007) also attributed pollen zone 18 to Mélisey II (and correlated it to MIS 5b), but only pollen zone 17e was assigned to St. Germain II (correlated to MIS 5b/5a). In contrast to Allen and Huntley (2000), pollen zones 17d-a were assigned to the short stadials/interstadials, which follow after the St. Germain II interstadial and correlated to MIS 5a. Brauer et al. (2007) also suggested that the end of the St. Germain II interstadial (pollen zone 17e) would coincide with a transition to glacial conditions. This, and the different assignments of the Monticchio pollen zones are confusing and would imply that the last interstadial (St. Germain II) ended during the middle part of MIS 5a. It is however likely that the short stadial (pollen zone 17d) seen in the Monticchio record after St. Germain II (pollen zone 17e) is correlative to stadial 1 in Iberian Margin core MD95-4042, that the short peak in mesic woody taxa in Monticchio (pollen zone 17c) correlates to the Ognon interstadial and the marked drop in mesic woody taxa (pollen zone 17b) to stadial 2 (Table 8-1).

  In terrestrial pollen records the shift between stadial and interstadial conditions is defined by changes in pollen assemblages, which is in contrast to ice cores and speleothems, where an atmospheric signal determines the end/start of stadials/interstadials.

The chronology for marine sediment core MD95-2042 cannot really be regarded as independent, since it was constructed using a number of assumptions and tie points: calibrated radiocarbon dates and correlations between planktonic foraminifera $\delta^{18}O$ values and the Greenland ice core record back to 50 ka; comparisons of the benthic $\delta^{18}O$ record to U/Th dated corals between 83 and 140 ka; interpolations between the two time scales to cover the gap (Shackleton et al. 2003, 2004). However, the multi-proxy record of MD95-2042, which combines deep-water and surface water signals with shifts in terrestrial vegetation, allows for a direct comparison between changes in marine and land proxies (Sánchez Goñi et al. 2005, Sánchez Goñi 2007). As such, leads and lags between the marine signal and the vegetation response can be evaluated.

The pollen records of the ancient lakes of Ioannina 284 (Tzedakis et al. 2002, 2003, 2004) and Tenaghi Philippon in Greece (Tzedakis et al. 2006) have also been described as independent chronologies, but since both are tuned to the astronomical time scale this is only partly true. Since changes in vegetation are a combined response to climate, soil conditions, and distance to refugias, among several other factors, the definition of when an interstadial starts or ends does not have to coincide with the atmospheric signal in the ice cores.

For a few other terrestrial records, such as for example the new long sequence from Tenaghi Philippon (TP-2005) in northern Greece (Müller et al. 2011) and Sokli in northern Finland (Alexanderson et al. 2008, Helmens et al. 2012) (Figure 1-2), U/Th and/or TL/OSL and IRSL dating of the sediments have provided some independent age points, which allow a general attribution to interstadials and stadials.

The fairly good correspondence between the ages of major stadials and interstadials determined in the NGRIP ice core (NGRIP Members 2004), in marine core MD95-2042 (Sánchez Goñi et al. 2005, Sánchez Goñi 2007) and in the NALPS speleothem records (Boch et al. 2011) (Table 8-1) justifies transferring these chronologies to the vegetation zones recorded from other sites in southern and central Europe. Such an approach allowed Müller and Sánchez Goñi (2007) to discuss differences in the timing of tree immigration and forest establishment between central and southern Europe. Müller and Sánchez Goñi (2007) showed for example that reforestation north of the Alps, at the start of St. Germain I and II, was delayed as compared to southern Europe, due to plant migration lags from more distant refugia.

Although age estimates for the end of the Eemian interglacial and for the end of the Mélisey I stadial are comparable between Lago Grande di Monticchio (Brauer et al. 2000, 2007, Allen and Huntley 2009), MD95-2042 and the NALPS data set (Boch et al. 2011), large differences exist in respect to other stadial/interstadial/stadial transitions (Table 8-1). The end of the St. Germain II interstadial is for example dated to 83 ka in Lago Grande di Monticchio, but to 78 ka in NGRIP, MD-95-2052 and NALPS. Whether these differences relate to uncertainties in the respective chronologies and/or to the definition of the pollen zones and their attribution to the stratigraphic scheme is not possible to decide.

Table 8-1. Comparison of stadial and interstadial ages in the NGRIP ice core (NGRIP Members 2004), MD95-2042 on the Iberian Margin (Sánchez Goñi et al. 2005, Sánchez Goñi 2007, Sánchez-Goñi M F, personal communication), Lago Grande di Monticchio in southern Italy (Brauer et al. 2000, 2007, Allen and Huntley 2009) and the NALPS data set (Boch et al. 2011). GS = Greenland stadial; GI = Greenland interstadial; C = North Atlantic sea surface temperature cooling event; LI Last interglacial, PZ = pollen zone. The marine isotope stages (MIS) as recognized in MD95-2042 are shown for comparison.

NGRIP		MD95-2042		LG di Monticchio		NALPS
End GS20	72.5 ka	End Stadial 2 – C19	73 ka	End PZ 17b	78 ka?	72 ka
End GI 20	74 ka	End Ognon I	74 ka	End PZ 17c	80 ka?	–
--------------------------------		*MIS4/5a transition*	------------			
End GS 21	77 ka	End Stadial 1 – C20	76 ka	End PZ17d	82 ka?	75.8 ka
End GI 21	78 ka	End St Germain II	78 ka	End SG 2/PZ 17e	82.73 ka	77.6 ka
--------------------------------		MIS5/5b transition	------------			
End GS 22	85 ka	End Mélisey II – C21	82.5 ka	End Mélisey 2	87.98 ka	85 ka
--------------------------------		MIS5b/5c transition	-------------			
End GI 23/22	88 ka	End St Germain Ic	87 ka	End St. Germain 1	90.65 ka	88.7 ka
End GS 24	104 ka	End Montaigu – C23	101.5 ka	End Montaigu	102.78 ka	103.5 ka
End GI 24	106 ka	End St Germain Ia	104 ka			105 ka
--------------------------------		MIS5c/5d transition	------------			
End GS 25	108.5 ka	End Mélisey I – C24	107 ka	End Mélisey 1	107.60 ka	108.3 ka
End GI 25	111 ka	End Eemian	109.7 ka	End LI	109.50 ka	
GS26	116.5 ka	C26/C25				
--------------------------------		MIS5d/5e transition	------------			

In contrast to southern Europe and to the alpine foreland, the chronology of environmental changes for sites in northern Europe (with the exception of Sokli) still remains uncertain and needs to be based on tuning of vegetation changes to independently dated archives. Kühl et al. (2007) for example tuned the pollen record of Gröbern in northern Germany (Figure 1-2) to the NGRIP chronology to obtain age estimates for the duration of stadial and interstadial vegetation changes. Since the end of the Eemian, Herning, Brörup, and Rederstall, respectively as defined by the pollenzones, was used as tie points to the NGRIP chronology, age estimates for these boundaries are basically the same as in NGRIP. Nevertheless, this exercise suggested that the length of north European interstadials was likely much shorter than their corresponding intervals in southern and central Europe (Table 8-2, Figure 8-1).

Table 8-2. Comparison of stadial and interstadial ages in Iberian Margin core MD95-2042 (Sánchez Goñi et al. 2005, Sánchez Goñi 2007, Sánchez-Goñi M F, personal communication), Lago Grande di Monticchio in southern Italy (Brauer et al. 2000, 2007, Allen and Huntley 2009) and Gröbern in northern Germany (Kühl et al. 2007). LI = Last interglacial, PZ = pollen zone.

MD95-2042		LG di Monticchio		NALPS	Gröbern	
End Stadial 2	73 ka	End PZ 17b	78 ka?	72–73 ka		
End Ognon	74 ka	End PZ 17c	80 ka?	–		
End Stadial 1	76 ka	End PZ17d	82 ka?	76 ka		
End St Germain II	78 ka	End St. Germain 2	82.73 ka	77.6 ka		
End Mélisey II	82.5 ka	End Mélisey 2	87.98 ka	85 ka	End Rederstall	85.5 ka
End St Germain Ic	87 ka	End St. Germain 1	90.65 ka	88.7 ka	End Brörup	96.5 ka
End Montaigu	101.5 ka	End Montaigu	102.78 ka	103.5 ka		
End St Germain Ia	104 ka					
End Mélisey I	107 ka	End Mélisey 1	107.60 ka	108.3 ka	End Herning	108.5 ka
End Eemian	109.7 ka	End LI	109.50 ka	116 ka	End Eemian	116.5 ka

Clearly, the transition from the Eemian interglacial into the subsequent stadial, as defined by changes in vegetation cover, seems to have occurred 5 ka earlier in northern Europe (Müller and Kukla 2004, Müller and Sánchez Goñi 2007, Kühl et al. 2007) as compared to central and southern Europe. The Eemian/Weichselian transition in northern Europe would approximately coincide with the start of GS26 in the NGRIP ice core at around 115–116 ka and with North Atlantic SST cooling event C26. Planktonic $\delta^{18}O$ records show that cooling of North Atlantic surface waters had started soon after the MIS 5e temperature optimum (Chapman and Shackleton 1999, Shackleton et al. 2002, Oppo et al. 2006) and first IRD, marking the advance of ice sheets/glaciers (on Greenland) to the coast, is already observed during the final stage of MIS 5e (Fronval and Jansen 1997, Müller and Kukla 2004, Oppo et al. 2006). The early end of the terrestrial Eemian (i.e. the change in vegetation composition) in northern Europe is thus likely a response to the first distinct North Atlantic sea-surface cooling event C26. In southern Europe, however, the end of the terrestrial Eemian coincides with event C24 during MIS 5d and corresponds to the GI25/GS25 transition at around 110 ka (Figure 8-1).

Detailed land-ocean-ice correlations for the last deglaciation (see for example Björck et al. 1996, Walker et al. 2001) and for MIS 3 (see for example Wohlfarth et al. 2008, Sánchez Goñi et al. 2008, Müller et al. 2011), i.e. time intervals for which much better chronological frameworks are available, show that cold intervals identified in the Greenland ice cores correspond to cold North Atlantic SSTs and to distinct ecosystem changes on the adjacent continents. The response to a cold event seems to have occurred within decades, but was felt differently in different regions due to differences in for example geology, topography, soil conditions and climatology. Transitions from stadial to interstadial or interglacial climatic conditions, as viewed from the Greenland ice cores, also occurred within less than a decade (Steffensen et al. 2008) and had an immediate impact on lake ecosystems and fast responding fauna (Björck et al. 1996). In contrast, the response of the vegetation was not immediate, but was governed by the distance to refugia from where trees had to re-immigrate and by local soil conditions, among several other factors. The use of vegetation records to delimit climatic shifts is thus greatly hampered by the fact that vegetation responds with a considerable time lag.

The NALPS speleothem data set shows rapid and immediate shifts in climate conditions in the northern Alpine foreland, which nicely match in time those recognized on Greenland (Boch et al. 2011) (Tables 8-1, 8-3). Moreover so-called precursor events recognized in the Greenland $\delta^{18}O$ record have a correspondence in the NALPS data set (Boch et al. 2011). This implies that the timing of cold/warm climate conditions was similar between Greenland and Europe, and that cooling/warming signals were transmitted and recognized over a wide region, and possibly with little or no time lags also during MID 5d-a.

The terrestrial stadials and interstadials of MIS 5d-a are primarily defined through shifts in vegetation composition. It can be argued that vegetation responses to cold events were more or less rapid and synchronous over a large region, since a rapid decline in annual temperatures and a concomitant change in precipitation lead to vegetation changes within less than a few decades. In contrast, the response of the vegetation to an abrupt warming will depend on many different factors, such as local conditions (soils, climate, exposure, sheltered location, etc), and the distance to tree refugia. In some regions, the vegetation response to a temperature increase may result in dense forest cover; however sparse forests or open vegetation may develop in another region, where tree immigration is delayed by several centuries (Müller and Sánchez Goñi 2007). Moreover, the duration of an interstadial will have an important impact on the development, expansion and type of vegetation.

Unless each of these regional responses is dated independently, comparisons based on vegetation patterns will remain incorrect and speculative. The detailed comparison of MIS 3 interstadials (Sánchez Goñi et al. 2005, 2008) along distinct latitudinal gradients has for example shown that large differences in forest cover can be reconstructed between the Atlantic and the Mediterranean during interstadials. Given these observations, even larger temporal differences may be expected between pollen records from terrestrial sites in northern and southern Europe, during the warmer interstadials of MIS 5, which makes simple correlations between undated pollenstratigraphic records from these areas ambiguous.

It can however be assumed that the distinct cold events Mélisey I, Montaigu and Mélisey II with expansion of steppe vegetation in southern and central Europe have counterparts in the cold Herning stadial, the intra-Brörup cold phase and the Rederstall stadial in northern Europe and that these in turn correlate with sea surface cooling events C24, C23, and C21 and with Greenland stadials GS25,

GS24, and GS22 (Figure 8-1). Furthermore, since the impact of the distinct cold events is seen as a regional North Atlantic feature, and is registered in ice core, marine, pollen and speleothem records, it seems safe to assume that the response of the vegetation to these cold events was more or less synchronous across Europe.

It may also be assumed that the warmer interstadials of southern and central Europe (St. Germain I and II) broadly correspond to the Brörup and Odderade interstadials of northern Europe (Figure 8-1). However, it remains unclear how fast the tree vegetation in northern Europe became re-established subsequent to a warming. The tentative comparison between the length of stadials and interstadials in southern, central and northern Europe shown in Figure 8-1 needs to be viewed on the background of the above outlined.

As shown in Figure 8-1 and in Table 8-3, the first post-Eemian stadial in northern Europe (Herning) extends over approximately 8 ka and would cover GS26, GI25 and GS25, while the corresponding Mélisey I stadial in central and southern Europe would have had a duration of 2–3 ka. The total length of the Brörup interstadial is much shorter in northern Europe (12 ka) than its correlative, St. Germain I, in southern and central Europe (ca 20 ka), and the Herning stadial seems again to have lasted much longer (11 ka) as compared to the Mélisey II stadial (2.5–4.5 ka). Whether these differences are real or due to the fact that the stadial/interstadial zones are defined by vegetation, is difficult to judge.
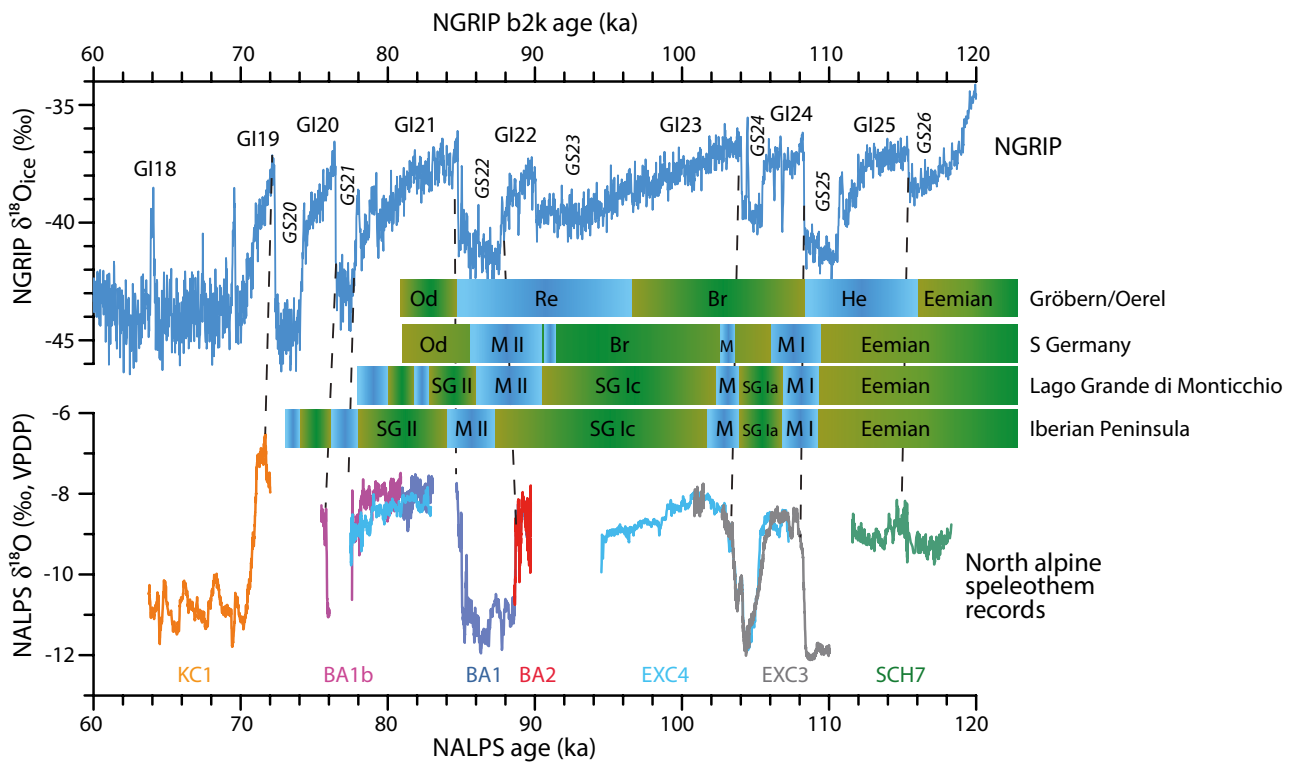
Figure 8-1. Tentative correlation of stadials and interstadials recognized in pollen records from northern (Kühl et al. 2007), central and southern Europe (Sánchez Goñi et al. 2005, Müller and Sánchez Goñi 2007, Sánchez Goñi 2007, Brauer et al. 2007) to the NGRIP ice core (NGRIP Members 2004) and the NALPS data set (Boch et al. 2011). Note that two stadials and one interstadial have been described in pollen records from southern Europe subsequent to the St. Germain II interstadial (Iberian Peninsula, Lago Grande di Monticchio). The last stadial marks the transition between MIS 5a and MIS 4. From the Alpine foreland, a further interstadial, termed Dürnten, has been reported after the Odderade/St. Germain II interstadial (not shown in the Figure) and marks the MIS 5a/4 transition. However in records from northern Europe, the Schalkholz stadial, which occurred subsequent to the Odderade interstadial, defines the MIS 5a/4 transition. See text for a further discussion. Original speleothem data was downloaded from ftp://ftp.ncdc.noaa.gov/pub/data/paleo/speleothem/ and ice core data from www.iceandclimate.dk/data.

Table 8-3. Best estimates for the duration of stadials and interstadials during the early part of the last Glacial period based on the NGRIP ice core (NGRIP Members 2004), Iberian Margin core MD95-2042 (Sánchez Goñi et al. 2005, Sánchez Goñi 2007, Sánchez-Goñi M F, personal communication), Lago Grande di Monticchio in southern Italy (Brauer et al. 2000, 2007, Allen and Huntley 2009) and Gröbern in northern Germany (Kühl et al. 2007).

	NGRIP	MD95-2042	LG di Monticchio	NALPS	Gröbern
Stadial 2/GS20	2.5 ka	1 ka	2 ka ?	–	
Ognon/GI20	3 ka	2 ka	2 ka ?	–	
Stadial 1/GS21	1 ka	2 ka	1 ka ?	1.6 ka	
Odderade/St Germain II/GI21	ka	4.5 ka	5.25 ka	7.4 ka	
Rederstall/Melisey II/GS22	3 ka	4.5 ka	2.67 ka	3.7 ka	11 ka
Brörup/St Germain Ic/GI23, GS23, GI22	16 ka	14.5 ka	12.13 ka	14.8 ka	12 ka
Brörup/St Germain Ib/Montaigu/GS24	2 ka	2.5 ka	2.79 ka	1.5 ka	
Brörup/St Germain Ia/GI24	2.5 ka	3 ka		2.03 ka	3.3 ka
Melisey I/GS25	2.5 ka	3 ka	1.90 ka		
Herning/GS26-25	8 ka				8 ka

Greenland stadials GS21 and GS20 correspond to the un-named Stadials 1 and 2 and to sea surface cooling events C20 and C19 recognized in Iberian Margin core MD95-2042, and are correlated to the later part of MIS 5a (Sánchez Goñi 2007) (Table 8-1, Figure 6-4). The short warm interval between these two stadials, the Ognon interstadial, can be correlated to GI20. Planktonic $\delta^{18}O$ values fluctuate markedly subsequent to SST cooling event C19, and increase around 66 ka into the stadial values of MIS 4 (Sánchez Goñi 2007) (Figure 6-4). The NGRIP ice core $\delta^{18}O$ values show a comparable pattern, i.e. a short interstadial (GI19) subsequent to GS20 and a rapid drop to much lower $\delta^{18}O$ values around 70 ka. The same pattern is recognized in the NALPS data set (Boch et al. 2011), where $\delta^{18}O$ values drop markedly at around 71–72 ka (Figure 8-1). MIS 5a thus does not end with the St. Germain II interstadial at 78 ka, but seems to encompass two further short stadials and one short interstadial (Ognon interstadial) (Figures 6-4, 8-1).

This scenario is partly in contrast to the pollen record of Lago Grande di Montocchio, where pollen zones 17e to 17c were originally assigned to St. Germain II, compared to the Odderade interstadial of northern Europe and correlated to MIS 5a. The subsequent stadial (pollen zone 17b) and interstadial (pollen zone 17a) were correlated to MIS 4 (Allen and Huntley 2000). Brauer et al. (2007) on the other hand assigned pollen zone 17e to St. Germain II, which was correlated to MIS 5b/5a, but pollen zones 17d-a to MIS 5a (Figure 8-1). If Brauer et al.'s (2007) suggested correlation to the marine isotope stratigraphy holds true, the pollen record of Monticchio would also support the idea that the end of the St. Germain II interstadial did not coincide with the end of MIS 5a.

In pollen records from northern Europe, the end of the Odderade interstadial (paralleled with St. Germain II in southern Europe) and the start of the Schalkholz stadial define the early/middle Weichselian boundary (Caspers and Freund 2001, Behre et al. 2005). The Oerel interstadial, which follows after the Schalkholz stadial, is ^{14}C dated to 58–55 ka, which would mean an age equivalent to early MIS 3 (Behre and van der Plicht 1992). Therefore, the early Weichselian in northern Germany would end with the Odderade interstadial (Figure 8-1).

9 Regional vegetation patterns in Europe and quantitative climate reconstructions

Most long, continuous terrestrial archives that document climatic and environmental changes throughout the last interglacial/glacial cycle are lake sediment and/or peat sequences, which have almost only been studied for pollenstratigraphy. In rare cases, have coleoptera or oxygen isotopes been analysed, and only few sites, e.g. Lago Grande di Monticchio in Italy (Allen and Huntley 2000, 2009), Gröbern in northern Germany (Litt et al. 1996, Hoffmann et al. 1998, Kühl et al. 2007) and Sokli in northern Finland (Helmens et al. 2000, 2007, 2012, Alexanderson et al. 2008, Väliranta et al. 2009, Helmens and Engels 2010) have been investigated using a multi-proxy approach.

9.1 The final phase of the Eemian

The transition period between the Eemian interglacial and the first early Weichselian stadial has been described as climatically unstable in several records. Boettger et al. (2007, 2009) and Novenko et al. (2008), among others, showed, based on sites in northern Germany that a number of short-term climate fluctuations, including a distinct warming had occurred just prior to the stadial. Late Eemian climate instability in the form of a distinct aridity event has been found in long sequences from the Eiffel Maar region in western Germany (Sirocko et al. 2005) and has been correlated with sea surface cooling event C26 in North Atlantic marine records. Quantitative precipitation and temperature estimates derived from pollen records from the northern alpine foreland (Klotz et al. 2003) suggest an initial decline in winter temperatures and a subsequent rise before the final temperature drop to overall stadial conditions. Diatom assemblages in the Ribain paleolake sequence from the Massif Central in France also indicate the occurrence of a warmer interval, characterised by mild and relatively dry winters during the final phase of the Eemian (Rioual et al. 2007). Quantified temperatures based on the long pollen record from Lago Grande di Monticchio, showed similar climate fluctuations during the transition zone, especially in respect to winter temperatures (Allen and Huntley 2009). A distinctly colder, but short-lived event (termed Woillard event) is recognized around 600–700 years before the end of the Eemian and has been correlated to sea surface temperature cooling event C25 (Brauer et al. 2007).

Since the ending of the terrestrial Eemian, as defined by a change in vegetation composition, is not time synchronous between northern and southern Europe, but occurred with a time lag of around 5 ka, the above described climatic fluctuations cannot be assigned to the same time interval. The climate shift described by Boettger et al. (2007, 2009) and Novenko et al. (2008) must have occurred earlier than those reported by Sirocko et al. (2005), Allen and Huntley (2009) and Brauer et al. (2007), since the end of the Eemian in northern Germany is equalled with the start of SST cooling event C26. Sirocko et al.'s (2005) aridity phase however has been correlated to SST cooling event C26, and the cooling event observed by Allen and Huntley (2009) and Brauer et al. (2007) has been assigned to SST event C25. Despite these differences, records in both regions point to marked climate instability during the transition from a warm interglacial to a cold climate state.

9.2 The MIS 5a/MIS 4 transition

In pollen records from northern Europe, the end of the Odderade interstadial (paralleled with St. Germain II in southern Europe) (Figure 8-1) and the start of the Schalkholz stadial define the early/middle Weichselian boundary (Caspers and Freund 2001, Behre et al. 2005). The Oerel interstadial, which follows after the Schalkholz stadial, is ^{14}C dated to 58–55 ka, which would mean an age equivalent to early MIS 3 (Behre and van der Plicht 1992).

A third interstadial (Dürnten) younger than the Eemian has been described from terrestrial sequences in the North Alpine foreland and has been correlated to the Ognon interstadial (Müller and Sánchez Goñi 2007). This so-called Dürnten interstadial was characterized by a spread of *Pinus* and *Picea* in southern Germany, and its end, which marks the onset of MIS 4, is indicated by a spread of steppe

biomes. In contrast, the NALPS $\delta^{18}O$ values (Boch et al. 2011) display the occurrence of two stadials (correlated to GS21 and GS20) and of two short interstadials (correlated to GI20 and GI19), before a distinct drop to low glacial $\delta^{18}O$ values at 68–70 ka. This pattern is comparable to the NGRIP ice core, where the end of GI19 leads into much lower (glacial) $\delta^{18}O$ values (Figure 8-1).

In the Iberian Margin cores, the end of MIS 5a is marked by a distinct increase in planktonic $\delta^{18}O$ values at around 68 ka, which compares in time to the climatic shift seen in both NGRIP and the NALPS data set (Figures 6-4, 8-1). These shifts occurred however much later than the end of the St. Germain II interstadial, as defined in the pollen record of Iberian Margin core MD95-2042, and indicate that the end of MIS 5a and the end of St. Germain II do not coincide. The terrestrial record of MD95-2042 displays two stadials and an interstadial (termed Ognon) subsequent to the St. Germain II interstadial (Sánchez Goñi 2007). The two stadials, correlated to SST cooling events C20 and C19, respectively (Figures 6-4, 8-1, Table 8-1) are defined by expansion of semi-desert plants on the Iberian Peninsula (Sánchez Goñi 2007). Since C19 marks the MIS 5a/4 boundary in the marine record, Stadial 2 would thus coincide with this transition.

The pollen record of Lago Grande di Monticchio also shows a stadial/interstadial/stadial succession with lower/higher/lower values, respectively of mesic woody plant pollen, following the St. Germain II interstadial (Brauer et al. 2007). Brauer et al. (2007) correlated this succession to the later part of MIS 5a, which would also suggest that the second stadial could possibly be paralleled with the MIS 5a/MIS 4 transition.

9.3 Vegetation and quantitative climate reconstruction

Table 9-1 summarizes the broad vegetation development along a North-south transect for a number of selected sites. It is however important to note that transitions between stadials and interstadials were time transgressive between northern, central and southern Europe (Müller and Sánchez Goñi 2007), which means that stadial vegetation became earlier established in northern and central Europe as compared to southern Europe, and that reforestation at the start of an interstadial was likely delayed and depended on the distance to the respective tree refugia (Figure 8-1).

As seen in Table 9-1, steppe or tundra-steppe biomes generally characterised the early Weichselian stadials at most sites across northern, central and southern Europe. One exception is the record from Lake Fimon in northern Italy (Figure 1-2), where *Pinus-Picea-Betula* forests have been reconstructed (Pini et al. 2010). The correlation between pollen records from sites north of the Alps and for the Iberian Peninsula suggested that the opening of forests, which marks the start of the Mélisey I stadial, had occurred earlier in more northerly areas than in southern Europe (Müller and Sánchez Goñi 2007). Moreover, Müller and Sánchez Goñi (2007) hypothesized that reforestation at the start of an interstadial should have been delayed in regions further north and that open vegetation biomes may thus have lasted longer in northern Europe than in southern Europe.

The vegetation development during the interstadials was not at all as uniform as compared to the stadials. Boreal forests seem to have prevailed in northern and central Europe, while temperate and broad-leaved trees dominated in southern Europe during the first interstadial (St. Germain I/Brörup) subsequent to the Eemian (Table 9-1). The site of La Grande Pile, sites in southern Germany and in Italy clearly show a progressive vegetation development with an immigration and/or spread of trees at the start of the interstadial, a replacement of the forest, and a final decline/change in forest composition (Table 9-1).

The Montaigu event, which had been observed as a distinct cooling event in for example La Grande Pile (Woillard 1978, de Beaulieu and Reille 1992a), Les Echets (de Beaulieu and Reille 1984), Lac du Bouchet (Reille et al. 1998), Lake Fimon (Pini et al. 2010), Lago Grande di Monticchio (Allen and Huntley 2000, 2009) and in the Iberian Margin cores (Sánchez Goñi et al. 2002, 2005) is also observed in sequences from southern Germany (Füramoos, Jammertal, Samerberg) by a minor opening of coniferous forests (Müller et al. 2003, Müller and Sánchez Goñi 2007) (Table 9-1). This short cooling phase has also been reported from sites in Poland (Komar et al. 2009), and sites from northern Germany, such as Gröbern, show a minor decrease in arboreal pollen percentages (Litt et al. 1996, Hoffmann et al. 1998, Kühl et al. 2007).

Boreal forests dominated in northern and central Europe throughout the second interstadial (St. Germain II/Odderade), while a development towards temperate forests is seen both at La Grande Pile and at sites in southern Germany during the middle part of the interstadial (Table 9-1). The end of the interstadial saw a renewed spread and subsequent decline of boreal/coniferous forests. At Lago Grande di Monticchio a steppe phase can be observed during the middle part of the interstadial, which suggests short-lived colder and or drier climatic conditions.

Pollen and plant macrofossil records and where available coleoptera, have been used to make climate reconstructions based on a wide number of different approaches and statistical techniques, see for example Guiot et al. (1992, 1993), Ponel (1995), Litt et al. (1996), Aalbersberg and Litt (1998), Hoffmann et al. (1998), Allen et al. (1999), Fauquette et al. (1999), Caspers and Freund (2001), Klotz et al. (2003, 2004), Kühl et al. (2007), Brewer et al. (2008), Allen and Huntley (2009), Väliranta et al. (2009) and Helmens et al. (2012) for details and further references. All of these methods assume that plants and animals responded in a more or less straight way to shifts in climate. However the use of biota as a proxy for quantitative temperature and precipitation estimates is not unproblematic, given that *sedimentary biological assemblages are a complex function of multiple chemical and physical gradients that are intimately linked through interaction of climate, human activity, and lake and catchment processes* (Juggins 2013, p 28). It is therefore important to note that the reconstructed temperature and precipitation estimates mentioned here, may not at all be representative.

Below I shortly describe inferred quantitative and qualitative climate estimates for selected sites and use these data sets as a template for the early Weichselian vegetation and climate in northern, central and southern Europe.

Table 9-1. Comparison of vegetation changes during the early Weichselian from selected sites along a north-south transect. Note that start and end of stadials/interstadial were not time synchronous between northern and southern Europe. Summarized after [1]Helmens et al. (2012), [2]Satkunas et al. (2003), [3]Behre and Lade (1986), Behre (1989), [4]Hoffmann et al. (1998), [5]Komar et al. (2009), [6]Woillard (1978), [7]Müller and Sánchez Goñi (2007), [8]Preusser (2004), [9]de Beaulieu and Reille (1992b), [10]Pini et al. (2010), [11]Allen and Huntley (2000, 2009).

Sites	Mélisey I/Herning	St. Germain I/Brörup	Mélisey II/Rederstall	St. Germain II/Odderade
Sokli[1]	Steppe-tundra with scattered trees	Mixed boreal forest		
Medininkai[2]	Tundra-steppe	Coniferous forest	Tundra-steppe	Dense coniferous forests
Oerel[3]	Tundra-steppe	Mixed boreal forest	Tundra-steppe	Boreal forests
Gröbern[4]	Tundra-steppe	Mixed boreal forest	Tundra-steppe	Mixed boreal forests
Poland[5]	Tundra-steppe	Dense birch forests – short cooling phase – spread of pine	Shrub-herb vegetation	Open pine and bine-birch forests
LG Pile[6]	Wooded steppe	(Ia) Sub-arctic tundra – boreal forest – cooling – (Ic) boreal forest – warm temperate forest – cold temperate forest – boreal forest	Steppe	Sub-arctic tundra – boreal forest – temperate forest – boreal forest
Southern Germany[7]	Open tundra-steppe	Spread of pioneer taxaco-niferous woodlands – minor opening of woodlands – recovery of forests and spread of thermophilous deciduous trees – increase and subsequent decline of coniferous forests	Steppe	Spread of Pinus and Picea – immigration of deciduous trees – coniferous forest – decline of coniferous forest
Switzerland[8]	Tundra	Coniferous forest	Steppe	Coniferous forest
Velay Plateau[9]	Steppe	Coniferous forest – mixed forest – coniferous forest – deciduous forest – coniferous forest	Steppe, sparse coniferous trees	Coniferous forest – mixed forest – coniferous forest
Fimon[10]	Pinus-Picea-Betula forests	Warm-temperate, broad-leaved forests – opening of forests – mixed forests	Boreal forest with dominance of Pinus	Expansion of warm-demanding trees and shrubs
LG di Monticchio[11]	Wooded steppe	Temperate deciduous forest – temperate deciduous/cool mixed forests	Cold/warm steppe	Temperate deciduous forest – steppe – temperate deciduous forest

9.3.1 Northern Europe

Aalbersberg and Litt (1998) (and references therein) compiled a variety of continuous and non-continuous terrestrial Eemian and Early Weichselian records covering northern Europe, assuming that non-forested intervals are comparable to stadial conditions and forested intervals to interstadial conditions. The compilation included coleoptera and paleobotanical data series. However given the fragmented nature of several of the sites included in the compilation, it is not sure if the stadial and interstadial records that were used were correlated correctly with each other.

A similar comparison was made by Caspers and Freund (2001) (see references therein) using different types of records from The Netherlands, Germany, Poland, Denmark, and Sweden. Also for this study it is difficult to know if the same time intervals were actually compared, given the fragmented nature and often, uncertain attribution of some of the sites to the early Weichselian interstadials. Caspers and Freund (2001) concluded that a cold continental climate prevailed during the Herning stadial, with frequent signs of cryoturbation, frost wedges, and solifluction. Climatic conditions were wetter and more maritime in Western Europe during the Brörup, while a more continental climate with cold and dry winters prevailed in Eastern Europe. Discontinuous permafrost during Rederstall and a more continental climate during Odderade are discussed. Continentality seems to have increased during Odderade as sea level lowered (Caspers and Freund 2001).
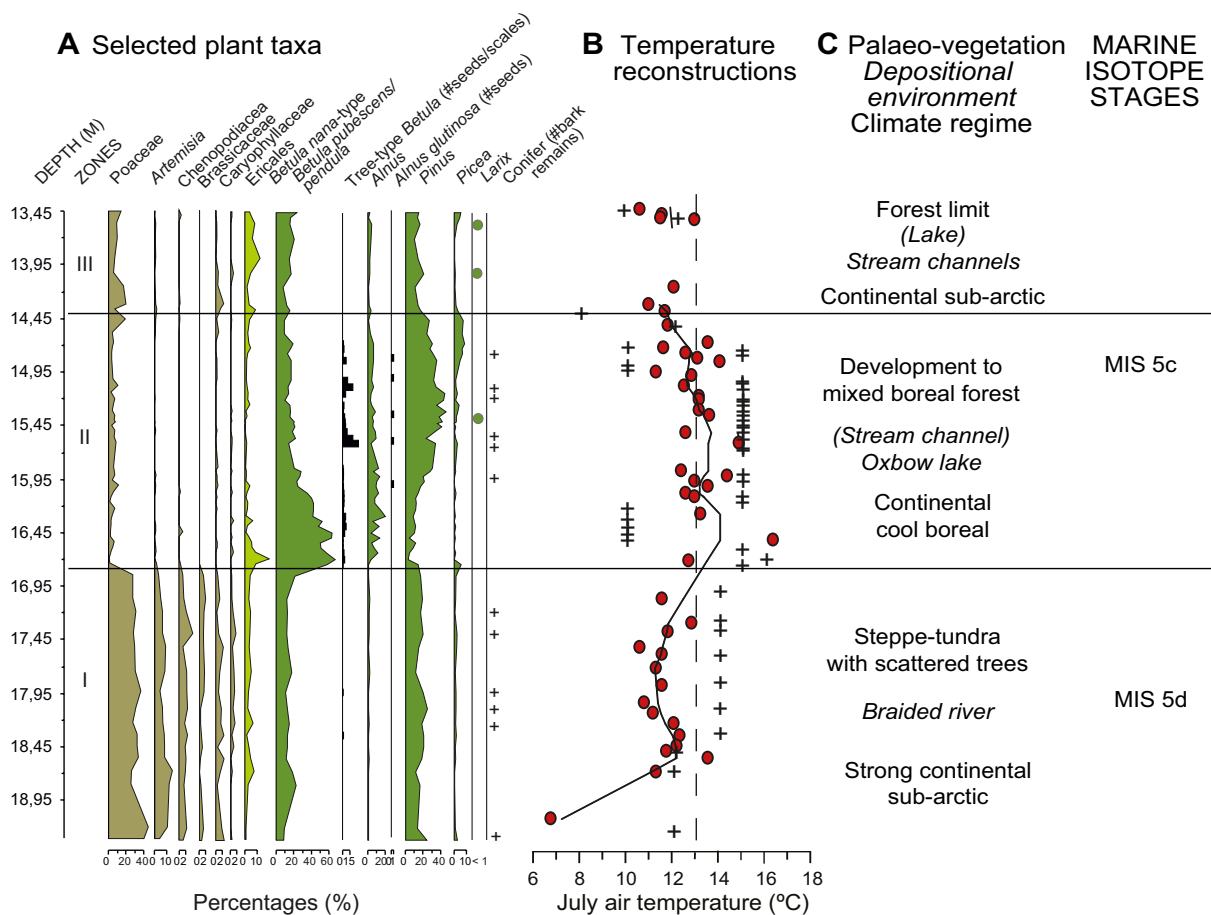

Figure 9-1. *(A) Selection of terrestrial pollen and plant macrofossil data from the last interglacial/glacial transition at Sokli correlated with MIS 5d-c. (B) Quantitative estimates of mean July temperatures based on chironomids (circles) and minimum mean July temperatures inferred from plant indicator species (crosses). (C) Summary of inferred paleo-environmental conditions. The present-day mean July temperature of 13°C is indicated for reference. The chironomid-inferred temperature values are given with a locally weighted scatterplot smoother (LOWESS, span = 0.20) applied to the reconstructed values; maximum bias is 1.05°C. Modified from Helmens et al. (2012).*

Sokli, north-east Finland

The lowermost sediments in the Sokli sequence, north-eastern Finland (Figure 1-2) are assigned to the Eemian interglacial, to MIS 5d (gravels and silty sediment) and to MIS 5c (gyttja and upper sands and gravels), based on stratigraphy, pollen assemblages and OSL ages (Helmens et al. 2000, 2007, 2012, Alexanderson et al. 2008, Helmens and Engels 2010).

Steppe-tundra vegetation, including Poaceae, *Artemisia*, Chenopodiaceae and *Betula nana* (Figure 9-1, Table 9-1), is inferred for the upper part of the MIS 5d deposit, sensu Helmens et al. (2012). Mean July temperatures of at least 12–14°C are indicated by chironomids and plant indicator species (Table 9-2) and are in agreement with the presence of conifer and birch trees as recorded by macrofossils. The presence of steppe-tundra vegetation and the recorded high summer temperatures, suggest severe continental climate conditions at Sokli during MIS 5d sensu Helmens et al. (2012) (Table 9-1). Birch forest became established during MIS 5c sensu Helmens et al. (2012) and was followed by the spread of pine and spruce. During late MIS 5c the vegetation was much more open. Rich plant indicator species assemblages indicate that the boreal environment during MIS 5c experienced July temperatures several degrees higher than the present-day value of 13°C (Table 9-2) The July-inferred temperatures for MIS 5c sensu Helmens et al. (2012) at Sokli are similar to those reconstructed for Germany by Behre et al. (2005) and Kühl et al. (2007) and suggest weaker north-south summer temperature gradients over northern Europe than at present. The high summer temperatures and presence of larch at Sokli suggest more continental conditions than at present.

Medininkai, Lithuania

The long, continuous record from Medininkai in Lithuania provides a sediment succession from the Eemian to the LGM (Satkunas et al. 2003). The pollen record allows assigning the vegetation changes to the Early Weichselian stadials and interstadials of northern Europe (Table 9-1). Similar to other sites, sparse birch forest with shrubs and herbs dominated during the Herning stadial (Satkunas et al. 2003). Macro remains of *Betula nana*, *Selaginella selaginoides* and *Potamogeton filiformis* may suggest minimum July temperatures of 4–7°C, and possibly up to 10–14°C following Kolstrup (1980), Hultén and Fries (1986), Brinkkemper et al. (1987) and Ran et al. (1990) (Table 9-2). Coniferous forests, dominated by *Larix*, expanded again during the Brörup interstadial. Macro remains of *Menyanthes trifoliata* and *Potamogeton natans* point to minimum July temperatures of 8°C (Kolstrup 1980) (Tables 9-1, 9-2). Presence of *Larix* also continued during the Rederstall stadial, although non-arboreal pollen increased markedly, indicating colder conditions (Satkunas et al. 2003). The Odderade interstadial was characterized by a re-expansion of dense coniferous forests. The occur-rence of *Ceratophyllum demersum* and *Selaginella selginoides* suggest minimum July temperatures of 10–14°C (Kolstrup 1980) (Table 9-2). The end of Odderade coincides with a sharp decrease in *Pinus* and *Picea* pollen percentages and an increase in Ericales pollen values (Satkunas et al. 2003).

Oerel, northern Germany

Pollen, coleopteran and plant macrofossils from the site Oerel in northern Germany (Figure 1-2) (Behre and Lade 1986, Behre 1989, Behre et al. 2005) provide estimates for MIS 5 summer and winter temperatures (Tables 9-2, 9-3). Macrofossils of *Typha* present in the Herning stadial indicate minimum mean July temperatures of 14–15°C (Table 9-1). During the Brörup birch phase, summer warmth-demanding *Stratiotes aloides* and *Ceratophyllum demersum* occur; macrofossils of *Ranunculus sceleratus* and *Typha* indicate minimum mean July temperatures of 15°C. On the other hand, mosses such as *Helodium blandowii* and *Meesia longiseta* (and later *Drepanocladus tundrae* as well as the midge *Corynocera ambigua*) have a specific northern distribution; this composition of species can be best explained by strong continental conditions with warm summers and cold winters. During the later part of the Brörup interstadial, a number of coleoptera species are found that today occur in temperate regions. Coleopteran-based reconstructions here give mean temperatures of the warmest and coldest month in the range of ca 15–19 and –8 to –14°C, respectively, while *Najas flexilis* indicate minimum mean July temperatures of 15°C (Tables 9-2, 9-3). The aquatic plants *Ceratophyllum demersum* together with *Stratiotes aloides* (minimum mean July temperatures of 12°C; tolerates very low January temperatures) indicate relatively high summer temperatures at the closing phase of the Rederstall stadial. Macrofossils of *Typha* indicate minimum mean July temperatures of 14–15°C (Table 9-2). The major part of the Odderade interstadial is dominated by

cold stenotherm insects. Coleoptera-based reconstructions give estimates of 8–12°C for the warmest month and –11 to –22°C for the coldest month (Tables 9-2, 9-3). In the lowermost part of the pine phase, however, coleopteran-based reconstructions are 19°C (warmest month) and 2–4°C (coldest month). *Typha* and *Ranunculus sceleratus* indicate minimum mean July temperatures of 15°C in the birch phase (Table 9-2), where also *Stratiotes aloides* and *Ceratophyllum demersum* are recorded (and *Potamogeton friesii*).

Gröbern and Klinge

The site of Gröbern in northeast Germany (Figure 1-2) has been the target of a number of different investigations. Coleoptera (Walkling and Coope 1996), pollenstratigraphy, plant macrofossil analysis (Litt et al. 1996, Hoffmann et al. 1998, Kühl et al. 2007) and isotope studies (Boettger et al. 2009) have been used to obtain quantified temperature reconstructions. Based on pollenstratigraphy, Litt et al. (1996) correlated the Gröbern sequence with the biostratigraphic zones established at Oerel.

Climate reconstructions using plant indicator species suggested that mean annual temperatures decreased by 6–11°C at the transition from the Eemian into the Herning stadial (Litt et al. 1996). Climate reconstructions using coleoptera (Walkling and Coope 1996) showed that mean summer temperatures were around 15°C during interstadials and around 10–15°C during stadials (Tables 9-2, 9-3, Figure 9-2). Hoffmann et al. (1998) combined plant macrofossil and pollen evidence to reconstruct mean annual and mean monthly temperatures during the different Early Weichselian stadials and interstadials. According to this reconstruction, climate conditions seem to have been oceanic to sub-oceanic during the Herning stadial with mean temperatures of the coldest month of around –7°C and mean temperatures of the warmest month of around 13 to 14°C (Hoffmann et al. 1998) (Tables 9-2, 9-3, Figure 9-2). In contrast a sub-continental climate prevailed during the Brörup interstadial, given lower reconstructed coldest month mean temperatures than during the previous stadial, and mean temperatures of the warmest month slightly higher (Hoffmann et al. 1998). Mean temperatures of the warmest month were a few degrees C lower during the Rederstall stadial, but the Odderade interstadial seems to have been again characterized by similar climate conditions as the Brörup interstadial (Table 9-2) (Hoffmann et al. 1998).
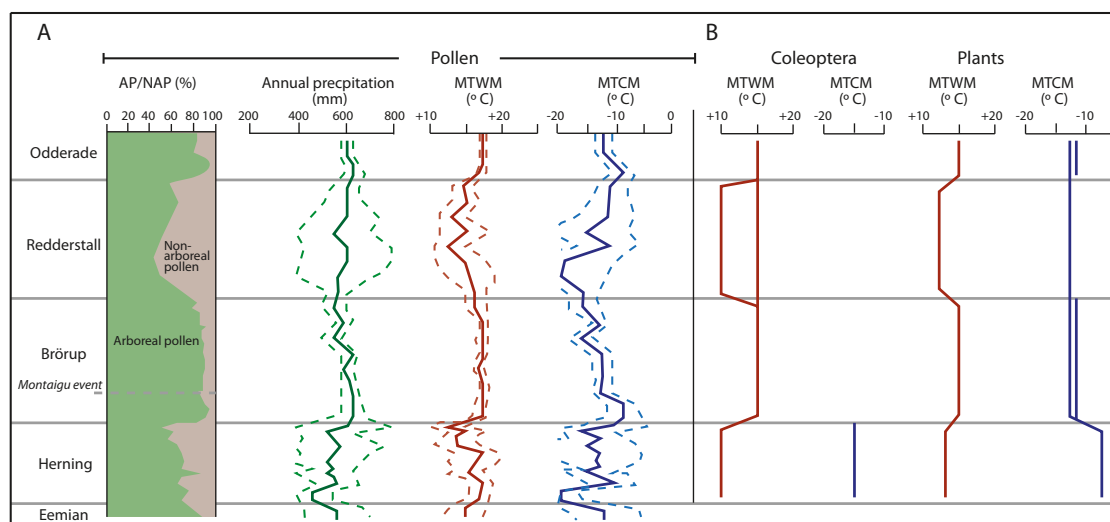

Figure 9-2. *Climate reconstructions for Gröbern in northeast Germany. A. Arboreal (AP) and non-arboreal (NAP) pollen percentages show forested interstadials and open vegetation stadials. Pollen-based climate reconstructions of annual precipitation, mean temperature of the coldest month (MTCM) and mean temperature of the warmest month (MTWM). Solid line = mean values; dashed line = standard deviation. Modified after Figure 4 in Kühl et al. (2007). B. Coleoptera-, plant macrofossil- and pollen-based climate reconstructions according to Walkling and Coope (1996) and Hoffmann et al. (1998).*

Table 9-2. Reconstructed minimum mean temperatures of the warmest month for northern Europe based on different types of proxies and methodological approaches. After [1]Helmens et al. (2012), [2]Satkunas et al. (2003), [3]Hoffmann et al. (1998), Walkling and Coope (1996), [4]Behre (1989), Behre and Lade (1986). *Coleoptera-based climate reconstruction; **pollen-based climate reconstruction; #plant macrofossil-based climate reconstruction; &chironomid-based climate reconstructions.

Sites	Mélisey I/Herning	St. Germain I/Brörup	Mélisey II/Rederstall	St. Germain II/Odderade
Sokli[1]	12–14°C#&	10–16°C#&		
Medininkai[2]	4–7°C#	>10°C#		10–14°C#
	(Max 10–14°C)#			
Oerel[3]	14–15°C#	15°C#	14–15°C#	15°C#
		15–19°C*	8–12°C*	19°C*
Gröbern[4]	<10°C*	15°C*	10–15°C*	15°C*
	15°C#**	c. 17°C**		c. +17°C**

Table 9-3. Reconstructed minimum mean temperatures of the coldest month for northern Europe based on different types of proxies and methodological approaches. After [1]Behre (1989), Behre and Lade (1986) and [2]Hoffmann et al. (1998), Walkling and Coope (1996). *Coleoptera-based climate reconstruction; **pollen-based climate reconstruction; #plant macrofossil-based climate reconstruction.

Sites	Mélisey I/Herning	St. Germain I/Brörup	Mélisey II/Rederstall	St. Germain II/Odderade
Oerel[1]	–	–8 to –14°C*	–11 to –22°C*	2 to 4°C*
Gröbern[2]	<–15°C*	–10 to –15°C**	–	–10 to –15°C**
	–7°C#**	–12 to –14°C#**		–12 to –14°C#**

A different method to reconstruct past climatic conditions was adopted by Kühl et al. (2007), who used a multivariate probabilistic approach to pollen and plant macrofossil taxa (Figure 9-2). To obtain a time scale for the Gröbern pollenstratigraphy, the interstadial/stadial transitions were tied to the NGRIP ice core chronology. The reconstructions suggest a strong shift to a continental climate at the Eemian/Herning transition, a decrease in July and January temperatures by c. 3°C and c. 15°C, respectively and a decrease in annual precipitation by c. 200 mm (Figure 9-2, Tables 9-2, 9-3). For the interstadials reconstructed July and January temperatures are around 17°C and between –10 and –15°C, respectively and mean annual precipitation is around 600 mm (Tables 9-2, 9-3). The pollen- and plant macrofossil based climate reconstructions compare quite well to those obtained using coleopteran.

9.3.2 Central and southern Europe

La Grande Pile

New sediment cores obtained at La Grande Pile (Figure 1-2) were studied for pollen (de Beaulieu and Reille 1992a) and coleoptera (Ponel 1995). The new pollen record was used as a basis for different climate reconstruction approaches (Guiot et al. 1989, 1992, Fauquette et al. 1999, Brewer et al. 2008). Cold conditions and dry winters seem to have prevailed towards the end of the Eemian interglacial and during the first stadial (Mélisey I) (Guiot et al. 1992). A continental climate characterized St. Germain II, although conditions seem to have become more oceanic before and after the cold and dry Montaigu event. The reconstructions suggest cold and relatively humid climatic conditions towards the end of St. Germain I. Expansion of steppe taxa during Mélisey II, again points to a cold and arid climate. Oceanic conditions seem to have prevailed during the early part of St. Germain II, continental conditions during the middle part, and cold and relatively humid conditions during the final part of St. Germain II.

Fauquette et al. (1999) reconstructed mean annual temperatures (MAAT) of –2 to 5°C and a mean annual precipitation (MAP) of <650 mm for Mélisey I and II. Reconstructions for St Germain I and II indicated MAAT of 8 to 12°C and MAP of 800–1,200 mm. The Montaigu event was characterised by MAAT of around 0°C, but MAP did not seem to decrease.

Northern alpine foreland

Temperature and precipitation reconstructions for the sites Füramoos and Samerberg in southern Germany (Figure 1-2) (Klotz et al. 2004) also imply strong continentality during the Mélisey I stadial (Figure 9-3). Reconstructed mean temperatures of coldest month (MTCM) for Füramoos, Samerberg and Jammertal are around −17 to −5°C, while reconstructed mean temperatures of warmest month (MTWM) range from 7 to 17°C (Tables 9-4, 9-5). Low temperatures and humidity, coincident with Mélisey I/GS25, can also be inferred from low $\delta^{18}O$ values in the NALPS speleothem data set (Boch et al. 2011) (Figures 7-1, 8-1), which supports the pollen-based reconstructions.

Only a minor rise in winter and summer temperatures however seems to have occurred at all three sites during the subsequent St. Germain I interstadial (Klotz et al. 2004). In contrast, $\delta^{18}O$ values in the speleothem data set (Boch et al. 2011) show a very distinct temperature rise at the stadial/interstadial transition, suggesting a marked increase in temperature and humidity.

Distinctly colder MTCM of −19 to −12°C are reconstructed for the second stadial (Mélisey II), while MTWM are in the range of 10–16°C (Tables 9-4, 9-5, Figure 9-3) (Klotz et al. 2004). The low $\delta^{18}O$ values of the NALPS data set (Boch et al. 2011) also point to a rapid and marked decrease in temperatures and suggest drier conditions (Figure 8-1).

The start of the St. Germain II interstadial was characterized by a shift to warm sub-oceanic to oceanic conditions, higher precipitation and slightly higher MTCM and MTWM. The temperature increase is most distinct at Füramoos, where MTCM are −5 to 0°C and MTWM around 13–17°C (Tables 9-4, 9-5, Figure 9-3). Towards the end of St. Germain II, winter and summer temperatures decline again and precipitation decreases (Klotz et al. 2004). A rapid increase in temperatures and humidity at the start of interstadial GI 21 is also seen in the NALPS $\delta^{18}O$ record, followed by gradual decreasing temperatures (Boch et al. 2011).

Long pollen sequences further to the west, in the Swiss alpine foreland suggest a similar vegetation and climatic development (Klotz et al. 2003, Preusser 2004) (see references therein). Steppe and/or tundra-like vegetation were described for the first stadial after the Eemian interglacial. Significant glacier advances in the high mountains and possibly as far as into the Swiss alpine foreland may have been triggered by these inferred cold and humid climatic conditions (Preusser 2004). Coniferous forests including deciduous trees became reestablished during the St. Germain I/Brörup interstadial, although a short interval with expansion of pine suggests the occurrence of an intermittent colder event. Climate conditions during the second stadial (Mélisey II/Rederstall) seem to have been less cold and less humid, as compared to the first stadial, although steppe vegetation again covered large areas (Preusser 2004). Less cold and less humid climatic conditions were not favourable for glacier advances. Coniferous forests with thermophilous elements, such as *Carpinus*, *Corylus*, *Quercus*, and *Ulmus*, again dominated the last interstadial (St. Germain II/Odderade), suggesting warmer climatic conditions.

Les Echets and Lac du Bouchet

Fauquette et al. (1999) climate reconstruction for Les Echets estimated a MAAT of around 8–12°C and MAP of 600–1,100 mm for St. Germain I and II, and a distinct decrease in MAAT to <0°C, but not in MAP during the Montaigu event.

Interestingly, although the pollen zones corresponding to Mélisey I and II were characterised by reworked pollen in the Les Echets sequence (de Beaulieu and Reille 1984), the climate reconstructions by Klotz et al. (2004) did not take this into account (Figure 9-3, Tables 9-4, 9-5). Using two different methods, modern analogue vegetation types and probability mutual climatic spheres, Klotz et al. (2004) suggested a decrease in winter temperatures to a minimum of about −17°C, and summer temperatures of 15–20°C for the Mélisey I stadial. Low reconstructed precipitation of around 590 mm, low winter temperatures and still high and stable summer temperatures indicate increased continentality (Figure 9-3, Tables 9-4, 9-5). Towards the end of the stadial, another reduction in winter temperatures with mostly stable or decreasing summer temperatures can be observed (Klotz et al. 2004). During St. Germain Ia, reconstructed MTCM rise to a maximum of 2°C, while MTWM remain at around 15–20°C. The Montaigu event was characterized by average winter temperatures of −15°C and average summer temperatures of 15°C (Klotz et al. 2004). Reconstructed MTCM and MTWM for the later part of the St. Germain interstadial are 0°C and 20°C, respectively (Figure 9-3, Tables 9-4, 9-5).

Cold winters and warmer summers seem to have prevailed during Mélisey II, for which reconstructed MTCM and MTWM are –20 to –2°C and 5–22°C, respectively (Klotz et al. 2004). During St. Germain II reconstructed MTCM are –10 to 2°C and MTWM attain 20°C (Figure 9-3, Tables 9-4, 9-5).

Climate reconstructions for Lac du Bouchet by Fauquette et al. (1999) suggest MAAT of –7 to –2°C and MAP of <650 mm for Mélisey I and II. Reconstructed MAAT are 8 to 12°C and reconstructed MAP is 800–1,200 mm for St. Germain I and II. This reconstruction shows no indication of the Montaigu event.
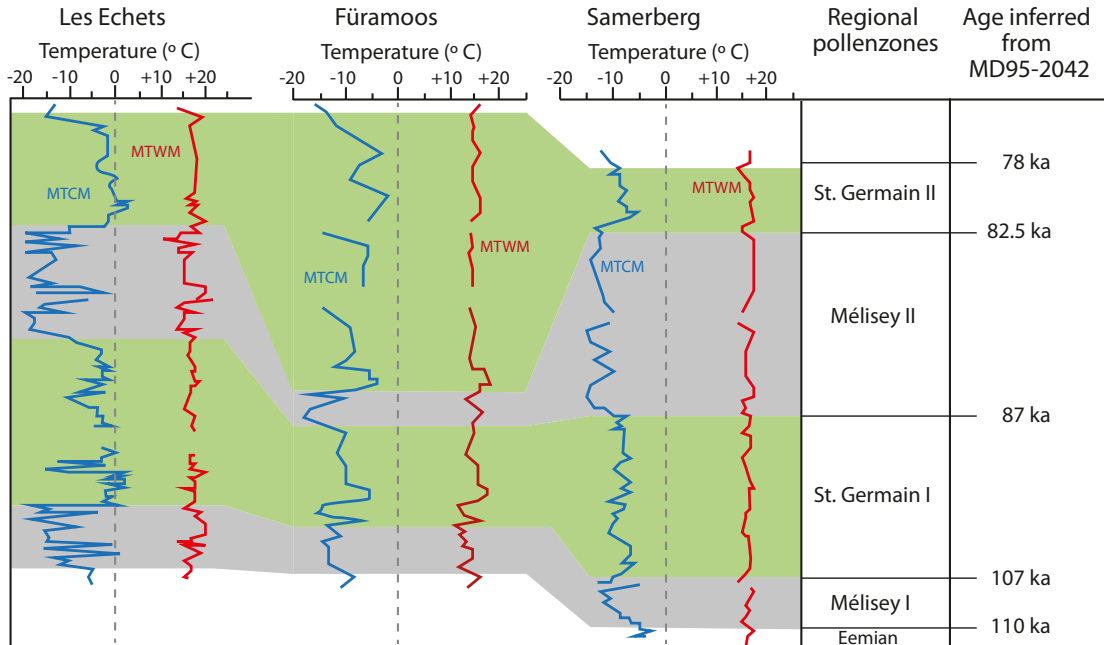

Figure 9-3. *Quantified mean temperatures of the coldest (MTCM) and warmest months (MTWM) for Les Echets, Füramoos and Samerberg, reconstructed using modern analogue vegetation types. The ages for the stadial/interstadial transitions have been inferred from Iberian Margin core MD95-2042. Modified after Figure 3 in Klotz et al. (2004).*

Table 9-4. Reconstructed minimum mean temperatures for the warmest month from long terrestrial sequences in central and southern Europe, after Klotz et al. (2004).

Sites	Mélisey I/Herning	St. Germain I/Brörup	Mélisey II/Rederstall	St. Germain II/Odderade
Les Echets	15 to 20°C	15 to 20°C	5 to 22°C	15 to 20°C
Füramoos	10 to 12°C	7 to 12°C	12 to 15°C	13 to 17°C
Samerberg	c. 15°C	15 to 16°C	14 to 16°C	15 to 16°C
Jammertal	7 to 17°C	10 to 15°C	10 to 16°C	6 to 17°C

Table 9-5. Reconstructed minimum mean temperatures for the coldest month from long terrestrial sequences in central and southern Europe, after [1]Klotz et al. (2004) and [2]Allen and Huntley (2000, 2009).

Sites	Mélisey I/Herning	St. Germain I/Brörup	Mélisey II/Rederstall	St. Germain II/Odderade
Les Echets[1]	–17 to 2°C	0 to 2°C Montaigu: –15°C	–20 to –4°C	–10 to 2°C
Füramoos[1]	–15 to –10°C	–15 to –7°C[2]	–17 to –12°C	–5 to –2°C
Samerberg[1]	–12 to –5°C	–10 to –5°C	–15 to –10°C	–12 to –10°C
Jammertal[1]	–17 to –10°C	–14 to –5°C	–19 to –15°C	–15 to –4°C
LG di Monticchio[2]	–4.4°C	0 to 3°C	–8 to –5°C	–14 to 1°C

Lago Grande di Monticchio

The vegetation development for Lago Grande di Monticchio has been investigated in very high resolution and provided estimates for mean temperatures of the coldest month, for the length of the growing season and for the ratio between actual and potential evaporation (Allen et al. 1999, Allen and Huntley 2000, 2009).

Local pollenzone 21a, which marks the end of the Eemian interglacial, shows the presence of temperate deciduous forests, although during the short cooling event (Woillard event), which is correlated to SST cooling event C25, wooded steppe seems to have occurred (Allen and Huntley 2009). Reconstructed average MTCM for pollen zone 21a are –0.7°C, although minimum temperatures seem to have reached –7.3°C. Local pollen zone 20 represents the first stadial following the Eemian interglacial and is correlative to Mélisey I. Wooded steppe biomes, maximum winter temperatures of –16°C (average mean –4°C) and low moisture availability, but relatively high annual temperature sums, suggest high seasonality (Allen and Huntley 2009) (Table 9-5). Re-expansion of temperate forests during St. Germain I (local pollen zones 19a, b) showed that MTCM had increased (Allen et al. 1999). Mélisey II (local pollen zone 18) is again characterised by wooded steppe biomes, by a decrease in MTCM to between –5 and –8°C (Table 9-5) and by low moisture availability. The expansion and establishment of temperate deciduous forests during the St. Germain II interstadial (local pollen zone 17e), was interrupted by a short phase with expansion of steppe biomes (local pollen zone 17d) (see Chapter 9.2 for a discussion of the St. Germain II interstadial in the Lago Grande di Monticchio record). The marked fluctuations in arboreal and non-arboreal pollen percentages during pollen zones 17e to 17c resulted in distinct fluctuations in MTCM (Table 9-5), ranging from +1 to –14°C and in reconstructed available moisture (Allen et al. 1999).

9.3.3 Temperature gradients in Europe

Overall, and taking the large uncertainties into account, the temperature reconstructions for northern Europe seem to agree broadly. MTWM for the Herning stadial range at 12–15°C at all four sites in northern Europe and MTCM (only available for Gröbern) are –15 to –7°C. Reconstructed MTWM for central and southern Europe are slightly warmer (7–20°C) and MTCM cover a range between –4 and –17°C. Severe continentality has been inferred for Sokli during MIS 5d (Herning) (Helmens et al. 2012), while Hoffmann et al. (1998) suggested oceanic to sub-oceanic climatic conditions for Gröbern. The large difference between warmest and coldest month temperatures for sites in central and southern Europe supports the idea of strong continentality.

MTWM for the Brörup interstadial are around 10–19°C at all four sites in northern Europe and coldest month temperatures (inferred for Gröbern) are –15 to –10°C. In central and southern Europe MTWM of 7–20°C and MTCM of 0 to –15°C are reconstructed for St. Germain I. The fairly large difference between MTWM and MTCM would suggest also strong continentality during the Brörup interstadial, but possibly weaker N-S temperature gradients (Helmens et al. 2012).

Temperature reconstructions for Oerel and Gröbern suggest MTWM of 8–15°C and MTCM of –22 to –11°C during the Rederstall stadial. MTWM of 5–16°C and MTCM of –4 to –20°C have been inferred from sites in central and southern Europe for Mélisey II. This suggests overall colder MTWM and MTCM as compared to the Herning/Mélisey I stadial.

For the Odderade interstadial, MTWM of 15–19°C and MTCM of 2–4°C (–10 to –14°C based on coleopteran) are reconstructed for Oerel and Gröbern. MTWM inferred for sites in central and southern Europe for St. Germain II are comparable (6–20°C) to those of northern Europe. MTCM of 1 to –15°C are much lower than those inferred for example for Oerel, but much closer to those reconstructed based on the coleopteran record of Gröbern.

This fairly coarse comparison of the different temperature reconstructions is limited by a number of issues. (1) Each of the methods used to reconstruct temperature has its own error margins, and none of these are accounted for here. (2) Plant-, and coleoptera-based temperature reconstructions use different types of biological data sets, which each respond differently to climate. (3) As shown by the NGRIP and NALPS δ^{18}O data sets, high frequency climate shifts are present within the broadly classified interstadials. These shifts are not accounted for in these temperature reconstructions, but might be the cause why some reconstructions result in very low or very high temperature estimates. (4) As explained in Chapter 8, correlations between interstadials and stadials in northern, central and southern Europe are difficult, given the lack of independent chronologies for individual sites and given that interstadials had a shorter duration in northern Europe as compared to southern Europe.

10 Scandinavian ice sheet and permafrost changes

The few and often discontinuous pre-Last Glacial Maximum (LGM) records that exist in Scandinavia only allow for a sketchy reconstruction of Early Weichselian paleoenvironmental and climatic changes, ice sheet expansion and ice sheet retreat. Sites that provide information were located in areas where the cold-based LGM ice sheet did not erode or dislocate older interglacial and interstadial deposits (Lundqvist 1978, 1992, Lagerbäck and Robertsson 1988, Robertsson 1991, Robertsson and García Ambrosiani 1992, Kleman 1994, Kleman and Hättestrand 1999, Helmens et al. 2000, 2007, 2012, Helmens and Engels 2010, Hättestrand and Robertsson 2010), or comprise a variety of marine, peat, lacustrine and glacial deposits mainly from more marginal areas of the former LGM ice sheet (Andersen 1961, Miller 1977, Berglund and Lagerlund 1981, Påsse et al. 1988, Larsen et al. 2009, Mangerud et al. 2011, Lemdahl et al. 2013). Moreover, recent focus on southern Sweden has shown that a fairly large number of last interglacial and possibly early Weichselian deposits may be burrowed beneath LGM till (Lemdahl et al. submitted, Möller 2013).

Assessing the areal extent and timing of MIS 5 ice sheet and glacier expansion is difficult, since the deposits left by these advances have been overridden and modified by subsequent ice sheet advances. One possibility to assess how far the Scandinavian ice sheet advanced to the coast and onto the continental shelf during MIS 5 is to analyse IRD in marine sediments. A first glaciation curve, based on marine sediment cores off the Norwegian coast, showed only short-lived ice advances during the two stadials MIS 5d and 5b (Baumann et al. 1995) and suggested that glaciers did not pass the coastline until during MIS 5b. Fronval and Jansen's (1997) study on the other hand indicated that the Scandinavian ice sheet advanced to the Norwegian coast during both stadials (Figure 5-2).

Mangerud et al. (2011) recently summarized the advance/retreat history of the Scandinavian ice sheet during the last interglacial/glacial cycle in Norway, mainly based on a few key localities (Fjösanger and Brumundalen, Figure 1-2). At Fjösanger, marine Eemian (MIS 5e) sediments are overlain by glaciomarine silt (termed Gulstein), by a beach deposit (termed Fana) and by thick till beds (termed Bones). The glaciomarine Gulstein sediments and the Bones till are clear indications for glacier/ice sheet advances, however only the younger Bones advance reached beyond the coastline (Mangerud et al. 2011) (Figure 10-1). The stratigraphic position of these deposits above Eemian sediments, suggested that the older advance occurred during MIS 5d (correlated to the Herning stadial), and the younger advance during MIS 5b (correlated to the Rederstall stadial) (Mangerud et al. 2011). The intercalated beach deposit however would indicate an interstadial, which might possibly be correlative to a peat layer described from Brumunddalen in south-central Norway (Figure 1-2) (Mangerud et al. 2011). This peat layer is intercalated between two till beds, which shows that glaciers advanced over the site. The pollenstratigraphy of the peat layer includes a succession from open pioneer vegetation to shrubs with some trees including *Larix*, and a reversion to arctic tundra near the top of the peat. This cold–mild–cold climate cycle exemplified by the vegetation development suggests a possible correlation to the Brörup interstadial (Mangerud et al. 2011). In analogy with the stratigraphy at Fjösanger, Mangerud et al. (2011) thus hypothesized that the beach deposit and the peat layer are of similar age and attributable to the Brörup interstadial or MIS 5c (Figure 10-1).

The detailed investigation of borehole stratigraphies from northern Denmark, combined with a re-evaluation of existing data sets allowed Larsen et al. (2009) to develop a model of ice sheet advance and retreat for the south-western sector of the Scandinavian ice sheet since the penultimate glaciation. Larsen et al. (2009) reconstruct an ice sheet over southern Norway, which extended eastwards into Sweden, between 115 and 65 ka. The first major ice sheet advance from the north (via the Norwegian Channel and the Kattegat) however only reached northern Denmark and southern Sweden around 65–60 ka, i.e. during MIS 4 (Larsen et al. 2009, Houmark-Nielsen 2010). These scenarios compare well to paleoenvironmental studies of the site Stenberget in southern Sweden (Figure 1-1), which showed a continuous last interglacial – early Weichselian sequence (Berglund and Lagerlund 1981). Boreal to sub-arctic woodlands are here reconstructed for the end of the Eemian interglacial. These are replaced by Arctic tundra and/or a polar desert suggesting cold and dry, but ice-free conditions during the first early Weichselian stadial (Herning) (Berglund and Lagerlund 1981). Subarctic to boreal coniferous woodlands developed during the succeeding interstadial, which has been correlated to the Brörup interstadial (Berglund and Lagerlund 1981).

Possible Early Weichselian interstadial sediments (Brörup) have also recently been reported from another site in southern Sweden, where semi-open woodlands dominated by pine, birch and hazel are reconstructed (Lemdahl et al. submitted).

Pollen-based vegetation reconstructions for sites in northern Sweden, where two interstadials follow above Eemian interglacial sediments, did not provide unequivocal correlations of the interstadial deposits to either of the two early Weichselian interstadials (Robertsson 1991, Robertsson and García Ambrosiani 1992, Hättestrand and Robertsson 2010). Hättestrand (2008) therefore suggested two alternative correlations for the two interstadials (Tärendö I and II), which are separated by glacial deposits. As one alternative, she proposed a correlation to interstadials MIS 5c (Brörup) and MIS 5a (Odderade), respectively and as a second possibility a correlation of the Tärendö I interstadial to MIS 5a (Odderade) and of the Tärendö II interstadial to the earlier part of MIS 3. In alternative I, the intermittent glacial deposit would be correlative to MIS 5b, but in alternative II it would correlate to MIS 4. The multi-proxy study of the Sokli sequence in northeast Finland suggested a more complex picture with ice-free conditions and steppe-tundra vegetation with scattered conifers and tree birch during MIS 5d (Helmens et al. 2012). The subsequent interstadial (termed Sokli interstadial), which is correlated to MIS 5c, shows a vegetation development starting with the establishment of birch forest, followed by the spread of pine and then of spruce, and towards the end of the interstadial a return to a more open vegetation (Helmens et al. 2012). Glacial sediments correlated to MIS 5b and interstadial sediments correlated to MIS 5a suggest an ice-sheet advance and subsequent retreat, respectively (Helmens et al. 2007) in northeastern Finland. Although the Sokli sequence would thus indicate ice free conditions throughout MIS 5d and 5c and an ice sheet advance only during MIS 5b, Johansson et al. (2011) argued for a first early Weichselian glaciation in NW Lapland, corresponding to MIS 5d (Herning) and a second, much more extensive glaciation during MIS 5b (Rederstall). However only the latter would have reached the Gulf of Bothnia (Figure 10-1).

Periglacial conditions starting already around 115 ka have been described from Denmark (Houmark-Nielsen 2007), which would mean as early as the first Early Weichselian stadial. Permafrost conditions for the Herning and Rederstall stadials have also been reported from The Netherlands and Belgium, but not for the site of Gröbern in northern Germany (Aalbersberg and Litt 1998). Modelling of permafrost for north-central Europe during the entire Weichselian suggested that permafrost deeper than 100 m was only present for a short time during the LGM (Delisle et al. 2003). According to these simulations, permafrost depths of about 50 m and less may have been reached during two time intervals, 67–49 ka and 42–37 ka, i.e. during MIS 4 and MIS 3. Following these studies, permafrost may not have been very severe during MIS 5d-a (Delisle et al. 2003).
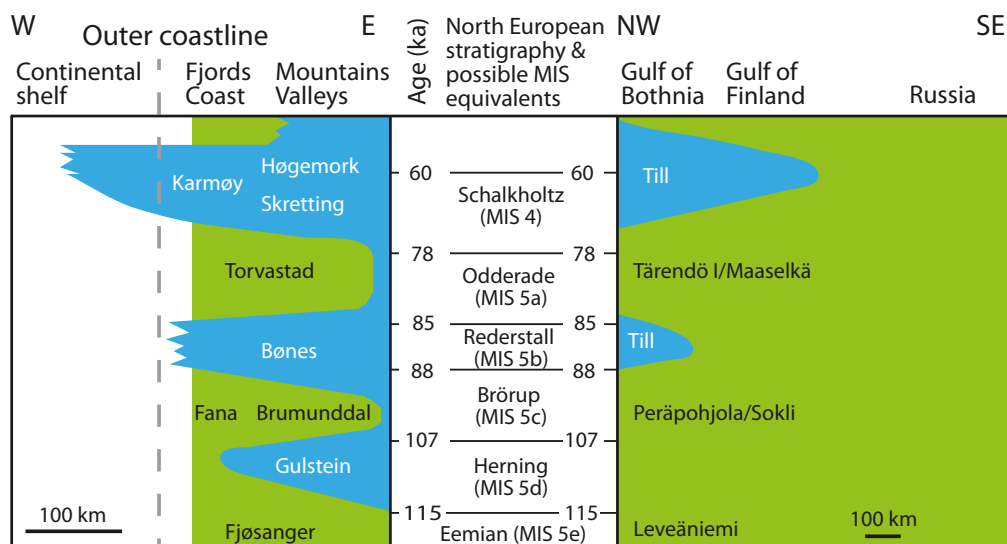

Figure 10-1. *Time-distance diagram of ice sheet extent for the southwestern, northeastern and southeastern flank of the Scandinavian ice sheet. After Svendsen et al. (2004) and Mangerud et al. (2011) using the NGRIP chronology as a time scale. The end of the terrestrial Eemian in northern Europe is set at 115 ka in comparison with the Eemian-Herning transition at Gröbern and follows Müller and Sánchez Goñi (2007). The age estimates for the interstadials and stadials follow the NGRIP chronology. The terminology for the NE part of the Scandinavian ice sheet is according to Hättestrand (2008).*

The most recent maps illustrating the development of the Scandinavian Ice Sheet through time (Figure 10-2) (Mangerud et al. 2011) suggest a minor ice sheet in the Scandinavian Mountains during the Herning stadial (= MIS 5d). This ice sheet reached the coast in south-western Norway and extended eastwards through central Sweden to the Gulf of Bothnia. Its north-eastern flank was located close to the Sokli site. This scenario is in contrast to Johansson et al. (2011), who suggested only a minor ice-sheet extent in NW Lapland, and also contrasts the findings of Helmens et al. (2012), who reconstructed steppe-tundra vegetation with scattered conifers and tree birch for the region around Sokli during MIS 5d. Pollen records from northern Germany and Poland indicate that the vegetation during the Herning stadial is attributable to mainly steppe or tundra biomes (see Chapter 9), whereas the maps in Figure 10-2 assume coniferous forest in northern Germany and Poland. During the subsequent interstadial (Brörup, MIS 5c), the ice sheet had decayed and only local glaciers may have been present. The areal extent of tundra and arctic steppe vegetation during the Brörup interstadial, as shown in Figure 10-2 might be slightly exaggerated given that birch, pine and spruce woodlands have been reported for MIS 5c at Sokli (Helmens et al. 2012).

The ice sheet, which is reconstructed for the Rederstall stadial (= MIS 5b) seems to have been concentrated to the Scandinavian mountains, Norway and central and northern Sweden and extended far into northern Finland and the Kola Peninsula, while southern Sweden and most of Finland remained ice free (Figure 10-2) (Mangerud et al. 2011). Large areas covered by tundra and arctic steppe are reconstructed to the south and east of the ice sheet (Figure 10-2). The birch forest shown on the map for northern Germany and northern Poland (Mangerud et al. 2011) is in contrast to pollen records, which indicate that the vegetation was mainly composed of steppe or tundra biomes (see Chapter 9). Local ice caps, somewhat larger than during MIS 5c and a northward movement of vegetation zones, are reconstructed for the Odderade interstadial (MIS 5a) (Figure 10-2) (Mangerud et al. 2011).
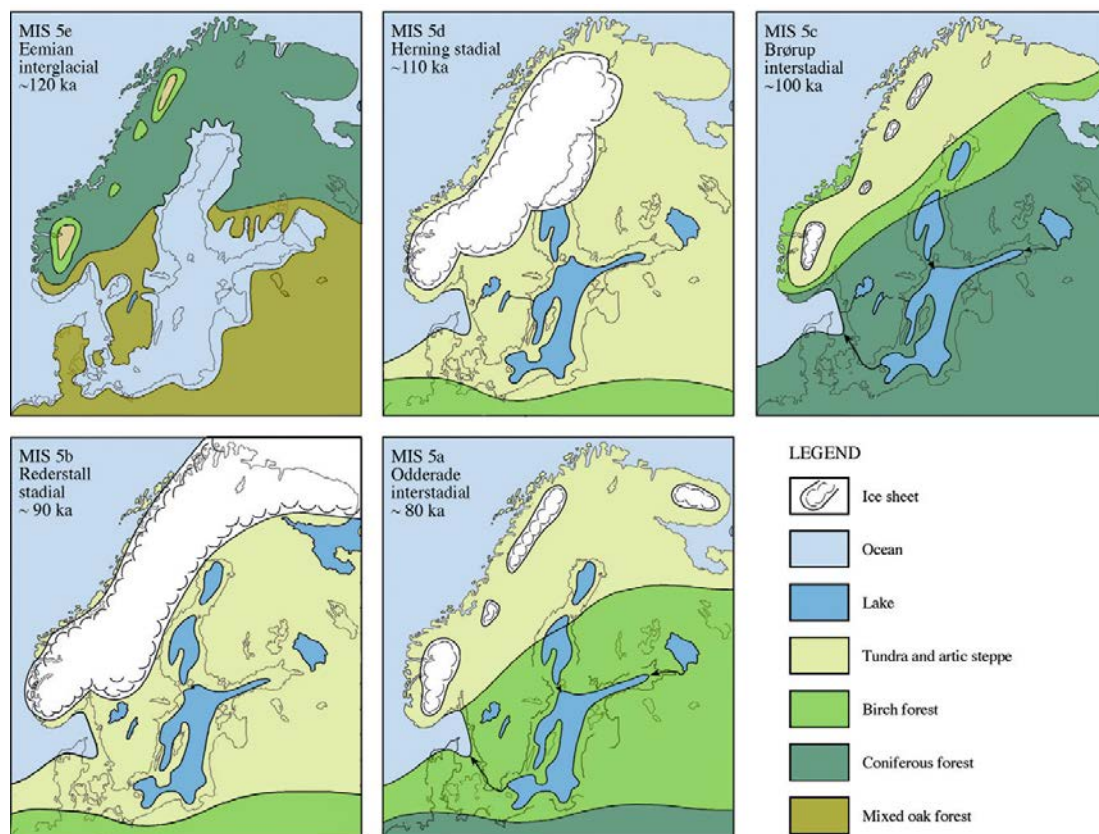

Figure 10-2. *Conceptual maps illustrating the development of the Scandinavian Ice Sheet during MIS 5e-a, modified after Lundqvist (1992). Modified from Mangerud et al. (2011).*

11 Sequence of change and magnitude

Glacial inception, and the sequence of changes leading into the last glacial period has been explored extensively from different view points. Some approaches relied on paleo records only (see for example Müller and Kukla 2004); others employed different types of models with different complexities and boundary conditions (see for example Crucifix and Loutre 2002, Donat and Kaspar 2006, Kaspar and Cubasch 2007, Lohmann and Lorenz 2007, Gröger et al. 2007, Kubatski et al. 2007, Kaspar et al. 2007, Bonelli et al. 2009, Calov et al. 2009) for overviews and references); others again compared paleo data and model output data (for example Sánchez Goñi et al. 2005, Risebrobakken et al. 2007).

North Atlantic records, of which the NGRIP δ^{18}O chronology is the most detailed, provide an idea of the atmospheric response to the decline in July insolation at northern latitudes (Figure 11-1). Correlations between ice core and marine records have shown that each of the stadials, recognized in the ice cores, is paralleled by a SST cooling event in North Atantic marine records. Some of these SST events show large amounts of IRD, which indicates surging of glaciers and ice sheets, and this in turn means that northern hemisphere glaciers/ice-sheets had grown large enough to reach the coastline. Correlations between NGRIP and the NALPS speleothem data set moreover imply that the temperature decrease/increase reconstructed for Greenland and the North Atlantic had an immediate impact on climate conditions in the Alpine region (Boch et al. 2011).
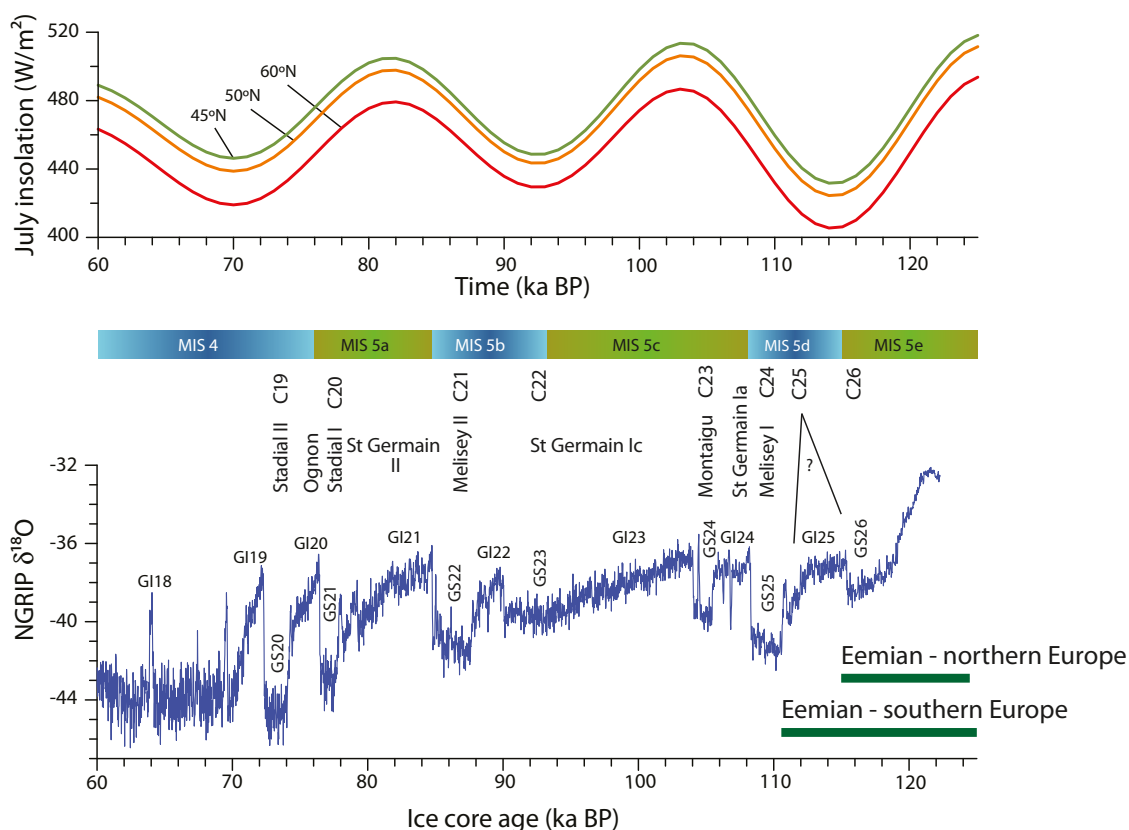

Figure 11-1. Summer insolation at 60°, 50° and 45° N (Berger 1978, Loutre M F, personal communication) compared to the NGRIP δ^{18}O record (NGRIP Members 2004). The North Atlantic sea surface cooling episodes (C26 to C19) and the terrestrial vegetation zones are according to Sánchez Goñi (2007). The correlation between marine and terrestrial events and the NGRIP record was inferred from Figure 13.1 in Sánchez Goñi (2007). The correlation between marine isotope stages (MIS 5e-4) and the NGRIP isotope record is tentative and partly follows Sánchez Goñi (2007) and partly Chapman and Shackleton (1999). The end of the terrestrial Eemian is according to Müller and Kukla (2004) and Sánchez Goñi (2007). GS = Greenland stadials; GIS = Greenland interstadials. Note that the correlation of C25 and C26 to Greenland stadials is not entirely clear. C26 likely corresponds to GS26.

Detailed land-sea correlations, using Iberian Margin cores MD95-2042 and MD99-2331, showed that each Greenland stadial and each marine surface-cooling event corresponds to stadial vegetation changes on the Iberian Peninsula. Further correlations between marine and terrestrial records, using the Iberian Margin records as templates, suggested that the response of the vegetation to these climatic shifts was time transgressive from north to south (Müller and Kukla 2004, Sánchez Goñi et al. 2005, Müller and Sánchez-Goñi 2007). This in turn means that the Eemian interglacial ended 5 ka earlier in northern Europe, as compared to southern Europe (Figure 11-1).

The sequence of changes around the North Atlantic has been illustrated by Müller and Kukla (2004), who aligned different marine and terrestrial records along a common time scale (Figure 11-2). Müller and Kukla (2004) concluded that the transition between MIS 5e and 5d, i.e. SST cooling event C26, at 115 ka was associated with a decrease in SSTs in the Nordic Seas and with a southward displacement of the North Atlantic current (Figure 11-2). However surface waters remained warm for another 5 ka south of the Iceland-Scotland ridge (south of 61°N), as shown by the low amount of the foraminifera *Neogloboquadrina pachyderma* (s) in marine cores (Müller and Kukla 2004). Warmer SSTs to the south and colder SSTs to the north would have led to a strong increase in the meridional SST gradient and to steep vegetation and climatic gradients. The study suggested that the southward displacement of the North Atlantic Current, associated with the C26 event, was accompanied by a shift of the polar timberline from 69°N in N Scandinavia to 52°N in N Germany and by an extinction of thermophilous trees north of 48°N. In contrast, model simulations (Crucifix and Loutre 2002) and paleodata (Sanchez Goñi et al. 2005) suggest a first southward displacement of the vegetation belts already at ~120 ka, which is earlier than the 115 ka estimate of Müller and Kukla (2004).

Landais et al. (2006) assembled ice core data from Greenland and Antarctica, and North Atlantic marine records over the last interglacial/glacial transition (Figure 11-3). Their comparison showed that the decline in $\delta^{18}O_{ice}$ on Greenland and in temperature over Antarctica, follow the general decrease in summer insolation, i.e. synchronous cooling occurred in the North and in the South (Landais et al. 2006). Superimposed on the general temperature decline over Antarctica is a short intermediate temperature drop at 115 ka. This short Antarctic temperature decrease compares in time to North Atlantic SST cooling event C26, but occurred before the lowest temperatures were attained over Greenland (GS26).

The rapid temperature increase associated with GI25 occurred during a period when atmospheric CO_2 levels start to decrease gradually (Figure 11-3), which would suggest a response of the biosphere to the gradual cooling. Moreover, this warming coincides in time with minimum temperatures inferred for Vostok (Figure 11-3). This observation compares well with the bipolar sea-saw concept (Stocker and Johnsen 2003), which suggests anti-phasing of Greenland and Antarctic temperatures during the rapid climate shifts of the last glacial period. This anti-phasing is explained by changes in Atlantic meridional overturning circulation, i.e. high freshwater influx into the North Atlantic slows down the thermohaline circulation, which leads to build up of warm waters in the southern Atlantic, but cools the northern North Atlantic region. Once deep-water formation is resumed, meridional heat transfer becomes re-established, and the northern hemisphere warms while the southern hemisphere looses heat.

During the warm phase of GI25 and during the preceding GS26, ice sheet volumes had reached a first relative maximum, as indicated by the distinct sea level lowering. The rapid temperature increase associated with GI25 and the subsequent decrease leading into GS25 seem to mark the onset of distinct and rapid climate variability in the North Atlantic. Sea surface temperatures initially fluctuated, but dropped distinctly (C24) coinciding with GS25, and first marked occurrences of IRD are observed in the sub-polar North Atlantic (Figure 11-3). Rapid climate variability seen in the Greenland ice core, as opposed to the Antarctic record, where a warming is seen during Greenland stadials, supports the importance of the North Atlantic meridional overturning circulation in modulating climate shifts (Landais et al. 2006).

The comparison between ice core records from Greenland and Antarctica thus suggests that both hemispheres cooled in response to decreased insolation at the last interglacial/glacial transition (Landais et al. 2006). However while Antarctica remained cold, warm surface waters reached the North Atlantic, which caused a rapid shift from cold stadial (GS26) to warmer interstadial (GI25) conditions. Higher sea surface temperatures in turn led to higher moisture supply to high northern latitudes, where ice sheets grew larger and reached the coastline. Surging of these ice sheets produced large amounts of icebergs, which were subsequently discharged, as seen by the large amount of IRD as far south as 42°N (MD99-2331) (Figures 1-2, 5-3).
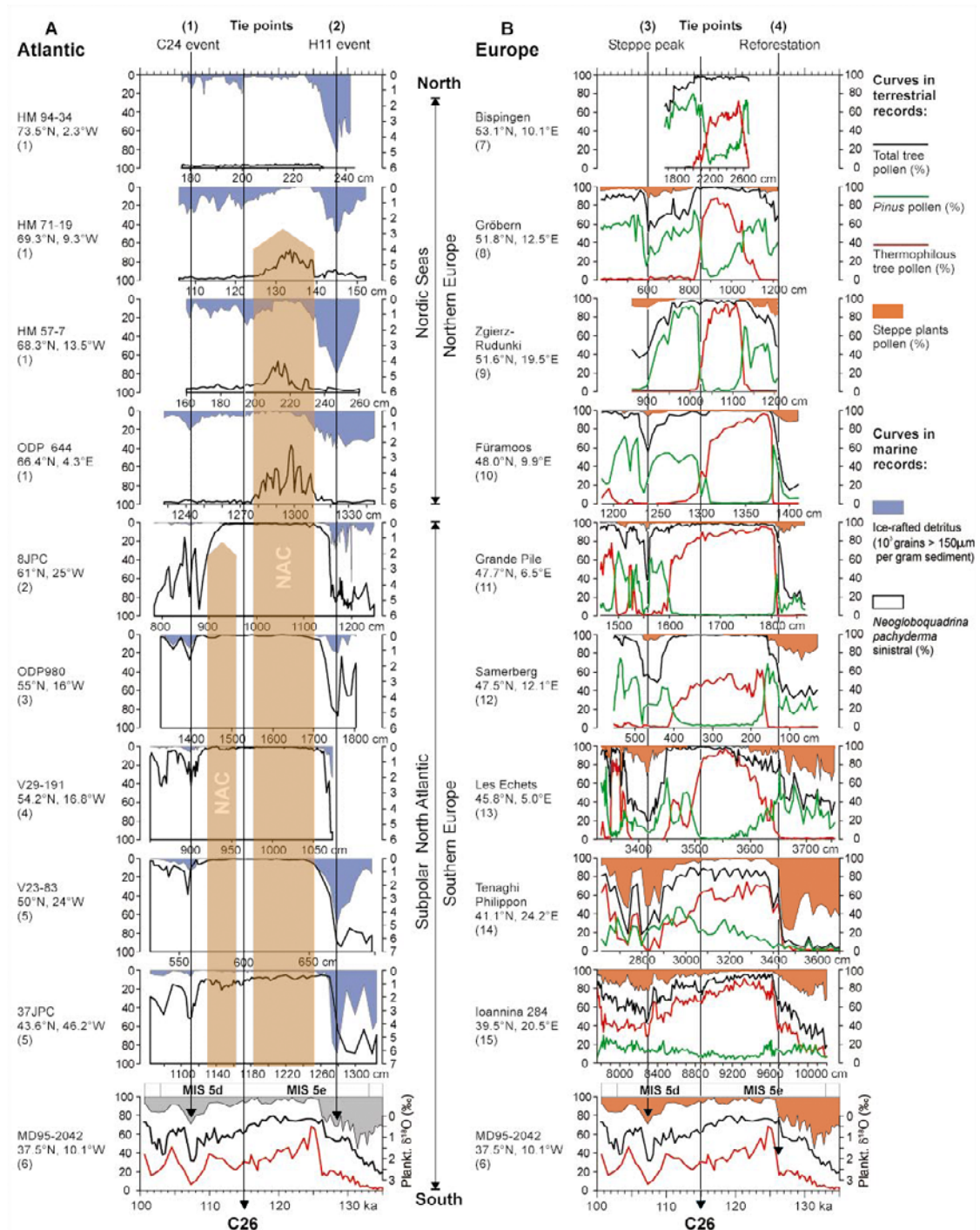
Figure 11-2. *Compilation of last interglacial records, modified from Müller and Kukla (2004). A. Using the time scale of Iberian Margin core MD95-2042 as a template, Atlantic SST records were aligned from north (top) to south (bottom) using two tie points: (1) event C24 event and (2) Heinrich event H11 event. The vertical gray-shaded bars show different extensions of the North Atlantic Current (NAC) during late MIS 5e and early MIS 5d as inferred from SST records. B. Correlation of European pollen records from north (top) to south (bottom) using two tie points: (3) the peak of steppe pollen percentages during the first stadial subsequent to the Eemian interglacial and (4) the reforestation at the onset of the last interglacial. Thermophilous tree taxa (red curves) and total tree taxa (black curves). See Müller and Kukla (2004) for references to the individual records.*
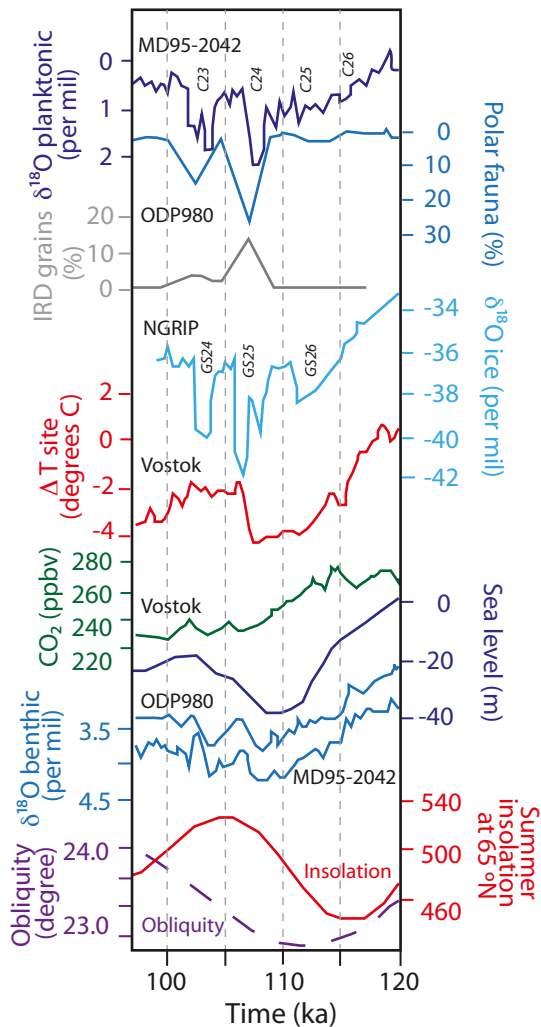
Figure 11-3. *Simplified schematic illustration of selected marine and ice core records covering the last interglacial – glacial transition, each on its own time scale. Modified after Figure 4 in Landais et al. (2006). From top to bottom: planktonic δ¹⁸O values for Iberian Margin core MD 95-2042; polar fauna and IRD from ODP site 980; the δ¹⁸O_ice record for NorthGRIP; reconstructed surface temperature at Vostok, Antarctica shown relative to the present mean annual surface temperature at Vostok; CO₂ record from the Vostok ice core; sea-level curve compared to δ¹⁸O benthic values from ODP 980 and MD 95-2042; obliquity and summer insolation at 65°N. The vertical dashed lines indicate transitions into SST cooling events. See Landais et al. (2006) for references to the individual records.*

The freshwater input and the associated disturbance of the meridional overturning circulation led to a chain of environmental and climatic responses: cooling of North Atlantic surface temperatures (C24), stadial conditions on Greenland (GS25), sea-ice formation, and cold and dry climatic conditions on adjacent land areas (Mélisey I/Rederstall). The southern Atlantic however warmed, coincident with GS25, as inferred from the temperature increase over Antarctica (Figure 11-3). The time interval of GI25 and GS25 thus seems to mark a shift in overall climatic conditions, with the decoupling between northern and southern hemisphere records.

Most model experiments for the last glacial inception suggest that changes in seasonal insolation alone are sufficient to decrease surface temperatures, but that changes in vegetation, ocean circulation, sea-ice extent, and albedo are important feedbacks. Cooler surface temperatures in response to lower insolation increase the atmospheric moisture supply to high northern latitudes and allow building up snow and ice over North America in one ocean-atmosphere model (Khodri et al. 2001). An atmosphere-ocean-vegetation-northern hemisphere-ice sheet model on the other hand suggested that changes in vegetation patterns are important to obtain a strong enough cooling that leads into glaciation over northern North America (Kageyama et al. 2004). Changes in vegetation patterns,

in response to orbital forcing and lower atmospheric CO_2 levels in the UVic Earth System Model lead to a southward shift of the northern treeline and to a replacement of 88% of broadleaf trees by shrubs and C4 grasses in tropical regions (Meissner et al. 2003). This suggests that vegetation changes are an important feedback, similar to the McGill Paleoclimate Model, in which extensive ice sheet growth over North America was facilitated through a reduction of high northern latitude forest areas in response to decreased warm season insolation (Wang et al. 2005). The importance of vegetation-climate feedbacks has also been exemplified by model – paleo-data comparisons using an Earth Model of Intermediate Complexity (MoBidiC) (Crucifix and Loutre 2000) and vegetation reconstructions for northern and southern Europe (Sánchez Goñi et al. 2005). MoBidiC simulated distinct environmental changes prior to glacial inception, most importantly, the replacement of boreal forest by tundra as early as 122–120 ka, which seems to have played a major role for ice accumulation. A southward migration of the treeline between 122–120 ka to 58°N is corroborated by paleo data (Sánchez Goñi et al. 2005). MoBidiC simulations moreover suggested that ocean-land interactions were less critical, but that the gradual growth of summer sea ice throughout the Eemian led to a more rapid replacement of taiga vegetation by tundra biomes (Sánchez Goñi et al. 2005).

In the CLIMBER-2 model, which is an Earth system model of intermediate complexity, glacial inception was triggered by a decrease in boreal summer insolation and an increase in albedo (Calov et al. 2005). This model simulation suggested that orbital forcing alone is sufficient to trigger interglacial-glacial transitions. However, once a threshold is passed, other mechanisms in the climate system, such as feedbacks through atmospheric CO_2 concentration, vegetation, and the ocean, provide amplifiers and contribute to the increase in inland ice cover (Calov et al. 2005). Moreover, dust deposition on the inland ice has been found to act as a regional negative feedback (Calov et al. 2005, Donat and Kaspar 2006).

In most model simulations the major part of the ice sheet build-up occurs in North America, in response to lower summer insolation, whereas the European ice sheet remains relatively small and is restricted to Scandinavia (for example Kageyama et al. 2004, Wang et al. 2005, Calov et al. 2005, Bonelli et al. 2009). Long-lasting ice cover over Eurasia was only reached with low insolation values and low CO_2 concentrations (Bonelli et al. 2009), and/or when an increase in sea ice cover (Kaspar and Cubasch 2007, Gröger et al. 2007) and/or the strength and location of storm tracks (Kaspar et al. 2007) were taken into consideration. In the scenario developed with the CLIMBER-2 model (Calov et al. 2005), the ice sheet cover over Scandinavia was closely linked to changes in the Atlantic meridional overturning circulation. When the convection area was located at a more northern position, ice over Scandinavia built up to a rather thick ice sheet located in the northern part of the region, due to more available moisture. However, when the convection area was located at a more southern position, the simulated ice sheet became rather thin and was located further to the south (Calov et al. 2005).

The influence of the Atlantic meridional overturning circulation on glacial inception was further explored by Risebrobakken et al. (2007), who compared an ocean–sea-ice model and North Atlantic marine paleo records. Their study suggested that lower summer insolation at high northern latitudes and the resulting lower sea surface temperatures led to an increase in the extent of sea ice in the northern North Atlantic (Risebrobakken et al. 2007). Reduced melting of sea ice during the summer season would have provided more saline waters to the high northern latitudes and would have led to an intensified overturning circulation (Risebrobakken et al. 2007). A stronger Atlantic meridional overturning circulation at the MID5e/5d transition has also recently been suggested by Guihou et al. (2011), but is explained by a large increase in the overturning rate of intermediate Atlantic waters. Independent of these differences, an increased overturning circulation and enhanced westerly winds, would have allowed penetration of warm Atlantic waters as far north as the northernmost Nordic Seas and the Barents Sea (Risebrobakken et al. 2007), where they would have supplied ample moisture to high northern latitudes. The strong ocean–land thermal gradient, a stronger Atlantic meridional overturning circulation, warm SSTs and decreasing high latitude insolation, and an increasing latitudinal insolation gradient could have further increased moisture transport towards the high north. Moist maritime air masses combined with cold atmospheric temperatures would have caused excess winter snow and reduced summer melting (Risebrobakken et al. 2007), which would have been essential for the onset of glacial growth, especially over Scandinavia. The MoBidiC simulations additionally showed that the gradual growth of summer sea ice throughout the Eemian was an important trigger to accelerate the transition from taiga to tundra biomes by about 1000 years (Sánchez Goñi et al. 2005).

12   Conclusions

Long and continuous records from ice core, marine and terrestrial archives provide a picture of climatic and environmental changes at the last interglacial/glacial transition. Each of these archives and each of the proxies analysed in the respective archives record different aspects of atmospheric, ocean, and land cover changes. The sequence of events leading from the last interglacial into the last glacial has been described using climate models with different complexities and boundary conditions, paleodata series, and comparisons between model output and paleo data.

The end of the last interglacial and the transition into the last glacial period was initially triggered by a decrease in incoming summer insolation at high northern latitudes around 125 ka. The change in orbital configuration subsequently led to a series of time-transgressive changes on land (e.g. gradual replacement of the existing vegetation) and in the North Atlantic (e.g. sea surface temperature, salinity, strength of the North Atlantic Current), which, as Northern Hemisphere ice sheets started to grow and expand, became more and more pronounced. Different scenarios exist to explain the sequence of events leading to glacial inception, such as summer sea ice development in the northern North Atlantic, a vigorous Atlantic meridional overturning circulation to supply moisture to high latitudes, and a shift in vegetation from forest to tree-less, increasing the albedo effect.

Only few paleo records (e.g. ice cores, speleothems, varved lake sequences) provide truly independent chronologies for the last glacial period. Most records rely on tuning to the astronomical time scale or on correlations to other dated archives to assess leads and lags and the response to the major climatic shifts of the last glacial. These exercises have shown that the vegetation in northern Europe may have responded as early as 122–120 ka to the decrease in summer insolation and to increased summer sea ice formation. The most distinct changes however seem to have occurred around 115 ka, when North Atlantic sea surface temperatures show signs of a first minor cooling. This cold event (labelled sea surface cooling event C26) defines the transition between Marine Isotope Stages (MIS) 5e/5d in marine cores and probably correlates with a decrease in temperatures over Greenland during Greenland Stadial (GS) 26. Parallel with this first cooling event seen in Greenland ice cores (GS26), temperatures also decrease in Antarctica, which would imply synchronous cooling in both hemispheres. However, while Antarctic temperatures subsequently remained cold, temperatures over Greenland started to warm again just before 110 ka, which suggests the start of the so-called bipolar see-saw mechanism.

The first marked cooling over Greenland at 110–108 ka (GS25) coincides with a distinct drop in North Atlantic sea surface temperatures (C24 event), by an increase in ice-rafted debris and by marked vegetation changes in southern Europe. This shift in vegetation defines the end of the terrestrial Eemian in southern Europe, which in comparison to marine records occurred during MIS 5d. Paleo records thus suggest that the response of the vegetation to North Atlantic cooling events was delayed in southern Europe by at least 5 ka as compared to northern Europe.

The gradual decrease in summer insolation at high northern latitudes thus led to a series of feedback mechanisms, which gradually became stronger as polar ice sheets grew larger. The initiation of the bipolar see-saw mechanism at around 110–112 ka seems to have triggered the series of abrupt and recurrent shifts between warmer interstadials and colder stadials that characterised the last glacial. While tundra and steppe-tundra developed in response to severe stadial conditions, the vegetation response to warmer interstadial temperatures was regionally different.

The duration of stadials and interstadials during the early part of the last glacial can be estimated based on records with independent chronologies. Stadials lasted between about 1000 and 4000 years, while interstadials had a length of between 2000 and 16,000 years. The magnitude of temperature shifts at the last interglacial/glacial transition and between stadials and interstadials varied greatly, depending on the location of the paleo-archive and the methods and proxies used for estimating climate conditions. Summer and winter sea surface temperatures reconstructed for marine core ODP 980 at 55°N for example suggest a temperature drop of 3 and 2°C, respectively at the MIS 5e/5d transition. Stadial/interstadial shifts in summer and winter temperatures are estimated at between 2–3°C and 2–4°C, respectively. Alkenone-based temperature reconstructions in Iberian Margin core

MD-2042 further to the south, show even larger temperature differences of up to 10°C between stadials and interstadials. Biological proxies derived from terrestrial sites indicate similar summer temperatures during stadials and interstadials, or only slightly higher temperatures during interstadials. In contrast winter temperatures seem to have been several degrees C colder during stadials as compared to interstadials. Probably the most detailed record of stadial/interstadial temperature shifts is derived from Greenland ice cores, where temperatures rose by between 8 and 16°C across stadial/interstadial transitions.

Although much progress has been made during the last years, new and independently dated terrestrial records are needed to being able to faithfully assess leads and lags to marine, ice core and speleothem archives. At the moment only few archives provide independent chronologies to assess the duration of stadials and interstadials.

Acknowledgements

References

SKB's (Svensk Kärnbränslehantering AB) publications can be found at www.skb.se/publications.

Aalbersberg G, Litt T, 1998. Multiproxy climate reconstructions for the Eemian and Early Weichselian. Journal of Quaternary Sciences 13, 367–390.

Alexanderson H, Eskola K O, Helmens K F, 2008. Optical dating of a Late Quaternary sediment sequence from northern Finland. Geochronometria 32, 51–59.

Allen J R M, Huntley B, 2000. Weichselian palynological records from southern Europe: correlation and chronology. Quaternary International 73–74, 111–125.

Allen J R M, Huntley B, 2009. Last Interglacial palaeovegetation, palaeoenvironments and chronology: a new record from Lago Grande di Monticchio, southern Italy. Quaternary Science Reviews 28, 1521–1538.

Allen J R M, Brandt U, Brauer A, Hubberten H-W, Huntley B, Keller J, Kraml M, Mackensen A, Mingram J, Negendank J F W, Nowaczyk N R, Oberhänsli H, Watts W A, Wulf S, Zolitschka B, 1999. Rapid environmental changes in southern Europe during the last glacial period. Nature 400, 740–743.

Allen J R M, Watts W A, Huntley B, 2000. Weichselian palynostratigraphy, palaeovegetation and palaeoenvironment: the record from Lago Grande di Monticchio, southern Italy. Quaternary International 73–74, 91–110.

Andersen K K, Svensson A, Johnsen S J, Rasmussen S O, Bigler M, Röthlisberger R, Ruth U, Siggaard-Andersen M-L, Steffensen J P, Dahl-Jensen D, Vinther B M, Clausen H B, 2006. The Greenland ice core chronology 2005, 15–42 kyr. Part 1: constructing the time scale. Quaternary Science Reviews 25, 3246–3257.

Andersen S T, 1961. Vegetation and its environment in Denmark in the Early Weichselian glacial (Last Glacial). Copenhagen. (Danmarks Geologiske Undersøgelse II)

Arrhenius G, 1952. Geology of the East Equatorial Pacific. In Pettersson H (ed). Reports of the Swedish deep-sea expedition 1947–1948. Vol 5, Sediment cores from the East Pacific. Göteborg: Göteborgs Kungl. Vetenskaps- och vitterhetssamhälle, 189–201.

Badertscher S, Fleitmann D, Cheng H, Edwards R L, Göktürk O M, Zumbühl A, Leuenberger M, Tüysüz O, 2011. Pleistocene water intrusions from the Mediterranean and Caspian seas into the Black Sea. Nature Geoscience 4, 236–239.

Bar-Matthews M, Ayalon A, Kaufman A, 1997. Late Quaternary paleoclimate in the Eastern Mediterranean region from stable isotope analysis of speleothems at Soreq cave, Israel. Quaternary Research 47, 155–168.

Bar-Matthews M, Ayalon A, Kaufman A, Wasserburg G J, 1999. The eastern Mediterranean paleoclimate as a reflection of regional events: Soreq cave, Israel. Earth and Planetary Science Letters 166, 85–95.

Bar-Matthews M, Ayalon A, Kaufman A, 2000. Timing and hydrological conditions of Sapropel events in the Eastern Mediterranean, as evident from speleothems, Soreq cave, Israel. Chemical Geology 169, 145–156.

Bar-Matthews M, Ayalon A, Gilmour M, Matthews A, Hawkesworth C J, 2003. Sea–land oxygen isotopic relationships from planktonic foraminifera and speleothems in the Eastern Mediterranean region and their implication for paleorainfall during interglacial intervals. Geochimica et Cosmochimica Acta 67, 3181–3199.

Baumann K-H, Lackschewitz K S, Mangerud J, Spielhagen R F, Wolf-Welling T C W, Heinrich R, Kassens H, 1995. Reflections on Scandinavian ice sheet fluctuations in Norwegian Sea sediments during the past 150,000 years. Quaternary Research 43, 185–197.

Behre K-E, 1989. Biostratigraphy of the last glacial period in Europe. Quaternary Science Reviews 8, 24–44.

Behre K-E, Lade U, 1986. Eine Folge von Eem und 4 Weichsel-Interstadialen in Oerel/ Niedersachsen und ihr Vegetationsablauf. Eiszeitalter und Gegenwart 36, 11–36.

Behre K-E, van der Plicht J, 1992. Towards an absolute chronology for the last glacial period in Europe: radiocarbon dates from Oerel, northern Germany. Vegetation History and Archaeobotany 1, 111–117.

Behre K-E, Hölzer A, Lemdahl G, 2005. Botanical macro-remains and insects from the Eemian and Weichselian site of Oerel (northwest Germany) and their evidence for the history of climate. Vegetation History and Archaeobotany 14, 31–53.

Berger A L, 1978. Long-term variations of daily insolation and Quaternary climatic changes. Journal of the Atmospheric Sciences 35, 2362–2367.

Berger W H, 2012. Milankovitch theory – hits and misses. Available at: http://escholarship.org/uc/item/95m6h5b9

Berglund B, Lagerlund E, 1981. Eemian and Weichselian stratigraphy in South Sweden. Boreas 10, 323–362.

Björck S, Kromer B, Johnsen S, Bennike O, Hammarlund D, Lemdahl G, Possnert G, Rasmussen T L, Wohlfarth B, Hammer C U, Spurk M, 1996. Synchronised terrestrial-atmospheric deglacial records around the North Atlantic. Science 274, 1155–1160.

Boch R, Cheng H, Spötl C, Edwards R L, Wang X, Häuselmann P, 2011. NALPS: a precisely dated European climate record 120–60 ka. Climate of the Past 7, 1247–1259.

Boettger T, Junge F W, Litt T, 2000. Stable climatic conditions in central Germany during the last interglacial. Journal of Quaternary Science 15, 469–473.

Boettger T, Junge F W, Knetsch S, Novenko E Y, Borisova O K, Kremenetski K V, Velichko A A, 2007. Indications to short-term climate warming at the very end of the Eemian in terrestrial records of Central and Eastern Europe. In Sirocko F, Claussen M, Sánchez Goñi M F, Litt T (eds). The climate of past interglacials. Amsterdam: Elsevier. (Developments in Quaternary Sciences 7), 265–275.

Boettger T, Novenko E Y, Velichko A A, Borisova O K, Kremenetski K V, Knetsch S, Junge F W, 2009. Instability of climate and vegetation dynamics in Central and Eastern Europe during the final stage of the Last Interglacial (Eemian, Mikulino) and Early Glaciation. Quaternary International 207, 137–144.

Bond G, Heinrich H, Broecker W S, Labeyrie L, McManus J, Andrews J T, Huon S, Jantschik R, Clasen S, Simet C, Tedesco K, Klas M, Bonani G, Ivy S, 1992. Evidence for massive discharges of icebergs into the glacial North Atlantic during the last glacial period. Nature 360, 245–249.

Bond G, Broecker W S, Johnsen S, McManus J, Labeyrie L, Jouzel J, Bonani G, 1993. Correlations between climate records from North Atlantic sediments and Greenland ice. Nature 365, 143–147.

Bonelli S, Charbit S, Kageyama M, Woillez M-N, Ramstein G, Dumas C, Quiquet A, 2009. Investigating the evolution of major Northern Hemisphere ice sheets during the last glacial-interglacial cycle. Climate of the Past 5, 329–345.

Brauer A, Mingram J, Frank U, Günter C, Schettler G, Wulf S, Zolitschka B, Negendank J F W, 2000. Abrupt environmental oscillations during the Early Weichselian recorded at Lago Grande di Monticchio, southern Italy. Quaternary International 73–74, 79–90.

Brauer A, Allen J R M, Mingram B, Dulski P, Wulf S, Huntley B, 2007. Evidence for last interglacial chronology and environmental change from southern Europe. Proceedings of the National Academy of Sciences 104, 450–455.

Brewer S, Guiot J, Sánchez Goñi M F, Klotz S, 2008. The climate in Europe during the Eemian: a multi-method approach using pollen data. Quaternary Science Reviews 27, 2303–2315.

Brinkkemper O, van Geel B, Wiegers J, 1987. Palaeoecological study of a Middle-Pleniglacial deposit from Tilligte, The Netherlands. Review of Palaeobotany and Palynology 51, 235–269.

Calov R, Ganopolski A, Petoukhov V, Claussen M, Brovkin V, Kubatski C, 2005. Transient simulation of the last glacial inception. Part II: sensitivity and feedback analysis. Climate Dynamics 24, 563–576.

Calov R, Ganopolski A, Kubatski C, Claussen M, 2009. Mechanisms and time scales of glacial inception simulated with an Earth system model of intermediate complexity. Climate of the Past Discussions 5, 595–633.

Capron E, Landais A, Chappellaz J, Schilt A, Buiron D, Dahl-Jensen D, Johnsen S J, Jouzel J, Lemieux-Dudon B, Loulergue L, Leuenberger M, Masson-Delmotte V, Meyer H, Oerter H, Stenni B, 2010. Millennial and sub-millennial scale climate variations recorded in polar ice cores over the last glacial period. Climate of the Past 6, 345–365.

Caspers G, Freund H, 2001. Vegetation and climate in the Early and Pleni-Weichselian in northern Central Europe. Journal of Quaternary Science 16, 31–48.

Caspers G, Merkt J, Müller H, Freund H, 2002. The Eemian interglaciation in northwestern Germany. Quaternary Research 58, 49–52.

Chapman M R, Shackleton N J, 1999. Global ice-volume fluctuations, North Atlantic ice-rafting events, and deep-ocean circulation changes between 130 and 70 ka. Geology 27, 795–798.

Chapman M, Shackleton N J, Duplessy J-C, 2000. Sea surface temperature variability during the last glacial–interglacial cycle: assessing the magnitude and pattern of climate change in the North Atlantic. Palaeogeography, Palaeoclimatology, Palaeoecology 157, 1–25.

Chappell J, 2002. Sea level changes forced ice breakouts in the Last Glacial cycle: new results from coral terraces. Quaternary Science Reviews 21, 1229–1240.

Crucifix M, Loutre M F, 2000. Transient simulations over the last interglacial period (126–115 kyr BP): feedback and forcing analysis. Climate Dynamics 19, 417–433.

Cutler K B, Edwards R L, Taylor F W, Cheng H, Adkins J, Gallup C D, Cutler P M, Burr G S, Bloom A L, 2003. Rapid sea level fall and deep-ocean temperature change since the last interglacial period. Earth and Planetary Science Letters 206, 253–271.

Dansgaard W, Johnsen S J, Clausen H B, Dahl-Jensen D, Gundestrup N S, Hammer C U, Hvidberg C S, Steffensen J P, Sveinbjörnsdottir A E, Jouzel J, Bond G, 1993. Evidence for general instability of past climate from a 250-kyr ice-core record. Nature 364, 218–220.

de Beaulieu J-L, Reille M, 1984. A long upper Pleistocene pollen record from Les Echets near Lyon, France. Boreas 13, 111–132.

de Beaulieu J-L, Reille M, 1992a. The last climatic cycle at La Grande Pile (Vosges, France): a new profile. Quaternary Science Reviews 11, 431–438.

de Beaulieu J-L, Reille M, 1992b. Long Pleistocene pollen sequences from the Velay Plateau (Massif Central, France). Vegetation History and Archaeobotany 1, 233–242.

Delisle G, Caspers G, Freund H, 2003. Permafrost in north-central Europe during the Weichselian: how deep? In Phillips M, Springman S M, Arenson L U (eds). Permafrost: proceedings of the Eighth International Conference on Permafrost, Zurich, Switzerland, 21–25 July 2003. Lisse: Swets & Zeitlinger, 187–191.

Donat M, Kaspar F, 2006. Simulations of the last interglacial and the subsequent inception with the Planet Simulator. Climate of the Past Discussions 2, 1347–1369.

Drysdale R N, Zanchetta G, Hellstrom J C, Fallick A E, Zhao J, 2005. Stalagmite evidence for the onset of the Last Interglacial in southern Europe at 129 ± 1 ka. Geophysical Research Letters 32, L24708. doi:10.1029/2005GL024658

Drysdale R N, Zanchetta G, Hellstrom J C, Fallick A E, McDonald J, Cartwright I, 2007. Stalagmite evidence for the precise timing of North Atlantc cold events during the early last glacial. Geology 35, 77–80.

Dutton A, Lambeck K, 2012. Ice volume and sea level during the Last Interglacial. Science 337, 216–219.

Dutton A, Bard E, Antonioli F, Esat T M, Lambeck K, McCulloch M T, 2009. Phasing and amplitude of sea-level and climate change during the penultimate interglacial. Nature Geoscience 2, 355–359.

Emiliani C, 1955. Pleistocene temperatures. Journal of Geology 63, 538–578.

Engels S, Helmens K F, Väliranta M, Brooks S J, Birks H J B, 2010. Early Weichselian (MIS 5d and 5c) temperatures and environmental changes in northern Fennoscandia as recorded by chironomids and macroremains at Sokli, northeast Finland. Boreas 39, 689–704.

EPICA Community Members, 2006. One-to-one coupling of glacial climate variability in Greenland and Antarctica. Nature 444, 195–198.

Fauquette S, Guiot J, Menut M, de Beaulieu J-L, Reille M, Guenet P, 1999. Vegetation and climate since the last interglacial in the Vienne area (France). Global and Planetary Change 20, 1–17.

Fleitmann D, Cheng H, Badertscher S, Edwards R L, Mudelsee M, Götürk O, Fankhauser A, Pickering R, Raible C C, Matter A, Kramers J, Tüysüz O, 2009. Timing and climatic impact of Greenland interstadials recorded in stalagmites from northern Turkey. Geophysical Research Letters 36, L19707. doi:10.1029/2009GL040050

Fletcher W J, Sánchez Goñi M F, Allen J R M, Cheddadi R, Combourieu-Nebout N, Huntley B, Lawson I, Londeix L, Magri D, Margari V, Müller U C, Naughton F, Novenko E, Roucoux K, Tzedakis P C, 2010. Millennial-scale variability during the last glacial in vegetation records from Europe. Quaternary Science Reviews 29, 2839–2864.

Follieri M, Magri D, Sadori L, 1988. 250,000-year pollen record from Valle di Castiglione (Roma). Pollen et Spores 30, 329–356.

Follieri M, Giardini M, Magri D, Sadori L, 1998. Palynostratigraphy of the last glacial period in the volcanic region of Central Italy. Quaternary International 47–48, 3–20.

Fronval T, Jansen E, 1997. Eemian and early Weichselian (140–60 ka) paleoceanography and paleoclimate in the Nordic seas with comparisons to Holocene conditions. Paleoceanography 12, 443–462.

Grant K M, Rohling E J, Bar-Matthews M, Ayalon A, Medina-Elizalde M, Bronk Ramsey C, Satow C Roberts A P, 2012. Rapid coupling between ice volume and polar temperature over the past 150,000 years. Nature 491, 744–747.

Grootes P M, Stuiver M, White J W C, Johnsen S, Jouzel J, 1993. Comparison of oxygen isotope records from the GISP2 and GRIP Greenland ice cores. Nature 366, 552–554.

Guihou A, Pichat S, Govin A, Nave S, Michel E, Duplessy J-C, Telouk P, Labeyrie L, 2011. Enhanced Atlantic Meridional Overturning Circulation supports the last glacial inception. Quaternary Science Reviews 30, 1576–1582.

Guiot J, Pons A, de Beaulieu J-L, Reille M, 1989. A 140,000-year continental climate reconstruction from two European pollen records. Nature 338, 309–313.

Guiot J, Reille M, de Beaulieu J-L, Pons A, 1992. Calibration of the climatic signal in a new pollen sequence from La Grande Pile. Climate Dynamics 6, 259–264.

Guiot J, de Beaulieu J L, Cheddadi R, David F, Ponel P, Reille M, 1993. The climate in western Europe during the last glacial/interglacial cycle derived from pollen and insect remains. Palaeogeography, Palaeoclimatology, Palaeoecology 103, 73–93.

Grüger E, 1979. Die Seeablagerungen vom Samerberg/Obb. und ihre Sellung im Jungpleistozän. Eiszeitalter und Gegenwart 29, 23–34.

Grüger E, 1989. Palynostratigraphy of the last interglacial/glacial cycle in Germany. Quaternary International 3–4, 69–79.

Gröger M, Maier-Reimer E, Mikolajewicz U, Schurgers G, Vizcaino M, Winguth A, 2007. Vegetation-climate feedbacks in transient simulations over the last interglacial (128,000–113,000 yr BP). In Sirocko F, Claussen M, Sánchez Goñi M F, Litt T (eds). The climate of past interglacials. Amsterdam: Elsevier. (Developments in Quaternary Sciences 7), 563–572.

Hays J D, Imbrie J, Shackleton N J, 1976. Variations in the Earth's orbit: pacemaker of the Ice Ages. Science 194, 1121–1132.

Helmens K F, Engels S, 2010. Ice-free conditions in eastern Fennoscandia during early Marine Isotope Stage 3: lacustrine records. Boreas 39, 399–409.

Helmens K, Räsänen M E, Johansson P, Jungner H, Korjonen K, 2000. The Last Interglacial-Glacial cycle in NE Fennoscandia: a nearly continuous record from Sokli (Finnish Lapland). Quaternary Science Reviews 19, 1605–1623.

Helmens K F, Johansson P W, Räsänen M E, Alexanderson H, Eskola K O, 2007. Ice-free intervals continuing into Marine Isotope Stage 3 at Sokli in the central area of the Fennoscandian glaciations. Bulletin of the Geological Society of Finland 79, 17–39.

Helmens K F, Väliranta M, Engels S, Shala S, 2012. Large shifts in vegetation and climate during Early Weichselian (MIS 5d-c) inferred from multi-proxy evidence at Sokli (northern Finland). Quaternary Science Reviews 41, 22–38.

Hoffmann M H, Litt T, Jäger E J, 1998. Ecology and climate of the early Weichselian flora from Gröbern (Germany). Review of Palaeobotany and Palynology 102, 259–276.

Houmark-Nielsen M, 1989. The last interglacial–glacial cycle in Denmark. Quaternary International 3–4, 31–39.

Houmark-Nielsen M, 2007. Extent and age of Middle and Late Pleistocene glaciations and periglacial episodes in southern Jylland, Denmark. Bulletin of the Geological Society of Denmark 55, 9–35.

Houmark-Nielsen M, 2010. Extent, age and dynamics of Marine Isotope Stage 3 glaciations in the southwestern Baltic Basin. Boreas 39, 343–359.

Hultén E, Fries M, 1986. Atlas of North European vascular plants. Vols I–III. Königstein: Koeltz.

Hättestrand M, 2008. Vegetation and climate during Weichselian ice free intervals in northern Sweden. PhD thesis. Department of Physical Geography and Quaternary Geology, Stockholm university.

Hättestrand M, Robertsson A-M, 2010. Weichselian interstadials at Riipiharju, northern Sweden – interpretation of vegetation and climate from fossil and modern pollen records. Boreas 39, 296–311.

Johansson P, Lunkka J P, Sarala P, 2011. The glaciation of Finland. In Ehlers J, Gibbard P L, Hughes P D (eds). Quaternary glaciations – extent and chronology: a closer look. Amsterdam: Elsevier. (Developments in Quaternary Sciences 15), 105–116.

Jouzel J, Stiévenard M, Johnsen S J, Landais A, Masson-Delmotte V, Sveinbjörnsdottir A, Vimeux F, von Grafenstein U, White J W C, 2007. The GRIP deuterium-excess record. Quaternary Science Reviews 26, 1–17.

Juggins S, 2013. Quantitative reconstructions in palaeolimnology: new paradigm or sick science. Quaternary Science Rewiews 64, 20–32.

Kageyama M, Charbit S, Ritz C, Khodri M, Ramstein G, 2004. Quantifying ice-sheet feedbacks during the last glacial inception. Geophysical Research Letters 31, L24203. doi:10.1029/2004GL021339

Kaspar F, Cubasch U, 2007. Simulations of the Eemian interglacial and the subsequent glacial inception with a coupled ocean-atmosphere general circulation model. In Sirocko F, Claussen M, Sánchez Goñi M F, Litt T (eds). The climate of past interglacials. Amsterdam: Elsevier. (Developments in Quaternary Sciences 7), 499–515.

Kaspar F, Spangehl T, Cubasch U, 2007. Northern hemisphere winter storm tracks of the Eemian interglacial and the last glacial inception. Climate of the Past 3, 181–192.

Khodri M, Leclainche Y, Ramstein G, Braconnot P, Marti O, Cortijo E, 2001. Simulating the amplification of orbital forcing by ocean feedbacks in the last glaciation. Nature 410, 570–574.

Kleman J, 1994. Preservation of landforms under ice sheets and ice caps. Geomorphology 9, 19–32.

Kleman J, Hättestrand C, 1999. Frozen-bed Fennoscandian and Laurentide ice sheets during the Last Glacial Maximum. Nature 402, 63–66.

Klotz S, Guiot J, Mosbrugger V, 2003. Continental European Eemian and early Würmian climate evolution: comparing signals using different quantitative reconstruction approaches based on pollen. Global and Planetary Change 36, 277–294.

Klotz S, Müller U, Mosbrugger V, de Beaulieu J-L, Reille M, 2004. Eemian to early Würmian climate dynamics: history and pattern of changes in Central Europe. Palaeogeography, Palaeoclimatology, Palaeoecology 211, 107–126.

Kolstrup E, 1980. Climate and stratigraphy in northwestern Europe between 30,000 B.P. and 13,000 B.P., with special reference to the Netherlands. Amsterdam: Universiteit van Amsterdam. (Publicaties van het Fysisch-geografisch en bodemkundig laboratorium van de Universiteit van Amsterdam 31), 181–253.

Komar M, Łanczont M, Madeyska T, 2009. Spatial vegetation patterns based on palynological records in the loess area between Dnieper and Odra Rivers during the last interglacial–glacial cycle. Quaternary International 198, 152–172.

Kubatski C, Claussen M, Calov R, Ganopolski A, 2007. Modelling the end of an interglacial (MIS 1, 5, 7, 9, 11). In Sirocko F, Claussen M, Sánchez Goñi M F, Litt T (eds). The climate of past interglacials. Amsterdam: Elsevier. (Developments in Quaternary Sciences 7), 583–593.

Kukla G J, McManus J F, Rousseau D-D, Chuine I, 1997. How long and how stable was the last interglacial? Quaternary Science Reviews 16, 605–612.

Kühl N, Litt T, 2003. Quantitative time series reconstruction of Eemian temperature at three European sites using pollen data. Vegetation History and Archaeobotany 12, 205–214.

Kühl N, Litt T, Schölzel C, Hense A, 2007. Eemian and Early Weichselian temperature and precipitation variability in northern Germany. Quaternary Science Reviews 26, 3311–3317.

Köhler P, Bintjana R, Fischer H, Joos F, Knutti R, Lohmann G, Masson-Delmotte V, 2010. What caused Earth's temperature variations during rthe last 800,000 years? Data-based evidence on radiative forcing and constraints on climate sensitivity. Quaternary Science Reviews 29, 129–145.

Lagerbäck, R, Robertsson A-M, 1988. Kettle holes – stratigraphical archives for Weichselian geology and palaeoenvironment in northernmost Sweden. Boreas 17, 439–468.

Lambeck K, Chapell J, 2001. Sea level change through the last glacial cycle. Science 292, 679–686.

Lambeck K, Esat T M, Potter E-K, 2002. Links between climate and sea levels for the past three million years. Nature 419, 199–206.

Lambeck K, Purcell A, Dutton A, 2012. The anatomy of interglacial sea levels: the relationship between sea levels and ice volumes during the Last Interglacial. Earth and Planetary Science Letters 315–316, 4–11.

Landais A, Jouzel J, Masson-Delmotte V, Caillon N, 2005. Large temperature variations over rapid climatic events in Greenland: a method based on air isotope measurements. Comptes Rendues Geoscience 337, 947–956.

Landais A, Masson-Demotte V, Jouzel J, Raynaud D, Johnsen S, Huber C, Leuenberger M, Schwander J, Minster B, 2006. The glacial inception as recorded in the NorthGRIP Greenland ice core: timing, structure and associated abrupt temperature changes. Climate Dynamics 26, 273–284.

Lang G, 1994. Quartäre Vegetationsgeschichte Europas: Methoden und Ergebnisse. Jena: Gustav Fischer Verlag.

Larsen E, Sejrup H P, 1990. Weichselian land–sea interactions: Western Norway – Norwegian Sea. Quaternary Science Reviews 9, 85–97.

Larsen N K, Knudsen K L, Krohn C F, Kronborg C, Murray A S, Nielsen O B, 2009. Late Quaternary ice sheet, lake and sea history of wouthwest Scandinavia – a synthesis. Boreas 38, 732–761.

Lemdahl G, Broström A, Hedenäs L, Arvidsson K, Holmgren S, Gaillard M J, Möller P, submitted. Eemian and Early Weichselian environments in southern Sweden: a multi-proxy study of till-covered organic deposits from the Småland peneplain. Submitted to Journal of Quaternary Science.

Litt T, Junge F W, Böttger T, 1996. Climate during the Eemian in north-central Europe – a critical review of the palaeobotanical and stable isotope data from central Germany. Vegetation History and Archaeobotany 5, 247–256.

Lisiecki L E, Raymo M E, 2005. A Plio-Pleistocene stack of 57 globally distributed benthic $\delta^{18}O$ records. Paleoceanography 20, PA1003. doi:10.1029/2004PA001071

Lohmann G, Lorenz S J, 2007. Orbital forcing on atmospheric dynamics during the last interglacial and glacial inception. In Sirocko F, Claussen M, Sánchez Goñi M F, Litt T (eds). The climate of past interglacials. Amsterdam: Elsevier. (Developments in Quaternary Sciences 7), 527–545.

Lundqvist J, 1978. New information about early and middle Weichselian interstadials in northern Sweden. Uppsala: SGU. (Sveriges Geologiska Undersökning C752)

Lundqvist J, 1992. Glacial stratigraphy in Sweden. Special Paper 15, Geological Survey of Finland, 43–59.

Magri D, 1999. Late Quaternary vegetation history at Lagaccione near Lago di Bolsena (central Italy). Review of Palaeobotany and Palynology 106, 171–208.

Mangerud J, Sønstegaard E, Sejrup H-P, 1979. Correlation of the Eemian (interglacial) Stage and the deep-sea oxygen-isotope stratigraphy. Nature 277, 189–192.

Mangerud J, Gyllencreutz R, Lohne O, Svendsen J I, 2011. Glacial history of Norway. In Ehlers J, Gibbard P L, Hughes P D (eds). Quaternary glaciations – extent and chronology: a closer look. Amsterdam: Elsevier. (Developments in Quaternary Sciences 15), 279–298.

Martinson D G, Pisias N G, Hays J D, Imbrie J, Moore T C, Shackleton N J, 1987. Age dating and the orbital theory of the ice ages: development of a high-resolution 0 to 300,000-year chronostratigraphy. Quaternary Research 27, 1–29.

McManus J F, Bond G C, Broecker W S, Johnsen S, Labeyrie L, Higgins S, 1994. High-resolution climate records from the North-Atlantic during the last interglacial. Nature 371, 326–329.

Meissner K J, Waever A J, Mathews H D, Cox P M, 2003. The role of land surface dynamics in glacial inception: a study with the UVic Earth System Model. Climate Dynamics 21, 515–537.

Meyer M C, Spötl C, Mangini A, 2008. The demise of the Last Interglacial recorded in isotopically dated speleothems from the Alps. Quaternary Science Reviews 27, 476–496.

Miller U, 1977. Pleistocene deposits of the Alnarp Valley, southern Sweden: microfossils and their stratigraphical application. PhD thesis. University of Lund, Department of Quaternary Geology.

Müller H, 1974. Pollenanalytische Untersuchungen und Jahresschichtenzählungen an der eemzeitlichen Kieselgur von Bispingen/Luhe. Geologisches Jahrbuch, A21, 148–169.

Müller UC, 2000. A late-Pleistocene pollen sequence from Jammertal, south-western Germany with particular reference to location and altitude as factors determining Eemian forest composition. Vegetation History and Archaeobotany 9, 125–131.

Müller UC, Klotz S, Geyh MA, Press J, Bond GC, 2005. Cyclic climate fluctuations during the last interglacial in central Europe. Geology 33, 449–452.

Müller U C, Kukla G J, 2004. North Atlantic current and European environments during the declining stage of the last interglacial. Geology 32, 1009–1012.

Müller U C, Pross J, Bibus E, 2003. Vegetation response to rapid climate change in Central Europe during the past 140,000 yr based on evidence from the Füramoos pollen record. Quaternary Research 59, 235–245.

Müller U C, Sánchez Goñi M F, 2007. Vegetation dynamics in southern Germany during Marine Isotope Stage 5 (~130 to 70 kyr ago). In Sirocko F, Claussen M, Sánchez Goñi M F, Litt T (eds). The climate of past interglacials. Amsterdam: Elsevier. (Developments in Quaternary Sciences 7), 277–287.

Müller U C, Pross J, Tzedakis P C, Gamble C, Kotthoff U, Schmiedl G, Wulf S, Christianis K, 2011. The role of climate in the spread of modern humans into Europe. Quaternary Science Reviews 30, 273–279.

Möller P, 2013. Drumlinised glaciofluvial and glaciolacustrine sediments on the Småland peneplain, South Sweden – new evidence on the growth and decay history of the Fennoscandian Ice Sheets during MIS 3. Submitted to Quaternary Science Reviews.

NGRIP Members, 2004. High-resolution record of Northern Hemisphere climate extending into the last interglacial period. Nature 431, 147–151.

Novenko E Y, Seifert-Eulen M, Boettger T, Junge F W, 2008. Eemian and Early Weichselian vegetation and climate history in Central Europe: a case study from the Klinge section (Lusatia, eastern Germany). Review of Palaeobotany and Palynology 151, 72–78.

Oppo D W, McManus J F, Cullen J L, 2006. Evolution and demise of the Last Interglacial warmth in the subpolar North Atlantic. Quaternary Science Reviews 25, 3268–3277.

Pini R, Ravazzi C, Reimer P J, 2010. The vegetation and climate history of the last glacial cycle in a new pollen record from Lake Fimon (southern Alpine foreland, N-Italy). Quaternary Science Reviews 29, 3115–3137.

Ponel P, 1995. Rissian, Eemian and Würmian Coleoptera assemblages from La Grande Pile (Vosges, France). Palaeogeography, Palaeoclimatology, Palaeoecology 114, 1–41.

Pons A, Reille M, 1988. The Holocene- and Upper Pleistocene pollen record from Padul (Granada, Spain): a new study. Palaeogeography, Palaeoclimatology, Palaeoecology 66, 243–263.

Preusser F, 2004. Towards a chronology of the Late Pleistocene in the northern Alpine Foreland. Boreas 33, 195–210.

Påsse T, Robertsson A M, Miller U, Klingberg F, 1988. A Late Pleistocene sequence at Margreteberg, southwestern Sweden. Boreas 17, 141–163.

Ran E T H, Bohncke S J P, van Huissteden J, Vandenberghe J, 1990. Evidence of episodic permafrost conditions during the Weichselian Middle Pleniglacial in the Hengelo Basin (The Netherlands). Geologie en Mijnbouw 44, 207–220.

Rasmussen T L, Thomsen E, Kuijpers A, Wastegård S, 2003. Late warming and early cooling of the sea surface in the Nordic seas during MIS 5e (Eemian Interglacial). Quaternary Science Reviews 22, 809–821.

Reille M, de Beaulieu J-L, 1988. History of the Würm and Holocene vegetation in the Western Velay (Massif Central, France): a comparison of pollen analysis from three corings at Lac du Bouchet. Review of Palaeobotany and Palynology 54, 233–248.

Reille M, de Beaulieu J-L, 1990. Pollen analysis of a long upper Pleistocene continental sequence in a Velay maar (Massif Central, France). Palaeogeography, Palaeoclimatology, Palaeoecology 80, 35–48.

Reille M, Andrieu V, de Beaulieu J-L, Guenet P, Goeury C, 1998. A long pollen record from Lac du Bouchet, Massif Central, France: for the period ca 325 to 100 ka BP (OIS 9c to OIS 5e). Quaternary Science Reviews 17, 1107–1123.

Reille M, de Beaulieu J-L, Svobodova H, Andrieu-Ponel V, Goeury C, 2000. Pollen analytical biostratigraphy of the last five climatic cycles from a long continental sequence from the Velay region (Massif Central, France). Journal of Quaternary Science 15, 665–685.

Rioual P, Andrieu-Ponel V, de Beaulieu J-L, Reille M, Svobodova H, Battarbee R W, 2007. Diatom response to limnological and climatic changes at Ribain Maar (French Massif Central) during the Eemian and Early Würm. Quaternary Science Reviews 26, 1557–1609.

Risebrobakken B, Dokken T, Otterå O H, Jansen E, Gao Y, Drange H, 2007. Inception of the Northern European ice sheet due to cotrasting ocean and insolation forcing. Quaternary Research 67, 128–135.

Robertsson A-M, 1991. The biostratigraphy of the Late Pleistocene in Sweden 150,000–15,000 B.P. – a survey. Striae 34, 39–46.

Robertsson A M, García Ambrosiani K, 1992. The Pleistocene in Sweden – a review of research, 1960–1990. Sveriges Geologiska Undersökning, Ser. Ca 81, 299–306.

Salgueiro E, Voelker A H L, de Abreu L, Abrantes F, Meggers H, Wefer G, 2010. Temperature and productivity changes off the western Iberian margin during the last 150 kyr. Quaternary Science Reviews 29, 680–695.

Sánchez Goñi M F, 2007. Introduction to climate and vegetation in Europe during MIS5. In Sirocko F, Claussen M, Sánchez Goñi M F, Litt T (eds). The climate of past interglacials. Amsterdam: Elsevier. (Developments in Quaternary Sciences 7), 197–205.

Sánchez Goñi M F, Eynaud F, Turon J L, Shackleton N J, 1999. High resolution palynological record off the Iberian margin: direct land–sea correlations for the Last Interglacial complex. Earth and Planetary Science Letters 171, 123–137.

Sánchez Goñi M F, Cacho I, Turon J L, Guiot J, Sierro F J, Peypouquet J P, Grimalt J O, Shackleton N J, 2002. Synchroneity between marine and terrestrial responses to millennial scale climatic variability during the last glacial period in the Mediterranean region. Climate Dynamics 19, 95–105.

Sánchez-Goñi M F, Loutre M F, Crucifix M, Peyron O, Santos L, Duprat J, Malaizé B, Turon J-L, Peypouquet J P, 2005. Increasing vegetation and climate gradients in Western Europe over the Last Glacial Inception (122–110 ka): data and model comparison. Earth and Planetary Science Letters 231, 111–130.

Sánchez Goñi M F, Landais A, Fletcher W J, Naughton F, Desprat S, Duprat J, 2008. Contrasting impacts of Dansgaard–Oeschger events over a western European latitudinal transect modulated by orbital parameters. Quaternary Science Reviews 27, 1136–1151.

Satkunas J, Grigiene A, Velichkevich F, Robertsson A-M, Sandgren P, 2003. Upper Pleistocene stratigraphy at the Medininkai site, eastern Lithuania: a continuous record of the Eemian-Weichselian sequence. Boreas 32, 627–641.

Sejrup H P, Larsen E, 1991. Eemian-early Weichselian N-S temperature gradients; North Atlantic – NW Europe. Quaternary International 10–12, 161–166.

Shackleton N J, 1967. Oxygen isotope analyses and Pleistocene temperatures re-assessed. Nature 215, 15–17.

Shackleton N J, 1969. The Last Interglacial in the marine and terrestrial records. Proceedings of the Royal Society of London B 174, 135–154.

Shackleton N J, 2006. Formal Quaternary stratigraphy – What do we expect and need? Quaternary Science Reviews 25, 3458–3462.

Shackleton N J, Pisias N G, 1985. Atmospheric carbon dioxide, orbital forcing, and climate. In Sundquist E T, Broecker W S (eds). The carbon cycle and atmospheric CO_2: natural variations, Archean to present. Washington, DC: American Geophysical Union. (Geophysical Monograph 32), 303–317.

Shackleton N J, Berger A Peltier W R, 1990. An alternative astronomical calibration of the lower Pleistocene timescale based on ODP Site 677. Transactions of the Royal Society of Edinburgh, Earth Sciences 81, 251–261.

Shackleton N J, Hall M A, Pate D, 1995a. Pliocene stable isotope stratigraphy of Site 846. In Pisias N G, Janacek L A, Palmer-Julson A, van Andel T H (eds). Proceedings of the Ocean Drilling Program. Vol 138. Scientific Results. College Station, TX: The Program, 337–355.

Shackleton N J, Crowhurst S, Hagelberg T, Pisias N G, Schneider D A, 1995b. A new Late Neogene time scale: application to Leg 138 Sites. In Pisias N G, Janacek L A, Palmer-Julson A, van Andel, T H (eds). Proceedings of the Ocean Drilling Program. Vol 138. Scientific Results. College Station, TX: The Program, 73–101.

Shackleton N J, Hall M A, Vincent E, 2000. Phase relationships between millennial-scale events 64,000–24,000 years ago. Paleoceanography 15, 565–569.

Shackleton N J, Chapman M R, Sánchez Goñi, M F, Pailler D, Lancelot Y, 2002. The classic marine isotope substage 5e. Quaternary Research 58, 14-16.

Shackleton N J, Sánchez Goñi M F, Pailler D, Lancelot Y, 2003. Marine Isotope Substage 5e and the Eemian Interglacial. Global and Planetary Change 36, 151–155.

Shackleton N J, Fairbanks R G, Chiu T, Parrenin F, 2004. Absolute calibration of the Greenland time scale: implications for Antarctic time scales and for Δ^{14}C. Quaternary Science Reviews 23, 1513–1522.

Sirocko F, Seelos K, Schaber K, Rein B, Dreher F, Diehl M, Lehne R, Jäger K, Krbetschek M, Degering D, 2005. A late Eemian aridity pulse in central Europe during the last glacial inception. Nature 436, 833–836.

Spötl C, Mangini A, 2006. U/Th age constraints on the absence of ice in the central Inn Valley (eastern Alps, Austria) during Marine Isotope Stages 5c to 5a. Quaternary Research 66, 167–175.

Steffensen J P, Andersen K A, Bigler M, Clausen H B, Dahl-Jensen D, Fischer H, Goto-Azuma K, Hansson M, Johnsen S J, Jouzel J, Masson-Delmotte V, Popp T, Rasmussen S O, Röthlisberger R, Ruth U, Stauffer B, Siggaard-Andersen M L, Sveinbjörnsdóttir A E, Svensson A, White J W C, 2008. High-resolution Greenland ice core data show abrupt climate change happens in few years. Science 321, 680–684.

Stocker T F, Johnsen S J, 2003. A minimum model for the bipolar seesaw. Paleoceanography 18, 1087. doi:10.1029/2003PA000920

Svendsen J I, Alexanderson H, Astakhov V I, Demidov I, Dowdeswell J A, Funder S, Gataullin V, Henriksen M, Hjort C, Houmark-Nielsen M, Hubberten H W, Ingólfsson Ó, Jakobsson M, Kjær K H, Larsen E, Lokrantz H, Lunkka J P, Lyså A, Mangerud J, Matiouchkov A, Murray A, Möller P, Niessen F, Nikolskaya O, Polyak L, Saarnisto M, Siegert C, Siegert M J, Spielhagen R F, Stein R, 2004. Late Quaternary ice sheet history of northern Eurasia. Quaternary Science Reviews 23, 1229–1271.

Svensson A, Andersen K K, Bigler M, Clausen H B, Dahl-Jensen D, Davies S M, Johnsen S J, Muscheler R, Rasmussen S O, Röthlisberger R, Steffensen J P, Vinther B M, 2006. The Greenland ice core chronology 2005, 15–41 ka. Part 2: Comparison to other records. Quaternary Science Reviews 25, 3258–3267.

Svensson A, Andersen K K, Bigler M, Clausen H B, Dahl-Jensen D, Davies S M, Johnsen S J, Muscheler R, Parrenin F, Rasmussen S O, Röthlisberger R, Seierstad I, Steffensen J P, Vinther B M, 2008. A 60,000 year Greenland stratigraphic ice core chronology. Climate of the Past 4, 47–57.

Thompson W G, Goldstein S L, 2005. Open-system coral ages reveal persistent suborbital sea-level changes. Science 308, 401–404.

Tzedakis P C, 2003. Timing and duration of Last Interglacial conditions in Europe: a chronicle of changing chronology. Quaternary Science Reviews 22, 763–768.

Tzedakis P C, 2005. Towards an understanding of the response of southern European vegetation to orbital and suborbital climate variability. Quaternary Science Reviews 24, 1585–1599.

Tzedakis P C, Andrieu V, de Beaulieu J-L, Crowhurst S, Follieri M, Hooghiemstra H, Magri D, Reille M, Sadori L, Shackleton N J, Wijmstra T A, 1997. Comparison of terrestrial and marine records of changing climate of the last 500,000 years. Earth and Planetary Science Letters 150, 171–176.

Tzedakis P C, Frogley M R, Heaton T H E, 2002. Duration of last interglacial conditions in northwest Greece. Quaternary Research 58, 53–55.

Tzedakis P C, Frogley M R, Heaton T H E, 2003. Last Interglacial conditions in southern Europe: evidence from Ioannina, northwest Greece. Global and Planetary Change 36, 157–170.

Tzedakis P C, Frogley M R, Lawson I T, Preece R C, Cacho I, de Abreu L, 2004. Ecological thresholds and patterns of millennial-scale climate variability: the response of vegetation in Greece during the last glacial period. Geology 32, 109–112.

Tzedakis P C, Hooghiemstra H, Pälike H, 2006. The last 1.35 million years at Tenaghi Philippon: revised chronostratigraphy and long-term vegetation trends. Quaternary Science Reviews 25, 3416–3430.

Väliranta M, Birks H H, Helmens K F, Engels S, Piirainen M, 2009. Early Weichselian interstadial (MIS 5c) summer temperatures were higher than today in northern Fennoscandia. Quaternary Science Reviews 28, 777–782.

Walker M J C, Björck S, Lowe J J, 2001. Integration of ice core, marine and terrestrial records (INTIMATE) from around the North Atlantic region: an introduction. Quaternary Science Reviews 20, 1169–1174.

Walkling A P, Coope G R, 1996. Climate reconstructions from the Eemian/Early Weichselian transition in Central Europe based on the coleoptera record from Gröbern, Germany. Boreas 25, 145–159.

Wang Z, Cochelin A-S B, Mysak L A, Wang Y, 2005. Simulation of the last glacial inception with the green McGill Paleoclimate Model. Geophysical Research Letters 32, L12705. doi:10.1029/2005GL023047

Watts WA, Allen JRM, Huntley B, 1996. Vegetation history and paleoclimate of the last glacial period at Lago Grande di Monticchio, southern Italy. Quanterary Science Reviews 15, 133–153.

Wohlfarth B, Veres D, Ampel L, Lacourse T, Blaauw M, Preusser F, Andrieu-Ponel V, Kéravis D, Lallier-Vergès E, Björck S, Davies S M, de Beaulieu J-L, Risberg J, Hormes A, Kasper H U, Possnert G, Reille M, Thouveny N, Zander A, 2008. Rapid ecosystem response to abrupt climate changes during the last glacial period in western Europe, 40–16 ka. Geology 36, 407–410.

Woillard G M, 1978. Grande Pile peat bog: a continuous pollen record for the last 140,000 years. Quaternary Research 9, 1–21.

Woillard G M, Mook W G, 1982. Carbon-14 dates at Grande Pile: correlation of land and sea chronologies. Science 215, 159–161.

Wulf S, Keller J, Paterne M, Mingram J, Lauterbach S, Opitz S, Sottili G, Giaccio B, Albert P G, Satow C, Tomlinson E L, Viccaro M, Brauer A, 2012. The 100–133 ka record of Italian explosive volcanism and revised tephrochronology of Lago Grande di Monticchio. Quaternary Science Reviews 58, 104–123.